MODELING FUTURE FIRE, VEGETATION, AND CARBON TRAJECTORIES UNDER CLIMATE CHANGE IN INTERIOR ALASKA BOREAL FOREST

by

SHELBY A. WEISS

A DISSERTATION

Presented to the Department of Geography
and the Division of Graduate Studies of the University of Oregon
in partial fulfillment of the requirements
for the degree of
Doctor of Philosophy

December 2022

DISSERTATION APPROVAL PAGE

Student: Shelby A. Weiss

Title: Modeling Future Fire, Vegetation, and Carbon Trajectories Under Climate Change in Interior Alaska Boreal Forest

This dissertation has been accepted and approved in partial fulfillment of the requirements for the Doctor of Philosophy degree in the Department of Geography by:

Melissa Lucash	Chairperson
Daniel Gavin	Core Member
Lucas de Carvalho Ramos Silva	Core Member
Joshua Roering	Institutional Representative

and

Krista Chronister	Vice Provost for Graduate Studies

Original approval signatures are on file with the University of Oregon Division of Graduate Studies.

Degree awarded December 2022

DISSERTATION ABSTRACT

Shelby A. Weiss

Doctor of Philosophy

Department of Geography

December 2022

Title: Modeling Future Fire, Vegetation, and Carbon Trajectories Under Climate Change in Interior Alaska Boreal Forest

Fire activity has increased in interior Alaska in recent decades and these trends are projected to continue under climate change. A greater frequency and severity of wildfires have been found to favor broadleaf-deciduous species across numerous field and modeling studies, impacting the resilience of black spruce forests and potentially impacting the carbon storage capacity in the region. This dissertation explores potential future trends in boreal forest fire regimes, vegetation composition, and carbon storage under climate change through three studies using the spatially explicit landscape simulation model, LANDIS-II. The modeling framework represented wildfire dynamically using the SCRPPLE fire extension and captured belowground carbon, hydrologic, and permafrost dynamics in addition to vegetation growth using the DGS succession extension. All three studies relied on simulations of a 380,400-hectare landscape (4-ha resolution) under both historic and future (RCP 8.5) climate projections. The first study explored impacts of wildfire under different climate change scenarios and found that annual area burned and average fire size were greater under climate change; climate change scenarios also resulted in a greater rate of areas burning multiple times during the simulation period. The second study focused on quantifying and identifying

drivers of potential shifts in dominant forest type following different numbers of wildfires. It showed that initially-conifer-dominated areas on the landscape that experienced greater numbers of fires more often shifted to broadleaf-deciduous dominance, and this effect was exacerbated by climate change. Vegetation type transitions away from conifer dominance were most strongly driven by percentage of biomass removed in the most recent wildfire. The third study quantified differences in carbon pools and vegetation productivity under different climate scenarios and found that while carbon and net primary productivity overall increased across the landscape under climate change, the amount of soil carbon available for decomposition also increased and associated increases in heterotrophic respiration led to the landscape being a net source of atmospheric carbon. Altogether these results reflect the importance of accounting for key ecosystem processes when modeling future change in interior Alaska and how climate change and wildfire behavior can interact to drive change in vegetation composition and future carbon storage.

CURRICULUM VITAE

NAME OF AUTHOR: Shelby A. Weiss

GRADUATE AND UNDERGRADUATE SCHOOLS ATTENDED:

University of Oregon, Eugene
Portland State University
The Ohio State University
Colorado State University

DEGREES AWARDED:

Doctor of Philosophy, Geography, 2022, University of Oregon
Master of Science, Environment and Natural Resources, 2017, The Ohio State University
Bachelor of Science, Fish, Wildlife, and Conservation Biology, 2014, Colorado State University

AREAS OF SPECIAL INTEREST:

Landscape Ecology
Disturbance Ecology
Forest Ecology

PROFESSIONAL EXPERIENCE:

Graduate Employee, Department of Geography, University of Oregon, 2020-2022

Graduate Research Assistant, Department of Geography, Portland State University, 2018-2020

Plant Recorder, Missouri Botanical Garden, 2017-2018

GRANTS, AWARDS, AND HONORS:

Rippey Dissertation Writing Grant, Modeling Future Fire, Vegetation, and Carbon Trajectories Under Climate Change in Interior Alaska Boreal Forest, Department of Geography, University of Oregon, 2022

Doug Foster Community Building Award, Department of Geography, University of Oregon 2022

IALE-North America Student Virtual Travel Award, Contexts mediating future shifts in vegetation composition in interior Alaska under climate change, IALE-North America, 2022

NEON Early Career Scholar Award for ESA 2020, How increasing fire frequency will change the forests of interior Alaska, Ecological Society of America, 2020

Dean's Oregon Sports Lottery Graduate Scholarship, Portland State University 2018, 2019

FAES Environmental Graduate Research Fellowship, The Ohio State University, 2016

University Fellowship, The Ohio State University, 2015

Magna cum Laude, Warner College of Natural Resources, Colorado State University, 2014

William D. Hatfield Memorial Scholarship, Warner College of Natural Resources, Colorado State University, 2011

Presidential Scholarship, Colorado State University, 2010

PUBLICATIONS:

Lucash, M.S., S.A. Weiss, M.J. Duveneck, R.M. Scheller. (2022). Managing for red-cockaded woodpeckers is more complicated under climate change. *The Journal of Wildlife Management 86*(8). https://doi.org/10.1002/jwmg.22309

Buma, B., K. Hayes, S.A. Weiss, M.S. Lucash. (2022). Short-interval fires increasing in the Alaskan boreal forest as fire self-regulation decays across forest types. *Scientific Reports 12*(4901). https://doi.org/10.1038/s41598-022-08912-8

Buma, B., S.A. Weiss, K. Hayes, M.S. Lucash. (2020). Wildland fire reburning trends across the US West suggest only short-term negative feedback and differing climatic effects. *Environmental Research Letters 15*. https://doi.org/10.1088/1748-9326/ab6c70

Weiss, S.A., E.L. Toman, R.G. Corace III. (2019). Aligning endangered species management with fire-dependent ecosystem restoration: manager

perceptions on red-cockaded woodpecker and longleaf pine management actions. *Fire Ecology 15*(19). https://doi.org/10.1186/s42408-019-0026-z\

Weiss, S.A., R.G. Corace III, E.L. Toman, D.A. Herms, P.C. Goebel. (2018). Wildlife implications across snag treatment types in jack pine stands of Upper Michigan. *Forest Ecology and Management 409*: 407-416. https://doi.org/10.1016/j.foreco.2017.10.013

Corace, R.G. III, S.A. Weiss, L.M. Shartell. (2018). Observer bias and sharp-tailed grouse lek counts in the Upper Midwest. *Journal of Fish and Wildlife Management 9*(2): 666- 667. https://doi.org/10.3996/112017-JFWM-095

Corace, R.G. III, S.A. Weiss, D.S. Marsh, E.L. Comes, F.J. Cuthbert. (2017). Novel method for monitoring common terns at a large colony in northern Lake Huron, USA. Journal of Great Lakes Research 43(6): 1160- 1164. https://doi.org/10.1016/j.jglr.2017.08.002

ACKNOWLEDGMENTS

I would first like to express gratitude to the chair of my committee, Dr. Melissa Lucash, who has been an unwavering supporter as I pursued this research. She has encouraged me through moments of frustration and given valuable feedback that has improved the way I think and write about ecology and landscape modeling. I feel very lucky to have had her as a mentor throughout this journey and as a model of how to collaborate and foster a supportive research community.

I am also thankful to my committee members, Dr. Dan Gavin, Dr. Lucas Silva, and Dr. Josh Roering. I have greatly appreciated their support and encouragement throughout each step of this process, especially when navigating a new Ph.D. program as a transfer student amidst the early days of the pandemic. Their interest in my research has been motivating and their feedback has strengthened my research.

I am grateful to have worked with a group of very talented and knowledgeable scientists through the Reburns Alaska project: Dr. Brian Buma, Kate Hayes, Dr. Tim Link, Dr. Melissa Lucash, Dr. Adrienne Marshall, Dr. Dmitry Nicolsky, Dr. Vladimir Romanovsky, Dr. Rob Scheller, Dr. Jason Shabaga, and Dr. Jason Vogel. They have supported me in providing expertise, reference data, and insights about boreal forest ecology and modeling that have been critical toward building my understanding of interior Alaska ecosystem dynamics and how to model them. I am also very grateful to John McNabb, whose coding of the DGS extension, patience, and help with troubleshooting bugs during model development was instrumental in creating the model extension used in this dissertation.

I would also like to acknowledge the CyVerse High Performing Computing Resources and thank Dr. Tyson Swetnam for his assistance and patience over many Zoom sessions and emails to help me create a Docker container for LANDIS-II. This has made the research in this dissertation possible and will hopefully help expand the modeling capacity for other LANDIS-II modelers. His assistance and the resulting products were made possible through CyVerse's External Collaborative Partnership program.

I would like to thank all the past, current, and associated members of the Terrestrial Ecosystem Ecology Lab who have consistently been a friendly and valuable community whom I can share progress with and seek advice. Thank you, Dr. Tom Brussel, Alison Deak, James Lamping, Colin Mast, Hana Matsumoto, Stuart Steidle, Gabriel Abreu-Vigil, and Dr. Neil Williams for providing support, positive words, and helpful comments at different stages of this research. Thank you to James for being a great office mate and friend; our conversations about Star Trek, R coding, Sierra, etc. have never failed to brighten my day. Thank you to Neil for many inspiring conversations about trees and ecology in the office and on outings in the Pacific Northwest. Thank you to Alison for helping me think through (and commiserating in) our shared modeling efforts and for improving my R scripts. Thank you to Dr. Zachary Robbins, who never failed to promptly and patiently answer all my SCRPPLE questions, and whose R scripts for parameterizing SCRPPLE were an incredibly helpful resource.

I owe immense thanks to my graduate student colleagues and friends in the Department of Geography at UO. I have benefitted greatly by learning from them and alongside them. Especially, I would like to thank Cy Abbott, Samantha Brown, Troy

Brundidge, Janice Chen, Emily Doerner, Sydney Katz, Lily Kuentz, and Kate Shields for the many interesting and meaningful conversations had in and outside of the classroom. Their kind words, humor, and encouragement have frequently lifted my mood and put me in a better place to tackle the challenges of grad school.

I am incredibly grateful to many friends and teachers outside of the UO community who have supported me in immeasurable ways. Alli Demonico and the Demonico family have made me feel a part of their family when I've been very far away from mine; they have brought me along on adventures, shared delicious food, and many entertaining stories. Thank you to Tessa Behnke for many reassuring conversations over the years and for going on adventures with me that provided much-needed breaks from grad school. Thank you to Ashley Guerra for your friendship, laughter, and support and for being willing to meet up for a beer no matter when I'm passing through. Thank you to Abbey Blue, who has supported my love of science since we met in the eighth grade and has cheered me on and made me laugh in both joyful and stressful times. Thank you to Barry Crook, who encouraged my love of reading and interest in science and gave me confidence at a young age that I could be a scientist.

I would like to thank Cameron Lund for his consistent support in all my academic and personal pursuits, regardless of how far away they have taken me. For always embracing the time we spend with one another, whether it be on the Current River or over the phone.

I am so grateful to my family, who have shown up for me in whatever I've pursued. Thank you, especially to my extended family in St. Louis, MO, and Godfrey, IL. It is hard to express what your presence in my life means to me in a few words, but I am

certain that who I am today has been shaped by your support and love. I would like to thank my parents for their unwavering confidence in me, and for inspiring in me inquisitiveness, empathy, and a sense of humor about the world. I wouldn't be where I am today without you.

I am also appreciative of the financial support received to do this research. This research was supported by the National Science Foundation Award 1737706, and by the University of Oregon Department of Geography Rippey Dissertation Writing Grant.

TABLE OF CONTENTS

LIST OF FIGURES

LIST OF TABLES

Table Page

CHAPTER 1

INTRODUCTION

The boreal forest biome is a critically important global carbon reservoir, storing an estimated one-third of the world's forest carbon (Pan et al. 2011). The balance between carbon sequestration and carbon emissions has important implications for climate change; when ecosystems that have historically been net storers of carbon become net emitters, this contributes to greater atmospheric greenhouse gas concentrations and leads to further warming. Most of the carbon in boreal ecosystems is stored belowground, where slow decomposition due to cool annual temperatures, substrate quality, and sometimes waterlogged soils allows organic, carbon-rich material to accumulate over time (Bradshaw and Warkentin 2015; Hobbie et al. 2000). Aboveground, vegetation communities also sequester carbon and their ability do so is influenced by climatic patterns and plant community age and composition. These critical carbon stores held in boreal forests are now vulnerable to a variety of climate change-mediated threats. For instance, in North American boreal forests, wildfires are becoming more frequent and severe (Kasischke et al. 2010). Numerous field studies have shown shifts in species dominance from conifers to hardwoods following high severity and/or short-interval fires (fires that burn the same area on the landscape twice with a shorter than typical interval in between events; Hart et al. 2019; Johnstone and Chapin 2006a; Whitman et al. 2019), prompting a growing concern that a changing fire regime will alter forest communities and prompt a large scale state shift that could impact how much carbon boreal forests in North America may be able to store in the future. However, there

is large uncertainty and disagreement on whether such shifts will result in a change in net carbon stored in the region (Bradshaw and Warkentin 2015).

Understanding how climate-driven changes in fire regime will impact boreal forest species composition at a large scale and how those potential changes may alter boreal forest carbon source-sink status in western North America require an integrated understanding of key ecosystem processes and how they interact. In Alaska, process-based models have generated valuable predictions of shifts to greater deciduous broadleaf dominance with greater fire activity (Foster et al. 2019; Mann et al. 2012; Mekonnen et al. 2019; Hansen et al. 2021). However, modeling efforts have yet to represent the full suite of woody plant species present on the landscape and some key belowground processes (e.g. soil CN dynamics) in a way that is spatially explicit and interactive at a landscape scale. The three studies presented here represent an effort to model a landscape in interior Alaska using a newly developed and sophisticated module to the LANDIS-II forest landscape simulation model (Scheller et al. 2007).

Study Region

Interior Alaska is characterized by a continental climate with cold winters reaching average temperatures of -23.5 degrees Celsius in January and warm, dry summers with average July temperatures of 16.3 degrees Celsius (Hinzman et al., 2006). The growing season is short, from early May to mid-September (Hinzman et al., 2006). Average precipitation in Fairbanks is 287 mm annually, with about 35% falling as snow (Hinzman et al., 2006).

Interior Alaska is dominated by black spruce forests, which account for ~ 44% of the area (Van Cleve & Dyrness, 1983). These forests are often underlain by permafrost, particularly on cool, northern aspects (Van Cleve & Dyrness, 1983; Viereck, 1983). Black spruce stands occur in a range of contexts from closed-canopy upland forests with feathermoss (*Pleurozium schreberi*, *Hylocomium splendons*) to more open lowland muskeg with Sphagnum moss and sedge tussocks (Van Cleve & Dyrness, 1983). Intermixed across the landscape with black spruce are stands of Alaska paper birch (*Betula neoalaskana*), quaking aspen (*Populus tremuloides*), and white spruce (*Picea glauca*), which typically occur on well-drained, permafrost-free south-facing upland sites and floodplain forests with balsam poplar (*Populus balsamifera*) and white spruce (L. A. Viereck et al., 1983).

Simulations were run on a modeling domain of 380,400 hectares in interior Alaska at a 0.2 km x 0.2 km resolution. The specific area was chosen to encompass field sites where reference data for validating the performance of the DGS extension (Figure 1). At the start of the simulation period, the dominant forest vegetation type across the landscape was mature black spruce, although the domain did include younger forest patches created by fires that had occurred within the past two decades.

Study Themes

The first chapter aims to quantify the impact of climate change on wildfire activity in the region of study and examine potential negative feedbacks to continued fire activity. The second chapter examines drivers of forest type transitions following different numbers of fires experienced through the simulation period. Finally, the third

chapter quantifies differences in carbon pools and fluxes between different climate change scenarios. Together, these three studies give a broad picture of how climate change may impact large-scale and interacting above and belowground ecosystem processes across a large landscape that is currently poised for change.

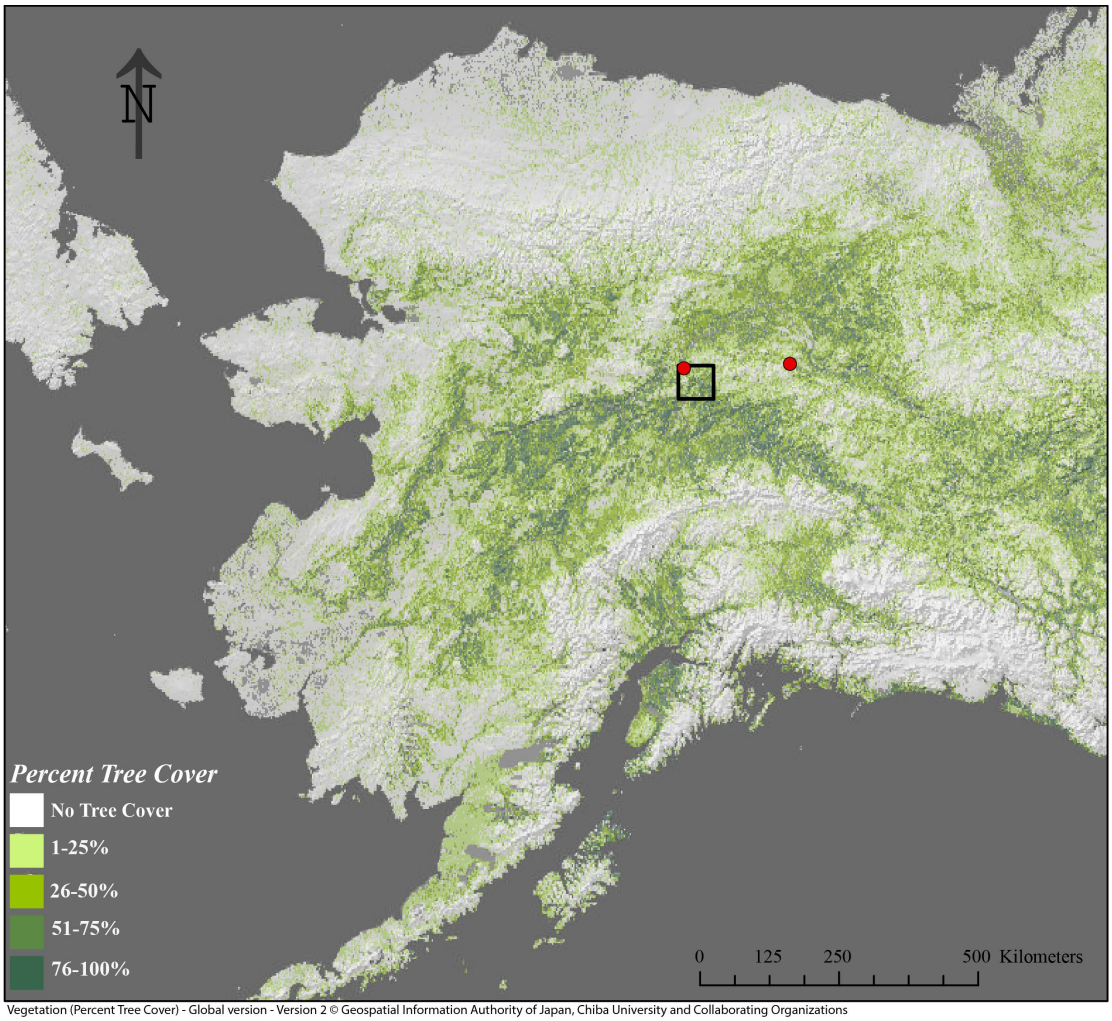

Figure 1. Map of modeling domain (black square) within interior Alaska and general location of reference field sites (red) for validating model behavior following multiple simulated fires. Percent tree cover is noted in shades of green.

CHAPTER 2

MODELING WILDFIRE DYNAMICS UNDER CLIMATE CHANGE OVER A LARGE LANDSCAPE IN INTERIOR ALASKA

Introduction

Under climate change, fire activity, i.e., fire occurrence, fire season length, and area burned, is increasing across many regions worldwide (Flannigan et al., 2009). This is of particular concern in boreal forests due to the large carbon reserves contained within these high-latitude ecosystems (Bradshaw & Warkentin, 2015; Pan et al., 2011). While wildfires have played an integral role in shaping and maintaining ecosystem dynamics across boreal regions for thousands of years (Hoecker & Turner, 2022; Kasischke et al., 2010), deviations in established fire regimes may translate to cascading effects on ecosystem processes. Current dominant species assemblages are not necessarily well-adapted to maintain dominance with more frequent and severe fire activity, thus making large-scale shifts in dominant vegetation type possible (Hoy et al., 2016; Johnstone et al., 2016). Such shifts have already been observed at small scales (J. F. Johnstone & Chapin, 2006; Viglas et al., 2013) but there is potential to alter regional vegetation composition (Mekonnen et al., 2019) and carbon pools and fluxes, potentially switching boreal forests from net carbon storers to emitters (Kurz et al., 2008; Turetsky et al., 2011; Walker et al., 2019). Understanding how patterns in fire activity interact with changing vegetation dynamics under continued climate change in boreal forest ecosystems is of great interest.

In North America, fire plays a central role in vegetation community assembly, both responding to and driving changes in fuel type. North American boreal forests are dominated by flammable and fire-intolerant conifers and fires are typically stand-

replacing every 70-130 years with high overstory mortality (>90%) (Johnstone et al., 2010; Van Cleve and Viereck 1981). Fire severity, in terms of the total consumption of carbon (inclusive of the soil organic layer), can be more variable (Boby et al., 2010). Around 10300-8250 years BP, the climate was warmer and drier and favored species as the dominant vegetation type (Higuera et al., 2009; Hu et al., 2006). Under these conditions, fires were relatively infrequent (>300-year fire return interval; Hu et al., 2006). However, after ~5500 years BP, the climate became cooler and wetter, and the dominant vegetation type shifted to white and black spruce (Higuera et al., 2009). Despite there being a cooler, wetter climate, the greater flammability of spruce, in particular black spruce, is thought to have driven an increase in wildfire frequency (Higuera et al., 2009; Hu et al., 2006; Kelly et al., 2013). In this way, shifts in climate can spur vegetation change and shifts in vegetation can also override climate influence on fire regime.

Under the current pressure of increasing global temperatures, boreal forest fire regimes are again undergoing significant change. In interior Alaska annual area burned in the 2000s was 50% higher than any prior decade (going back to 1940; Kasischke et al., 2010) and has been increasing more rapidly in areas defined as suppression zones in the 1980s, when the U.S. Forest Service institution instituted a fire suppression policy (Calef et al., 2015). Large-scale projections of future fire behavior support the idea that increases in annual area burned, fire size, and lightning ignitions are expected to continue in North American boreal forests with climate change (Bachelet et al., 2005; Hessilt et al., 2022; Mann et al., 2012; Wang et al., 2020). With greater overall wildfire frequency and more frequent large fire years, areas of forest are reburning within the typical 100-200 years recovery period that forests in the region have experienced for the past 5000-

6000 years. The greater presence of younger stands across the landscape due to reburning is thought to exert a negative feedback on fire spread due to their lower fuel levels, at least for a short period (Héon et al., 2014). Buma et al. (2022) quantified short-term negative feedback on short-interval fires (those areas which experienced > on fire < 20 years apart), which declined with time since the fire and the negative feedback disappeared after 20 years postfire. Similarly, should projected changes in vegetation communities occur as a result of greater fire activity, transforming the dominant vegetation type to broadleaf deciduous species, it is thought that a negative feedback to wildfire spread may be expected due to the lower flammability of broadleaf deciduous forest communities. This fuel-driven influence on broad-scale fire regime in boreal forests has occurred in the past periods prior to the modern establishment of conifer forest dominance in boreal western North America (ca. 10,300–8,250 years BP). During this time, deciduous species were the dominant vegetation type at a landscape scale and fire activity was relatively lower (Higuera et al., 2009).

Some process modeling efforts have sought to capture these complex feedbacks between vegetation, climate, and wildfires in North American boreal forests, but with conflicting results and differences of scale. While some recent work has captured fire in mechanistic ways that capture climate change influence and differences in flammability between fuel types (Foster et al., 2022), capturing a high level of detail in modeling the process of wildfire was done at the cost of interactivity. A study by Foster et al. (2022) lacked spatial propagation of wildfire, and so could not describe the extent to which feedbacks drove patterns of wildfire at larger scales. Larger scale models, in contrast, have captured enormous extents (i.e., the entirety of interior AK), but modeled the

process of fire at coarser spatial (1 km) and temporal (monthly- annual) resolutions (Bachelet et al., 2005; Mann et al., 2012; Mekonnen et al., 2019). This study attempts to strike a balance between these two ends of the modeling spectrum, by simulating daily dynamic wildfire (which interacts with weather, fuel, and topography) across a 380,400-hectare landscape with a 0.2 x 0.2 km resolution in interior Alaska, while doing so in a spatially-explicit and interactive manner to answer the following questions:

1. How may projected climate change affect the fire regime of a large landscape in interior Alaska?
2. To what extent do bottom-up drivers of fire, vegetation type and stand age, impact subsequent wildfire occurrence under climate change?
3. Will projected changes in climate affect the contexts in which wildfires occur in interior Alaska?

Materials and Methods

Study Area

The modeling domain for this study consists of a 380,400-hectare landscape in interior Alaska. The specific area was chosen to encompass field sites where reference data for validating the performance of the DGS extension (Figure 1). The total area of the domain is ~ 4 times the area of the largest recorded fire size in eastern interior Alaska, so it was thought to be appropriate for capturing potential changes in future fire regime characteristics. The elevation within the domain ranges from 93 - 950 m, with a mean elevation of 331.4 m (SD = 140.01 m). It is situated within the intermontane basin and plateau region of Alaska, which lies between the Alaska and Brooks mountain ranges; it

features rolling hills intersected with river valleys (Begét et al., 2006). The region falls within the discontinuous permafrost zone, and cool and wet lowland areas as well as north facing slopes are often underlain with permafrost Stralberg et al., 2020). Within the study area, the mean slope is 6.28 degrees (SD = 5.01 degrees) and ranges up to 36.13 degrees. Between 1992 and 2015, the study area experienced 1.05 wildfires per year (SD=1.12) with an average fire size of 3,794.53 hectares (SD=9,872.60 ha) and a fire rotation of 119 years (Karen Short). Wildfires in interior Alaska are typically large, stand-replacing events, and historically, forests experienced wildfires with a return interval of 50-100 years (L. A. Viereck, 1983).

LANDIS-II Model

I used LANDIS-II (v. 7), an open-source spatially explicit forest landscape simulation model (R. M. Scheller et al., 2007). LANDIS-II is modular, with a variety of extensions available to represent ecosystem processes such as forest growth as well as disturbances such as wildfire (https://www.landis-ii.org/extensions), which offers flexibility in the complexity that can be captured. Multiple extensions may be implemented with LANDIS-II simultaneously to simulate multiple processes. It operates on grid cells populated with species-age cohorts, and these cohorts may grow and compete with one another within a cell over time and based on species-specific attributes, which include longevity, reproductive ages, shade tolerance, seeding distances, and post-fire regeneration strategies (e.g., serotiny and resprouting). Individual cells may have multiple cohorts of each species, allowing for complex species age structures. The processes captured within LANDIS-II extensions are typically calibrated using historical

reference data, however, simulations have no single pathway once, executed, as processes such as regeneration (e.g. seed dispersal and resprouting) and disturbances (e.g., fire, wind, insects) are stochastic and interact spatially across the landscape.

Description of DGS Extension

I used the DAMM-GIPL-SHAW Succession (DGS) extension to LANDIS-II (https://github.com/LANDIS-II-Foundation/Extension-DGS-Succession; Lucash et al. *in prep*) to simulate plant growth, hydrological dynamics, and the soil temperature regime over time and under both historic and future climate scenarios. The DGS extension was designed specifically for use in the boreal regions, as it includes the below ground water and temperature dynamics unique to high latitude systems. DGS couples together the Simultaneous Heat and Water (SHAW) model and the Geophysical Institute Permafrost Laboratory (GIPL) heat flow model within the LANDIS-II framework. The SHAW model is a physically based model which simulates soil profiles and the vertical transfer of heat, water, and solutes down to 30m which is influenced by live and dead vegetation and snow. SHAW captures evapotranspiration, snow accumulation and ablation, and surface runoff and infiltration (Flerchinger, 2000). The GIPL model simulates ground temperature down to 75m and active layer thickness and receives water and ice content values from SHAW. GIPL calculates the solution to a nonlinear heat equation that was developed to simulate permafrost dynamics across a variety of contexts in Alaska (Marchenko et al., 2008; Nicolsky et al., 2017) and simulates phase changes. lower

Vegetation Inputs

To make a map of the initial tree, shrub, and moss species composition for the simulation landscape, U.S. Forest Service Forest Inventory and Analysis data (FIA) from the Tanana region surveys in interior Alaska (USDA-Forest Service 2019) were used in combination with the Alaska Center for Conservation Science Mosaic Landcover Map of Alaska (AKCCS, 2019). Six tree species, three shrub genera, and three moss functional types were initiated on the landscape (Appendix A). Following the methodology of Lucash et al., 2017, FIA plots were associated with cover types from a detailed landcover map (AKCCS, 2019), an elevation map (USGS, 2020a), and a climate region map (see below). Tree ages within FIA plots were estimated using site index curves (Carmean et al., 1989). Then, species-age cohort data from FIA plots were imputed within each cell on the landscape according to which plots most closely matched the cell's corresponding characteristics and stand age (estimated from a fire history dataset; FRAMES, 2016). When multiple FIA plots were a match, a random plot was selected from the pool of potential matches. The FIA database did not contain biomass information for shrub species but included percent cover by height class for each plot, so biomasses were inferred based on percent cover, height class, and associated stand ages. I developed linear models relating shrub biomasses at specific height classes and associated percent cover using Bonanza Creek LTER data archive datasets (Viereck et al., 2005, 2010) and allometric equations provided by Berner et al. (2015). The product was a map where age cohorts of each tree species, shrub species, and select moss function types and their relative biomasses were defined for each cell.

Biophysical Inputs

Maps of soil texture, soil depth, soil drainage class, field capacity, wilting point, and organic matter were created using the State Soil Geographic data available from USDA-NRCS for the state of Alaska at a 1:1,000,000 scale. A map of dead coarse root biomass was created using published relationships between dead coarse roots and live belowground biomass data provided in the FIA-Tanana dataset (USDA-Forest Service, 2018). A map of woody debris was created using the downed wood table in the FIA-Tanana dataset and linking it to the corresponding imputed FIA plot for each cell.

Climate Inputs

Daily weather inputs were needed to provide necessary climatological information for the succession and fire extensions of LANDIS-II. Climate data from two GCMs were used to create historical (1970-2000, NCAR-CCSM4 only) and RCP 8.5 future (2000-2100, GFDL-CM3 and NCAR-CCSM4) climate streams. The source dataset was downloaded from the Scenarios in Arctic Planning Group (SNAP) and had been dynamically downscaled at a 20 km resolution (Bieniek et al., 2016; Lader et al., 2017). Relative to other CMIP5 GCMs, NCAR-CCSM4 and GFDL-CM3 GCMs exhibit patterns that are close to the average across models (NCAR CCSM4) as well as the high end of both temperature and precipitation out of CMIP5 models (GFDL-CM3; Marshall et al. 2021, Figure S2; Figure 2). While finer-scale downscaled climate data are available for Alaska, this source both included all required variables at a daily temporal resolution to run the fire extension.

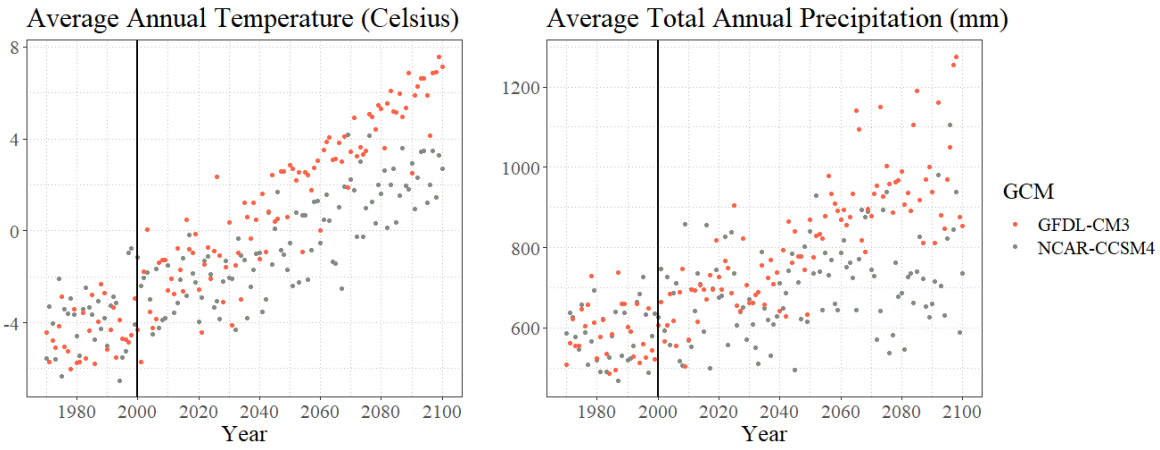

Figure 2. Climate data from two GCMs used in simulations. The vertical line indicates the division between historical scenario data (1970-1999) and future scenario data (2000-2100).

LANDIS-II uses 'climate regions', which group areas on the landscape which have similar climates to one another and provide the same climate stream to all cells within a given region. This is more computationally efficient than using gridded climate data. Following the methodology of Lucash et al., 2019, a k-means cluster analysis of climate normal was done to identify areas of similar climate. Average monthly projected precipitation and temperature from 2000-2100 (PRISM Climate Group: Oregon State University, 2021) was used with the package 'cluster' in R (Maechler et al., 2021) to inform the aggregation of cells into noncontiguous climate regions. Temperature inversions often form in valley bottoms in interior Alaska, making these areas common refugias for permafrost (Jorgenson et al., 2010). To allow for this phenomenon to be captured within the model and capture greater climatic variation due to winter temperature inversions, I ran an additional cluster analysis for each region, grouping each into two subregions (warmer and cooler) based on mean winter temperature from 30-year normals from PRISM. Altogether, this process resulted in ten climate regions.

The climate data had not been bias-corrected to ensure that the climate outputs are relatively more consistent with historical observations; therefore, I used a quantile mapping approach using the qmap package in R (Gudmundsson & Gudmundsson, 2012) with ERA-Interim reanalysis data (downscaled and provided by the same SNAP data source) to bias correct each variable for each climate region on the landscape. Values were then extracted from each climate region for all climate variables at the cell center of the cell with data residing closest to the center of each k-means cluster. Lastly, precipitation was further adjusted to limit the effect of spatial aggregation which creates days where there are exceptionally small amounts of precipitation: days where precipitation fell below one mm, were set to zero and the aggregate precipitation lost due to this correction was proportionally distributed across days where precipitation fell above 1 mm.

Description and Parameterization of SCRPPLE Extension

I modeled fire dynamically using the SCRPPLE fire extension (v. 3.2; R. Scheller et al., 2019). This extension allows for fire behavior to respond to climatic variables (e.g., fire weather index, wind velocity) and changes in fuel loading throughout the simulation period. Fire ignition probability is based on a (zero-inflated) Poisson model (Zuur et al., 2009) of historic daily ignitions and fire weather index (FWI), which were fit using records of historic ignitions specific to the region (Short, 2021; Appendix B) and corresponding daily fire weather derived from met station data. Fire spreads from cell-to-cell based on a probability function of daily fire spread, which calculates spread success based on the FWI, effective wind speed, and fine fuels (Scheller et al., 2019; Appendix

B). Parameters within this function were fit using historic daily fire perimeter data (GeoMAC 2019, GeoMAC 2020), met station data (Menne et al., 2012), topographic data (USGS, 2020a), and fine fuels data(USGS, 2020b). Each fire may spread until the maximum daily spread area is reached (Scheller et al., 2019). This area is calculated for a given day based on a generalized linear model of historic daily fire areas versus FWI and effective wind speed. The mortality from fires is driven by two functions, one determining the site-level mortality and one the cohort-level mortality. Site-level mortality is determined by an inverse link function of the percentage of clay in the soil, evapotranspiration in the year prior, effective wind speed during the fire, climatic water deficit the year prior, and fine fuels present during the fire. Cohort-level mortality is then determined by a combination of the site level severity value, cohort age, and individual species' bark thicknesses. More information on the SCRPPLE fire extension v. 3.2 may be found on GitHub (https://github.com/LANDIS-II-Foundation/Extension-SCRPPLE).

Simulations

I ran a total of 30 simulations; 10 were replicates of the historic climate data stream, which served as the reference historic climate forcing scenario in the analysis. Ten replicates each of NCAR-CCSM4 (hereafter 'NCAR') and GFDL-CM3 (hereafter 'GFDL') RCP 8.5 scenarios were run to represent potential future conditions. Here, GFDL is interpreted as the more extreme (highest temperature and precipitation values by end of the century) of the two future scenarios (Figure 2). Simulations were run for 100 years, with historic scenarios randomly sampling one year of data from the 30 available

years in the stream annually. RCP 8.5 scenarios used sequenced climate data. All simulations were run on the CyVerse computing cluster (cyverse.org).

Analysis

Fire regimes across the three climate scenarios were characterized based on the number of fires per year, annual area burned, fire size distribution, and fire rotation. These statistics were calculated for each replicate and the distributions of these characteristics were compared between scenarios using Wilcoxon rank sum test statistics, chosen because fire size and annual area burned data did not fit a normal distribution.

I compared spread probability between scenarios and examined differences based on vegetation type, stand age, and burn history (previous fire(s)). Four vegetation types were used in the analysis based on relative tree species dominance: conifer dominant, mixed broadleaf deciduous-conifer dominant, broadleaf deciduous dominant, and non-forest. Cells were classified as broadleaf deciduous dominant if the percentage of total tree biomasses of paper birch, quaking aspen, and balsam poplar together exceeded 66.66%; mixed conifer-broadleaf deciduous if the percentage of those same species out of the total were in between 33.33% and 66.66%, and conifer dominant if broadleaf tree species percentage was less than 33.33%. If tree biomass for a given cell was equal to zero, that cell was classified as non-forest. These dominance categories are similar to those adopted by Mack et al. (2021), though do not include any relative tree species density information because individual stems are not tracked within the LANDIS-II model framework.

To compare the relationship between fire and stand age, I also examined patterns in stand age over time and compared landscape stand age to the stand ages of cells in the year before their burning (i.e., pre-fire stand age). Stand age was defined by the age of the oldest cohort in each cell. Landscape stand age was calculated by averaging the calculated stand age for all cells in each year and each replicate.

To better understand which cells were tending to burn and reburn, I analyzed data from cells the year before they burned in the simulation, extracting both the pre-fire vegetation type and stand age. The percentage of burned or reburned area that had been classified as each vegetation type was then calculated, and the average stand age in the year before the fire. Overall differences in stand age and percentage vegetation type were compared between scenarios using Wilcoxon rank sum test statistics as well as plotted by simulation year to examine temporal trends.

The annual reburn rate was calculated for each replicate by isolating cells at each time step that burned and which had already burned in a previous time step. This number of cells was then divided by the total number of cells to give a percentage of the landscape that experienced a reburn. These percentages were plotted over time and examined differences in temporal trends between scenarios.

Results

There was no significant difference in the average number of fires per year between the historical scenario and both climate change scenarios (GFDL and NCAR; Figure 3), however, exceptionally large fires happened with greater frequency under climate change (Figure 4). The largest fire years occurred in the latter half of the century

across all/most replications (Figure 5). The historical scenario had greater numbers of 'no fire' years or years where there was no fire activity, whereas, under climate change, there were more years with back-to-back fires on the landscape. Average fire size was larger under climate change as well ($p < 0.05$), however, the overall magnitude in mean differences in fire size was relatively small, so this difference was largely driven by a large number of outlier (exceptionally large) fires present under climate change. The annual area burned was larger and fire rotation was shorter under climate change (Figure 6, 7), further illustrating the outcome of a greater frequency of large fires.

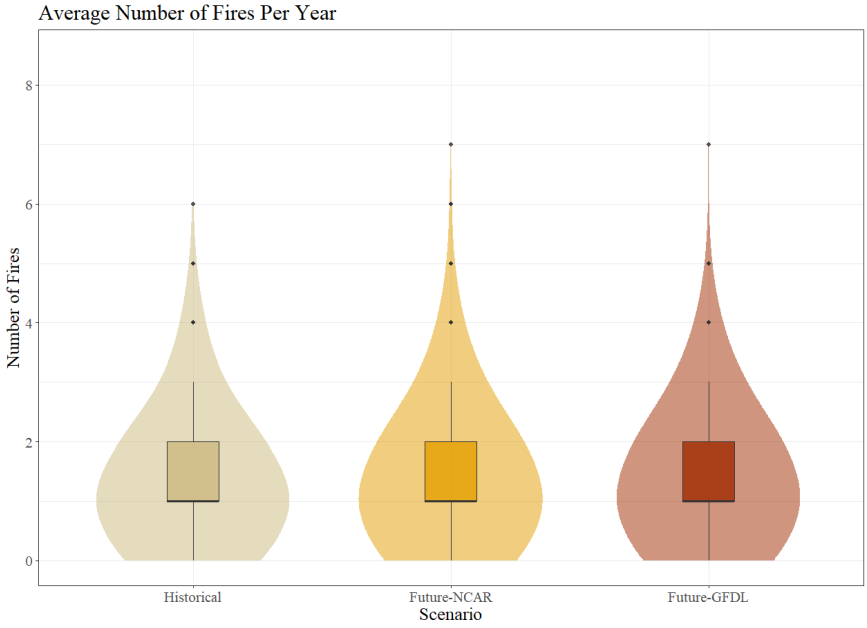

Figure 3. Boxplots of average number of fires per year experienced across the landscape across all ten simulation replicates for each scenario.

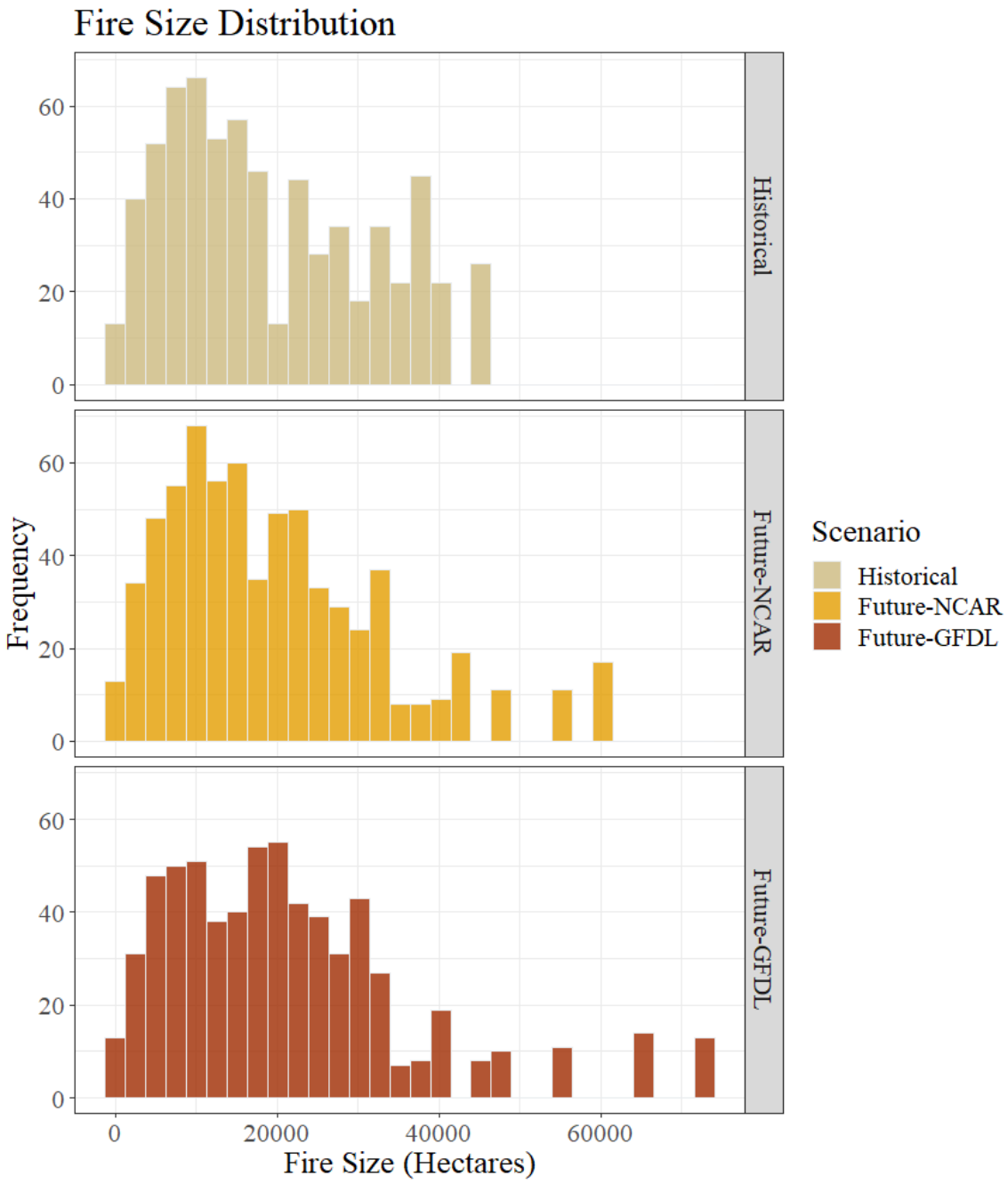

Figure 4. Fire size frequency distributions (hectares) across all ten simulation replicates for each scenario.

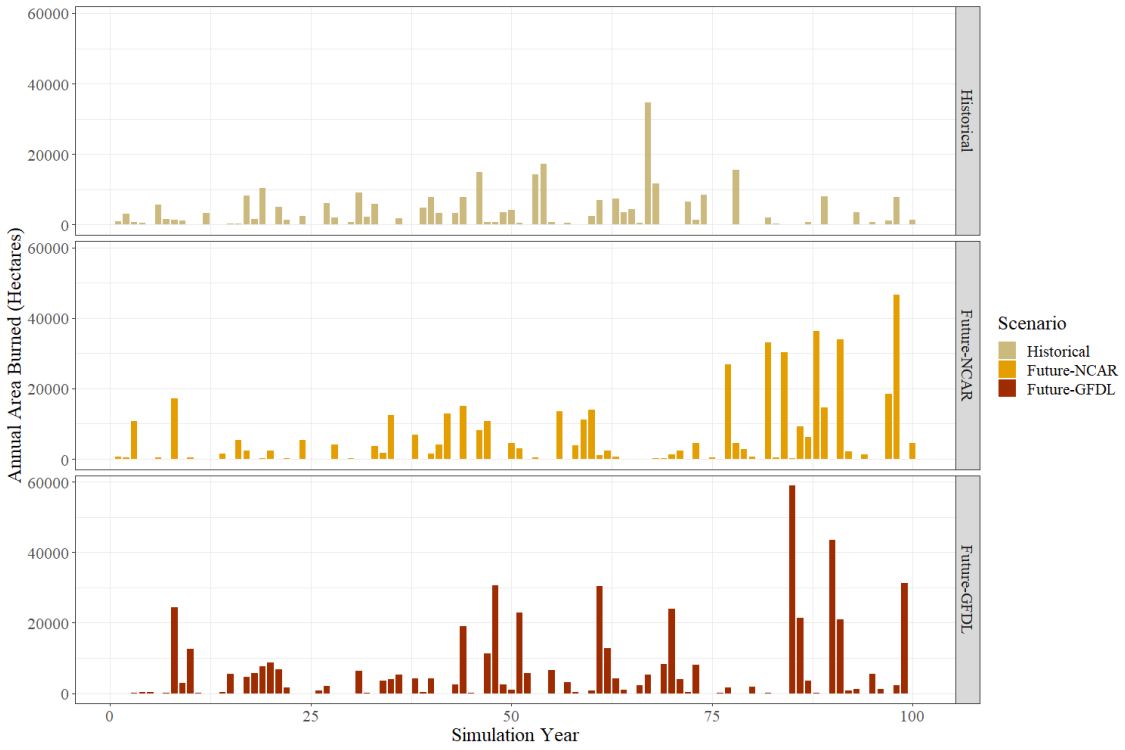

Figure 5. Annual area burned (hectares) by simulation year of one replicate from each scenario. One replicate was used for plotting to illustrate temporal patterns in annual area burned over time.

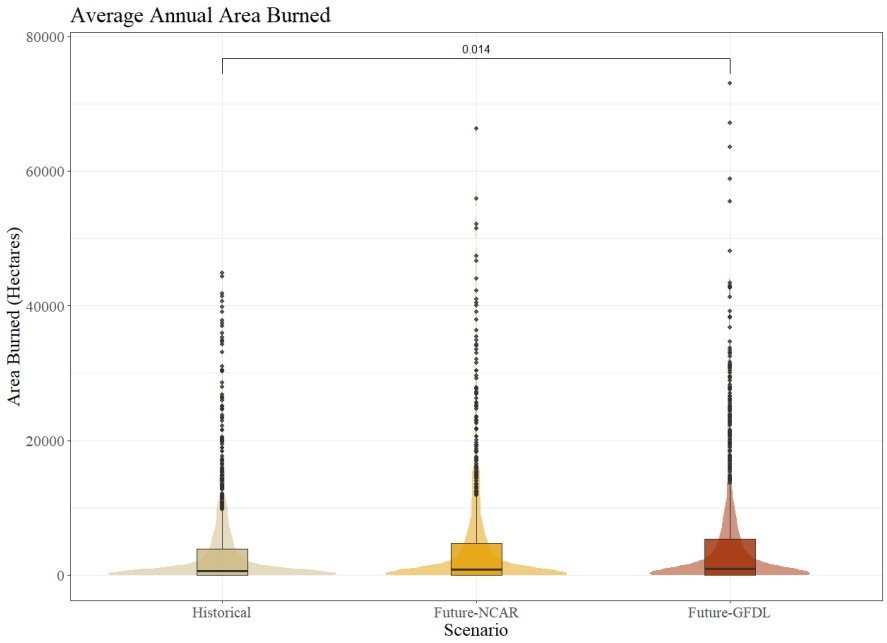

Figure 6. Boxplot of average annual area burned (hectares across all replicates for each scenario.

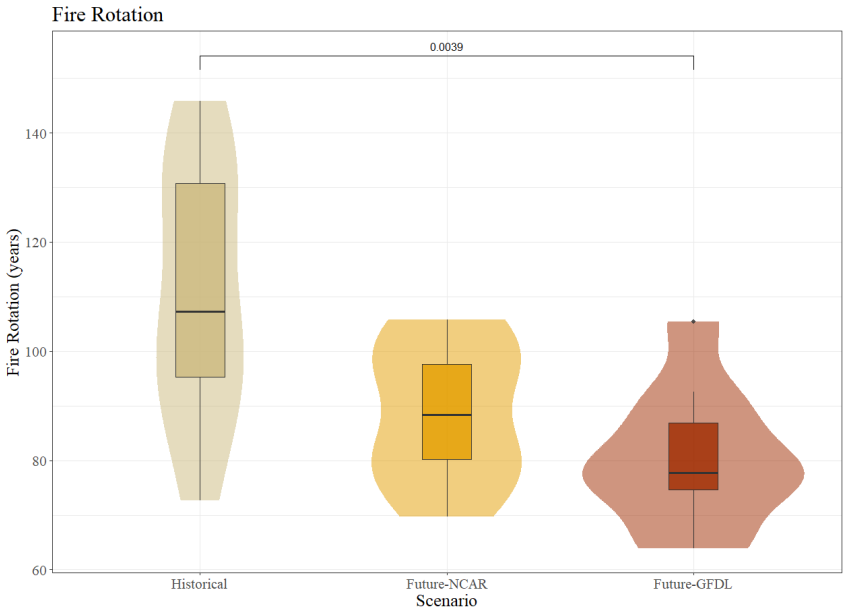

Figure 7. Distribution of fire rotation across all replicates between scenarios. P-value shown is the result of a Wilcoxon rank sum test statistic.

Changes to the annual burned area and frequency of large fire years prompt questions of what factors play the greatest role in influencing fire spread. Average spread probability across the landscape held relatively static through time and was similar across vegetation types (Fig 8). However, cells that burned under climate change exhibited slightly higher spread probabilities than under historic climate. I examined patterns in stand age within cells before burning and across the landscape as a whole and found that overall stand age increased throughout the simulation. Compared to the landscape average stand age, fires tended to burn cells that were greater in age than the overall landscape average under all scenarios, but there was an interaction with climate forcing; the most extreme climate scenario (Future-GFDL) tended to burn cells that were relatively younger than under historic climate forcing (Fig 9).

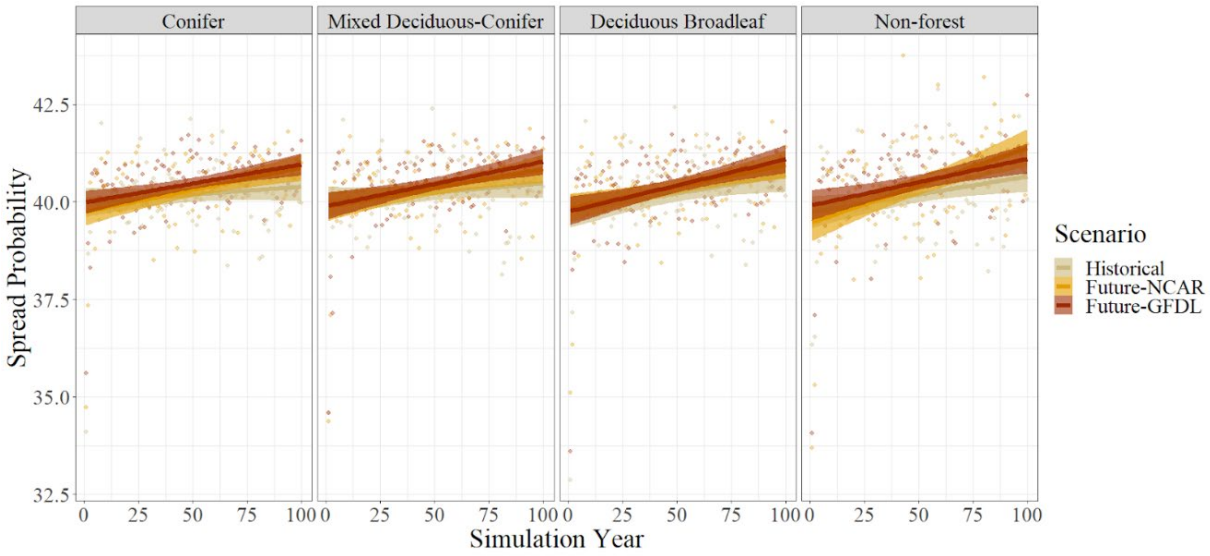

Figure 8. Average spread probability calculated from SCRPPLE spread probability output maps. Vegetation types represent the dominant vegetation type present in the year before a fire. Bands represent 95% confidence intervals.

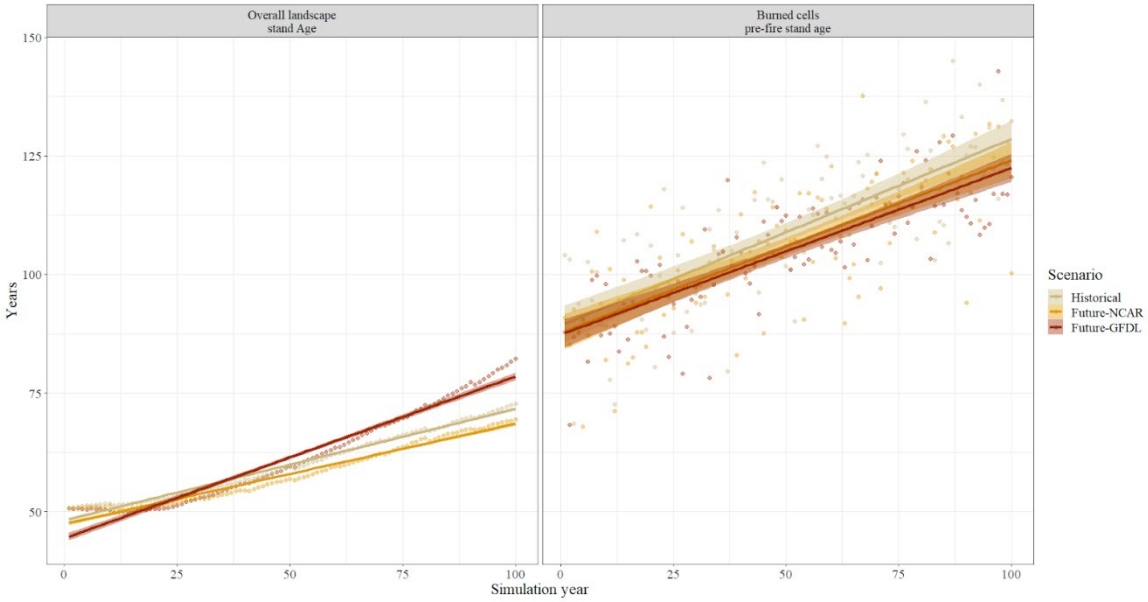

Figure 9. Average stand age over time for the overall landscape (left) and the stand age of cells one year before they burned (right) for each scenario with bands representing 95% confidence intervals.

There were also differences in the vegetation types that tended to burn and their relative frequency of being burned was different with different climate forcing. The highest percentages of area burned across scenarios were in conifer vegetation (Fig 10),

however, this percentage declined throughout the simulation and became lowest under climate change (Figure 11). Conversely, deciduous broadleaf vegetation type accounted for a greater proportion of the area burned over time and was greatest under climate change (Figure 11). It is possible, however, that these trends are at least in part reflective of the overall relative proportions of these vegetation types on the landscape.

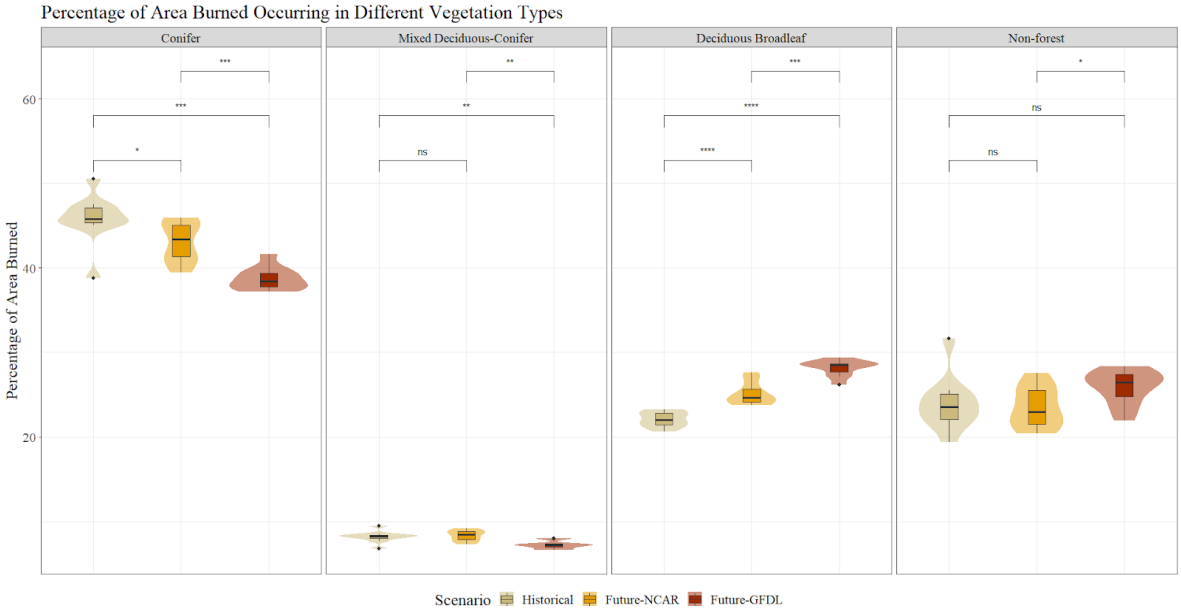

Figure 10. Boxplots of percent area burned within four vegetation type groups across all replicates and compared between scenarios. Significance was evaluated using Wilcoxon rank sum pairwise tests at a 0.05 significance level.

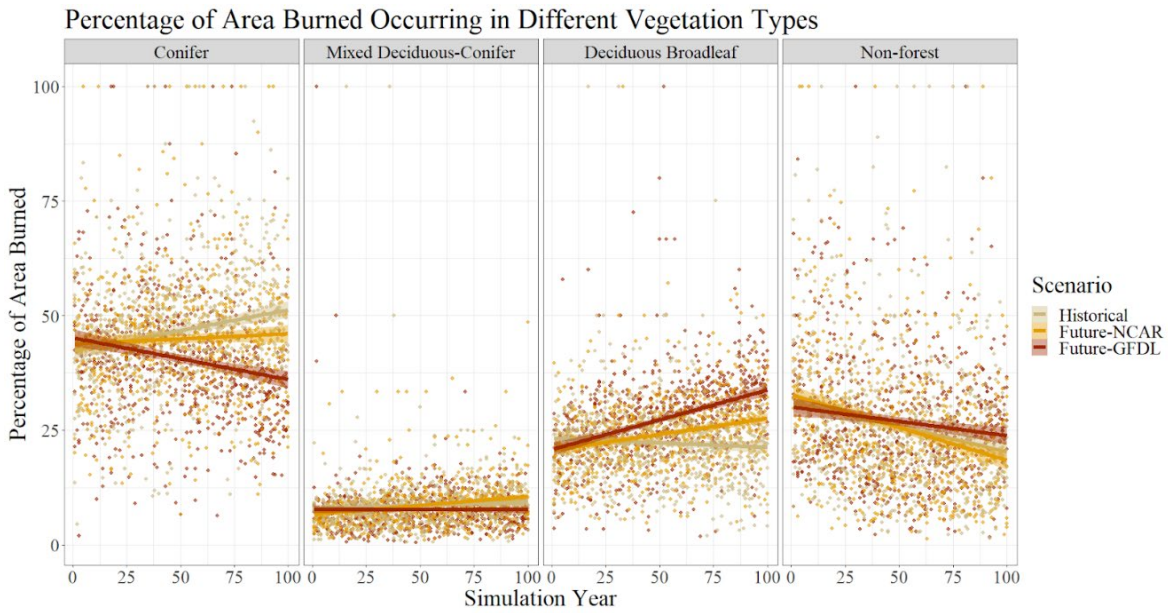

Figure 11. Trends in the percentage of area burned within different vegetation types over time. Trend lines represent a linear model fit to each climate scenario over time and ribbons represent 95% confidence intervals.

All three scenarios saw increases in reburn rates throughout the simulation period (Figure 12), which was calculated here as the percentage of the landscape at each timestep that had experienced two or more fires. Given, this, an increase in reburn rate was expected in the later years of the simulation as the opportunity for fire overlap increases over time. While reburn rates increased in all three scenarios, the slope of these rates diverged through time. Under the most extreme climate change scenario, annual reburn rates increased the most rapidly over time and were greatest by the end of the simulation period. The variation in the reburning rate from year to year also increased with time. In the final decade of the simulation, the reburn rate ranged from approximately 0.1% to over 2%.

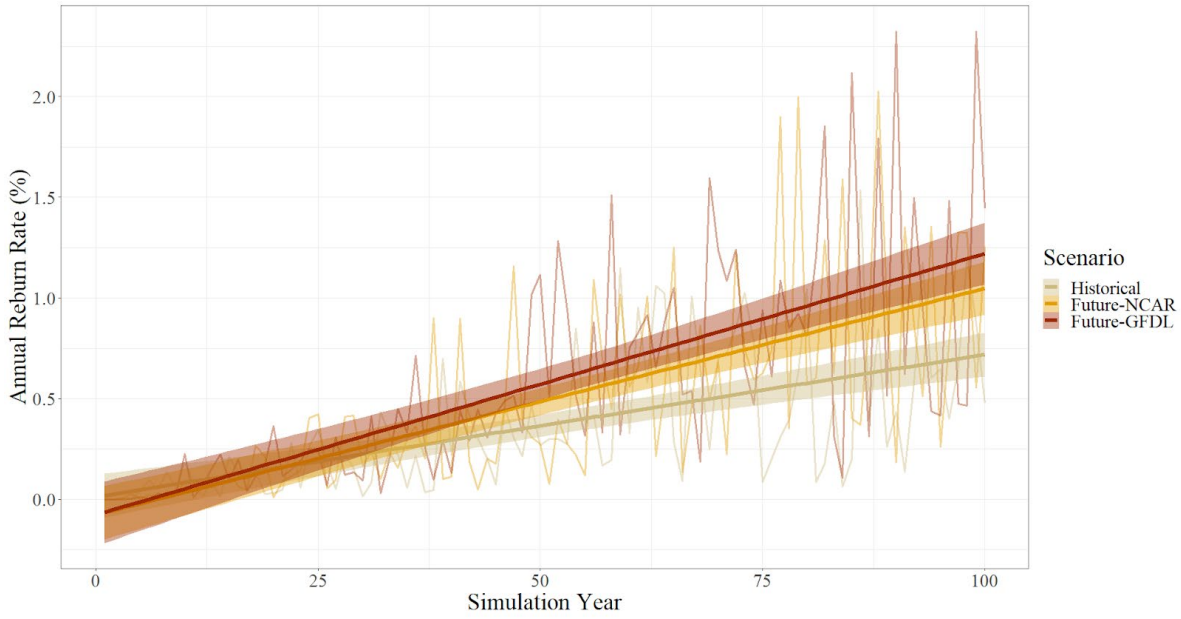

Figure 12. Annual reburn rate across the landscape over the simulation period averaged across all replicates for each scenario. Trend lines represent a linear model fit to each climate scenario over time and ribbons represent 95% confidence intervals.

Short-interval fire trends were evaluated at two thresholds; those areas that burned with less than 10 years since the last fire, and those that burned with 11-20 years since the last fire. Neither threshold showed increasing trends in short-interval fires, with the relative proportions of the burned area experiencing a short interval fire staying relatively consistent, and even modestly declining over the course of the simulation period (Figure 13). Under the climate change scenarios, short-interval proportion was consistently higher than the historical scenario.

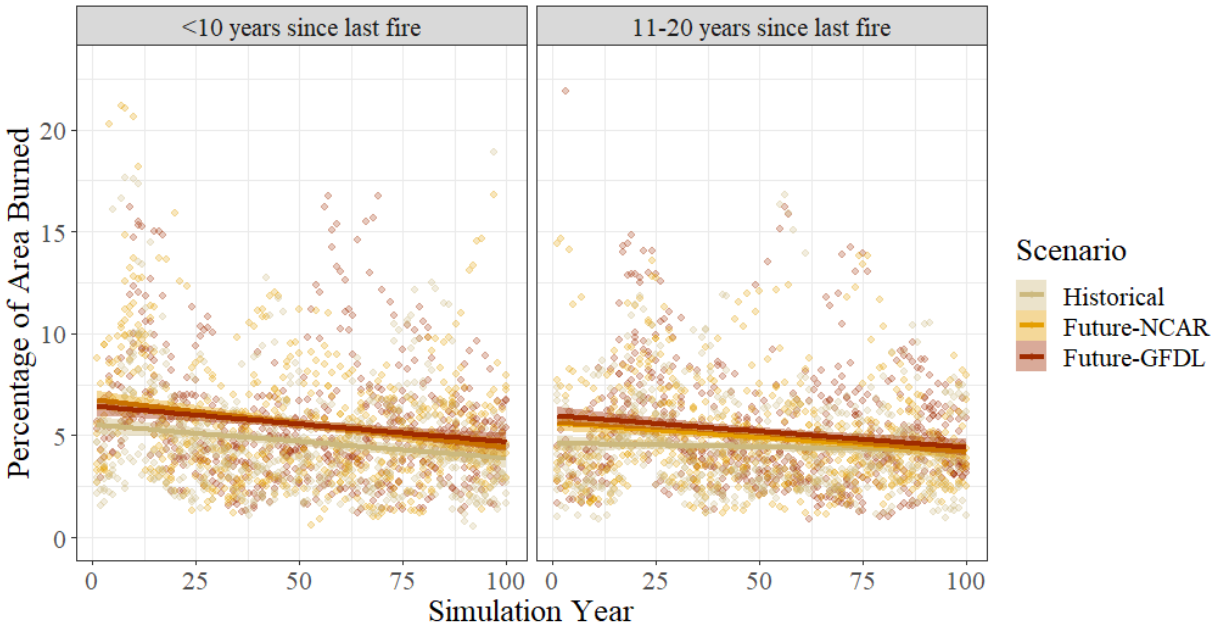

Figure 13. Proportions of short-interval burned area relative to total burned area at each timestep across all ten replicates, evaluated at two short-interval fire thresholds: < 10 years since last fire and 11-20 years since last fire.

There were differences in vegetation types that reburned as well. Different from the general burn patterns across all fire frequencies, conifer was not the most prevalent pre-fire vegetation type for reburns; proportions of reburned area were shared more evenly by conifer, deciduous broadleaf, and non-forest vegetation types (Figure 14). The conifer vegetation type accounted for less of the reburned area under climate change while deciduous broadleaf vegetation and non-forest vegetation accounted for more. There were also temporal patterns to which vegetation types experienced reburning and these patterns differed by climate forcing (Figure 15). The percentage of reburns in both conifer and deciduous broadleaf forests increased over the simulation period, however, the more extreme climate change scenario yielded a less rapid increase in conifer reburn percentage compared to the increases in deciduous broadleaf reburn frequency. Non-forest reburned area declined over time across all climate scenarios. Surprisingly, mixed

broadleaf deciduous-conifer accounted for the least amount of reburned area and this remained consistent over time.

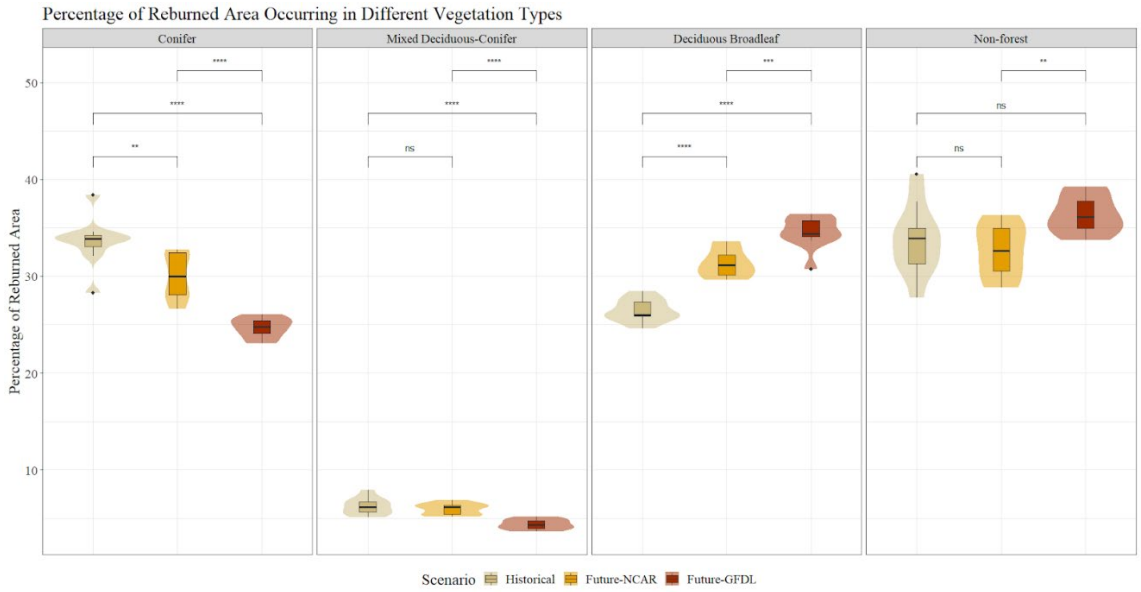

Figure 14. Boxplots of the percentage of area that reburned within different vegetation types averaged across replicates for each scenario and vegetation group. Significance was evaluated using Wilcoxon rank sum pairwise tests at the 0.05 level.

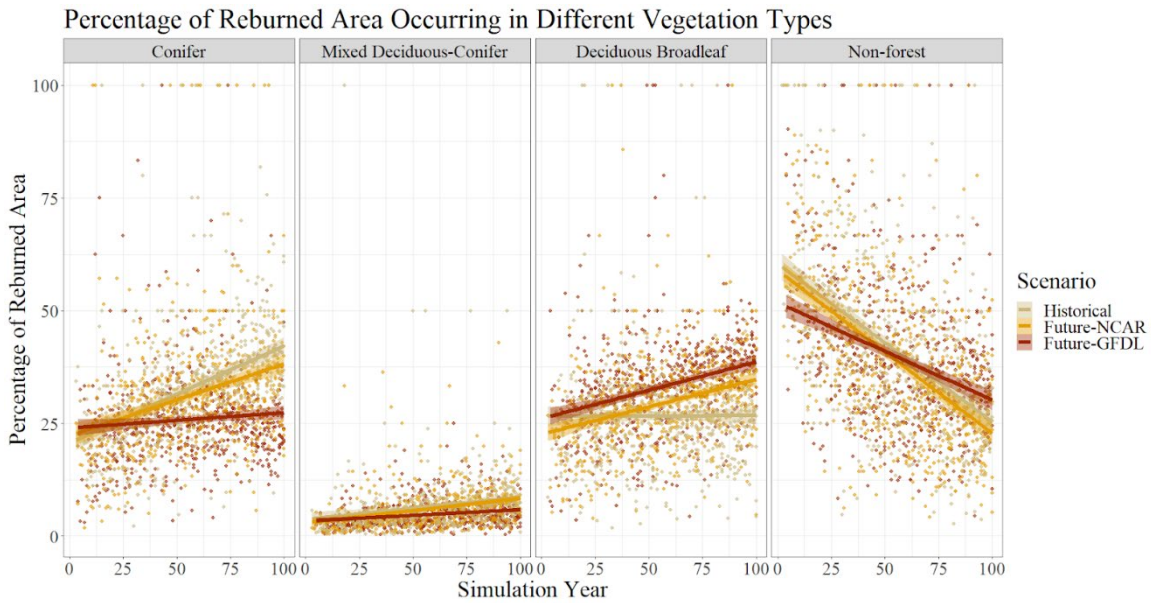

Figure 15. Percentage of the area that reburned within each vegetation type at each time step for all replicates within each scenario. Trend lines represent a linear model fit the data with ribbons delineating 95% confidence intervals.

Discussion

I found that climate change scenarios resulted in greater annual area burned and larger average fire size. This continues observed trends from recent decades in Alaska, where the region has seen increases in annual area burned that are 50% higher than in decades before the 2000s (Kasischke et al., 2010). Consistent with these results, climate-driven increases in North American boreal fire behavior across a variety of metrics have been projected to continue under numerous empirical and process modeling frameworks (Bachelet et al., 2005; Balshi et al., 2009; Hessilt et al., 2022; Mann et al., 2012; Wang et al., 2020) and this study further supports this.

While climate-driven changes in fire regimes have paleoecological precedent, shifts in dominant vegetation type have also been known to override climate drivers when a new vegetation regime is less flammable (Higuera et al., 2009). While fires tended to occur more in cells with older stand ages, pointing to more fuel-driven fire behavior, these simulations lend contrary support to a strong and persistent negative vegetation feedback, and instead, over time, fires increasingly began burning younger vegetation under climate change. Within this the parameterization of SCRPPLE for this study, the probability of spread is influenced by both fine fuel loads and FWI (Appendix B), both of which appear to be at play here, where fuels greater fuels in older stands tend to increase their probability of burning, but more extreme fire weather can increase the probability of younger stands burning under the climate change scenarios.

Reburned areas were also distributed more evenly across vegetation types rather than occurring predominantly within the conifer forest type as they do in single-burned locations. In simulations, large fire events continued to be common even toward the end

of simulations, despite the accumulation of previously burned areas over time. Mann et al. (2012) also found a shift in dominant vegetation type was not a strong enough negative feedback to limit future fire activity due to climate change influence, and consistent with these results, found that annual area burned increased despite vegetation change. Wang et al. (2020) modeled continued increases in annual area burned as well, and attribute this to the continued potential for fire-conducive weather conditions under climate change that support sustained high fire potential.

Overall reburning rates and the proportion of short-interval burned area under climate change simulations surpassed those simulated with a historical climate, further supporting the idea that climate drivers are strong enough to at least modestly override negative vegetation feedbacks. Rather than fire behavior (i.e. fire size, annual area burned) increasing linearly, however, a greater frequency in exceptionally large fire years was observed; this is a trend that has been observed in past studies as well; Wang et al. (2020) project that the potential for extreme fire years will increase by over four-fold by the end of the century across Canada. Whitman et al. (2022) also document an increase in specifically large wildfires (> 200 ha) in Alberta, CA. This increase in fire size variability rather than only the mean fire size points to a complex interplay between top-down and bottom-up drivers that are impacted by context, location, and scale. Héon et al. (2014) found that fuel age overall exerts a negative feedback to higher burn rates, however, they also note that extreme weather conditions have pushed the ecosystems in boreal Canada to sustain higher than expected burn rates. Additionally, paleo fire records show evidence that biomass burning increased during warm periods throughout the Holocene, even during periods of substantial vegetation change, demonstrating strong past climate

controls on fire (Hoecker & Turner, 2022). Buma et al. (2022) found that while boreal forests in interior Alaska are resistant to reburning within the first decade following a fire, this fuel-driven resistance to reburning declines with time (between 10-20 years), thus allowing additional fires to reburn areas after a couple of decades recovery time and giving way to climate drivers. Within the modeling domain this study, reburns were able to occur at short intervals as well and remained a consistent proportion of the total burned area each year throughout each scenario, so while they had a decreasing trend, potentially indicating a negative fuel feedback, their occurrence was elevated under climate change, indicating that a reduction in fuels in these areas was not entirely limiting.

Interestingly, there was not a significant increase in the overall number of ignitions. This study's modeling framework models ignition probability as a function of the fire weather index and uses records of historic ignitions and met station data to fit internal algorithms governing SCRPPLE. Recent work has suggested that lightning ignition frequency (i.e., the likelihood that a lightning ignition will start a fire) will increase with warming due to greater drying of fuels allowing for more successful ignitions (Hessilt et al., 2022). While there was not as strong of an effect on ignitions in the simulations, the coupling between fire weather index and specific ignition locations used to estimate this parameter was coarse due to the low availability of weather station data in the region, so it is possible that the strength of the relationship between fire weather index and ignition probability was underestimated, muting stronger emergent increases.

This study had a few limitations that are important to consider when interpreting the results. The parameterization of SCRPPLE relies heavily on empirical data on past

fires and associated weather and fuel variables, making it a valuable tool for realistically replicating the real-world relationships between these feedbacks within the model. However, these parameterizations are then limited by data quality and the availability of data necessary to fit them. In interior Alaska, options for fire and weather station data are limited, and so the behavior of SCRPPLE on this landscape will be limited by the constraints of available data. SCRPPLE also requires daily climate projections from GCMs for its weather inputs, which in Alaska, strongly limits the options and quantity of GCM data to use. For this reason, this study was only able to capture two GCMs representing one RCP scenario (8.5). Lastly, flammability within SCRPPLE is represented in the probability of spread from cell to cells, which is driven by FWI and fine fuel loads and does not distinguish between the specific geometries of leaf litter between species that could affect flammability at a finer scale. Some have argued that the higher moisture content and geometry of broadleaf deciduous tree litter make them less likely to carry fire, and so able to limit future fire activity should broad-scale shifts to broadleaf deciduous dominance occur (Chapin et al. 2010). However, this version of SCRPPLE (v. 3.2) is not able to capture this component of the fuel feedback, if present.

Overall, simulations captured not only increases in overall fire activity in the model but also consistent proportions of short-interval fires through time and relative increases in the rate of reburning under climate change projections. While stand age influenced where fires primarily took place across the landscape overall, the more extreme climate change stream burned relatively younger vegetation, indicating that increases in more fire-conducive weather in the region could counteract the strength of vegetation feedbacks in the future.

CHAPTER 3

DRIVERS OF VEGETATION STATE SHIFTS IN RESPONSE TO INCREASING FIRE FREQUENCY UNDER CLIMATE CHANGE IN INTERIOR ALASKA

Introduction

In interior Alaska, there is growing concern that black spruce (*Picea mariana*) forest communities will undergo a state shift from spruce- to broadleaf deciduous-dominance due to climate-driven changes in fire regime. Such a shift has global implications due to the large carbon sink contained within boreal Alaska forest ecosystems and whether a state shift would reduce carbon sink strength (Berner et al., 2011). Black spruce has been the dominant forest type in interior Alaska for the past 5,000-6,000 years (Higuera et al., 2009; Lynch et al., 2002) and several mechanisms have helped maintain its long-term dominance. The serotinous cones of black spruce allow for prolific seed dispersal and rapid regeneration post-fire (Zasada et al., 1992). In mature black spruce stands, thick soil organic layers often develop due to slow decomposition and slow nutrient turnover that are promoted by and help maintain moist, cool soils (Johnstone et al., 2016). Post-fire residual organic matter can inhibit seedling establishment for most tree species in the region, however, the relatively larger size of black spruce seeds allows them to regenerate with greater success on poorer quality seedbeds (Greene et al., 2007; Johnstone, Chapin, et al., 2010; Johnstone & Chapin, 2006a). The shallow rooting depths of black spruce also allow it to grow on top of permafrost while most other species in the region cannot (Van Cleve et al., 1983). These competitive advantages allow for early establishment at the exclusion of would-be

competitors and continued dominance as stands mature. Successional trajectories in black spruce communities are typically self-replacing following disturbance for these reasons (Fastie & Ott, 2006; Johnstone et al., 2020; Kurkowski et al., 2008).

Fires recurring every 70-130 years (Johnstone et al., 2010) have allowed black spruce to retain competitive advantages over other species. However, feedbacks between fire and climate change are altering dynamics such that those advantages may no longer operate as effectively. In recent decades, annual area burned, fire season length, and fire severity has increased while fire return intervals have decreased and these changes in Alaska's fire regime are projected to continue (Flannigan et al., 2009; Kasischke et al., 2010). Wildfire events in black spruce forests, while stand-replacing, are typically characterized as low severity concerning the depth of soil consumption (Johnstone et al., 2010). High-severity fires have been documented as promoting persistent shifts from black spruce to deciduous dominance via consumption of the soil organic layer (Johnstone et al., 2010; Johnstone & Chapin, 2006a; Shenoy et al., 2011). Declines in fire return interval similarly disrupt successional pathways in black spruce forests in several ways. First, multiple fires with less recovery time in between prevent the soil organic layer from building up between fires, such that when areas reburn, the soil organic layer is more readily consumed, exposing mineral soil much in the same way a single high severity fire might (Hayes & Buma, 2021; Johnstone et al., 2016; Shabaga et al., 2022). Second, a reduction in fire return interval reduces seed availability of black spruce for post-fire regeneration. Black spruce sexual maturity is ~30 years, and often does not maximize seed productivity until much later (e.g., >100 years; Viglas et al., 2013) so a reduction in fire return interval may prevent black spruce from reaching maturity in the

time between fires, preventing seed dispersal via aerial seedbanks post-reburn (Johnstone & Chapin, 2006b).

The size, shape, and distribution of wildfires within previously burned areas also has important implications for future stand composition. If a second fire occurs within a relatively young former black spruce stand and the distance to the burn perimeter exceeds the seeding distance, this limits opportunities for reestablishment within burn perimeters (Johnstone et al., 2016). As such, the size and shape of individual fires and where reburns occur within previous burn scars are also likely influential to future black spruce reproductive success within reburns. Additionally, while black spruce are semi-serotinous and burned mature stems act as a seed source within fire scars, nearby reserves of unburned trees are an important contributor to total viable seed rain, particularly when high severity fires compromise the aerial seed bank (Johnstone et al., 2009).

While much of the work in interior Alaska on vegetation compositional shifts has focused on overstory functional groups, understory components such as shrubs play an important role as well. Shrub expansion linked to warming temperatures at high latitudes has been well documented, specifically in tundra ecosystems and in response to the degradation of permafrost and subsequent mineralization of nutrients (Bret-Harte et al., 2002; Chapin et al., 1995). In boreal forest ecosystems, shrub growth has been noted as responding more positively to climate change than its overstory counterparts (Yang et al., 2020). However, other climatic and biotic factors interact with the direct effects of increasing annual temperatures (e.g., insect outbreaks; Boyd et al., 2019; Williams et al., 2011), making the direct effects of increasing annual temperatures on growth rates

difficult to disentangle. Nonetheless, climatic variables may influence interspecific dynamics between functional groups throughout succession.

Impacts from fire and climate change are not felt uniformly across the landscape and local site conditions can buffer climate and wildfire impacts. Past work has found site variables related to higher soil moisture tend to be associated with greater reproductive success and growth following a fire in black spruce forests. Less consumption of the soil organic layer and a lesser decline in black spruce regeneration has been observed following two short-interval fire events in wetter, lowland areas, compared to drier upland sites (Hayes & Buma, 2021). Patterns in annual primary productivity over time have been found to diverge between dry and mesic sites, increasing linearly on mesic sites over time, while peaking mid-succession before declining on drier sites where deciduous species and willow become dominant midway through in succession (Mack et al., 2008). These findings are consistent with those of Johnstone et al. (2010), who found that sites with higher moisture initially had greater densities of black spruce and greater black spruce re-establishment post-fire.

Several modeling studies from interior Alaska have examined potential shifts in forest composition and while they have used different models to do so, they commonly predict greater relative deciduous dominance triggered by climate-driven fire regime change (Foster et al., 2019; Hart et al., 2019; Mann et al., 2012; Mekonnen et al., 2019). Hansen et al. (2021) used the forest stand model, iLand to investigate the persistence of stands converted from conifer to deciduous in Alaska and found that continued short intervals between fires maintained stands in a deciduous state. While prior modeling work has made significant progress toward improving our predictive capacity in North

American boreal forest ecosystems, several areas have remained unexplored. Past large-scale modeling efforts have largely operated at coarser resolutions (e.g., 1 km^2 or larger; Mann et al., 2012; Mekonnen et al., 2019) and studies have limited the species represented to the functional group-level (Mann et al., 2012; Mekonnen et al., 2019) or limit the number of species represented to tree species (Hansen et al., 2021). Those modeling efforts focused at finer scale interspecific dynamics have also largely lacked spatial interactivity (i.e. allowing processes to overlap spatially, tracking their cumulative effects; (Foster et al., 2019; Hansen et al., 2021), and so do not capture how impacts of climate change and wildfire on vegetation composition trajectories may be mediated by spatial contagion effects from the surrounding landscape. This study aims to fill these gaps by using a spatially explicit, spatially interactive forest landscape model to explore how climate change and increasing fire frequency alter species composition, dominance, and spatial arrangement, and quantify the relative influences of fire history, seed source patterns, climate, and soil conditions on future post-fire successional trajectories.

Materials and Methods

Study Area

For this study, a modeling domain of 380,400 ha in interior Alaska was used. Simulation study area and replicates used in analysis were identical to those used in Chapter 2 and encompasses locations where reference data from multiple short-interval fires were collected (Figure 1).

Model Description

This study used the DGS extension to LANDIS-II (https://github.com/LANDIS-II-Foundation/Extension-DGS-Succession; Lucash et al. *in prep*), which simulates vegetation succession, hydrology, and ground temperature across a large range of depth, and carbon and nitrogen dynamics. The extension was created to capture boreal processes and in the case of this study, was used in conjunction with the SCRPPLE fire extension. Within the DGS extension, climate zone, vegetation type, topographic information, and time-since-fire are used to assign cells at each time step to a specific temperature-hydrology unit (THU). Each THU has specific sets of SHAW and GIPL inputs. Based on the THU assigned at each timestep in combination with climate data inputs, GIPL computes a soil temperature profile (Nicolsky et al., 2017), the lower boundary of which is shared with SHAW, and this information is used in combination with THU assignment to compute soil moisture and the soil temperature profile (Flerchinger, 2000). Soil moisture and temperature information are then shared with the vegetation in DGS, aggregated to two depths: from 10cm to the surface, and from 10cm to a species-specific rooting depth. LANDIS-II uses this integrated soil moisture and temperature information in its calculations of species cohort growth. Within the DGS extension, growth is simulated monthly based on life-history attributes which are specified for each species as well as temperature, age, competition, water availability, nitrogen availability, and disturbances. Regeneration is influenced by species attributes, light, and water availability. Soil CN dynamics rely upon the DAMM-McNiP model (Abramoff et al., 2017), which simulates seven measurable soil pools (soil organic C, dissolved organic C,

dissolved organic N, microbial biomass C, microbial biomass N, and extracellular enzymes).

Model Inputs

The same model runs from Chapter 2 were used for analysis here. For full details on vegetation, climate, and soil inputs used, see Chapter 2.

Calibration of DGS Model Extension

Inputs to the SHAW module of DGS were sourced from a combination of literature values and GLUE analyses conducted by Marshall et al. (2021). Inputs to the GIPL soil temperature module of DGS were sourced from literature values and observations of ground temperatures across a range of soil depths across interior Alaska and when necessary, calibrated to ground temperature data from two Ameriflux sites representative of black spruce (Smith Lake 2) and paper birch dominance (UPA1). Greater detail of parameterization and validation of these model components will be described in Chapter 4.

Maximum relative gross primary productivity data across a range of soil water contents and soil temperature at 10cm depth from Ameriflux sites (Kobayashi et al., 2019; Ueyama et al., 2019b, 2018b, 2018a) in interior Alaska were used to fit nonlinear temperature and soil moisture response functions for four species functional groups: conifer, hardwood, shrubs, and mosses. Ameriflux sites were chosen based on a predominance of a particular functional group to serve as representatives (Appendix C).

The individual growth of each species was calibrated by running single-cell simulations populated with single young (cohort age of one year with 100 gm^{-2} biomass) cohorts for 200 years under historic climate forcing. Biomass trends from each single cell simulation were compared with FIA tree biomass data plotted against stand age, as a proxy for a reference growth trajectory. Simulations were repeated with a set of variables, selected based on their having high uncertainty around their values (KLAI, MaxANPP, FCFRAC, MAXLAI, K) being adjusted iteratively within acceptable ranges using a particle swarm optimization algorithm approach with the hydroPSO package in R (Zambrano-Bigiarini & Rojas, n.d.) to find a solution where species single cohort trajectories best-matched tree reference data (Appendix D).

To validate that the simulated biomass trajectories were consistent with field data, a 20,000-ha test landscape was populated using field reference data of woody plant composition from plots measured at sites that had not experienced a fire for 12-15 years. Simulations of 200 years were run under historic climate forcing with wildfires. Trends in species biomass from cells that experienced a fire history consistent with reference plots from two sites (one categorized as upland and one as lowland) were analyzed and compared.

Simulations

The same model output was analyzed for this study as in Chapter 2. Ten simulations each of a historical climate stream (NCAR 1970-2000) and two RCP 8.5 (2000-2100, NCAR and GFDL) climate streams were run for a total of 30 simulations. Simulations were run for 100 years, with historic scenarios randomly sampling one year's

data from the 30 available years in the stream annually to build the climate stream. RCP 8.5 scenarios used sequenced climate data. All simulations were run on the Cyverse computing cluster (cyverse.org).

Analysis

Average landscape biomasses for each species were summarized over time to examine broad, landscape-level trends for each scenario type across replicates. To analyze which cells changed vegetation state from a conifer-dominant condition and the site-specific variables associated with those cells, species biomass maps output from the Output Biomass extension (Scheller & Mladenoff, 2004) were used to create datasets of vegetation type biomasses for each cell at every timestep. Time series datasets of cell-level vegetation type were used to calculate at each time step, the proportions of cells transitioned from the conifer dominant state.

Random Forests were trained to classify whether cells on the landscape would change vegetation state different from conifer dominant within the 10 years following the most recent wildfire and to assess the relative importance of potential drivers. Predictors included a combination of continuous and categorical variables related to climate, climate variability, biomass loss from fire, the proportion of starting broadleaf biomass, topography, and the mature conifer biomass in adjacent cells (Table 1). The 10-year post-fire benchmark was selected because boreal forest communities most commonly follow a species replacement successional trajectory (Kurkowski et al., 2008) and those species which establish dominance within the first decade following a fire are likely to retain dominance until subsequent disturbances are experienced (Johnstone et al., 2020;

Johnstone & Chapin, 2006b). The Random Forest algorithm was chosen because it can be reliably used when predictors are highly correlated, and predictors may also be a combination of categorical and continuous as is the case for this study and can handle high-order interactions well (Strobl et al., 2008).

Variable
Percent biomass removed (i.e., vegetation killed)
Starting deciduous fraction
Aspect
Lowland vs Upland status
Percent total carbon removed
Variance in total annual precipitation postfire
Variance in mean annual temperature postfire
Time 1 soil temperature at 3 m
Variance in soil temperature at 3m postfire
Soil temperature at 3m postfire
Mean annual temperature change
GCM
Mean annual temperature all years
Total annual precipitation variance
Scenario
Total annual precipitation postfire
Number of adjacent mature black spruce cells
Scenario
Average total annual precipitation all years
Mean annual temperature postfire
Change in total annual precipitation
Mean annual temperature variance all years
Time 1 soil moisture at 0.55m
Soil moisture at 0.55m
Number of adjacent mature black spruce cells
Soil moisture variance at 0.55m postfire
Fire year

Table 1. Predictor variables included in Random Forest analyses.

Raster cells within the modeling domain that began the simulation with the majority of mature biomass coming from conifer species (and so classified as conifer-

dominant at the start of the study) were isolated and their fire histories (the number of fires experienced) were determined using output maps of wildfires that are produced at each timestep by the SCRPPLE extension. 478 cells each (10% of those that began the simulation as mature conifer) were then sampled from three fire categories: once burned, twice burned, or three times burned throughout the simulation up until the 90th year. This stratification was done to ensure a more balanced sampling from each fire category. While the time between fires for twice and thrice burned cells was not controlled for, the 100-year model duration, naturally drives the fire return interval down for reburns.

Input datasets of predictors were then constructed by extracting associated values for variables of interest from sampled cells. Three random forest analyses- one for each fire history type (one, two, and three wildfires) were run for each replicate of the three simulated climate scenarios (Historical, Future NCAR, Future GFDL) for a total of 30 random forests. Forests of 500 trees were trained for each with five variables sampled as candidates at each split. Forests were trained on 80% of each random forest dataset set and prediction accuracy was determined using the remaining 20%. Conditional variable importance was extracted for each variable from the random forests and distributions of those values were plotted for comparison. Conditional variable importance gives higher values to those variables that are most important in successfully classifying the variable of interest (here, the transition from or retention of conifer dominance), while accounting for shared contributed importance (i.e., collinearity) among variables, thus ranking variables that offer information above that which is shared higher. Lastly, additional exploratory analyses were conducted on variables that were identified as most important for each fire history model classifier to better understand the direction of those variables

concerning post-fire retention or transition of conifer dominance. Vegetation type classifications used in this exploratory analysis were consistent with the thresholds defined for vegetation types in Chapter 2.

Results

Validation of Successional Trends

Simulated post-fire biomasses of broadleaf, coniferous trees, and shrubs matched field data within one standard deviation for all woody species groups except shrubs at the lowland sites after two and three fires, where biomasses were elevated above plot data. Simulations yielded more variable post-fire biomasses in most cases, although they were the least variable for lowland broadleaf trees postfire. In general, simulated tree biomasses were the most variable following one fire relative to subsequent fire events (Figure 16).

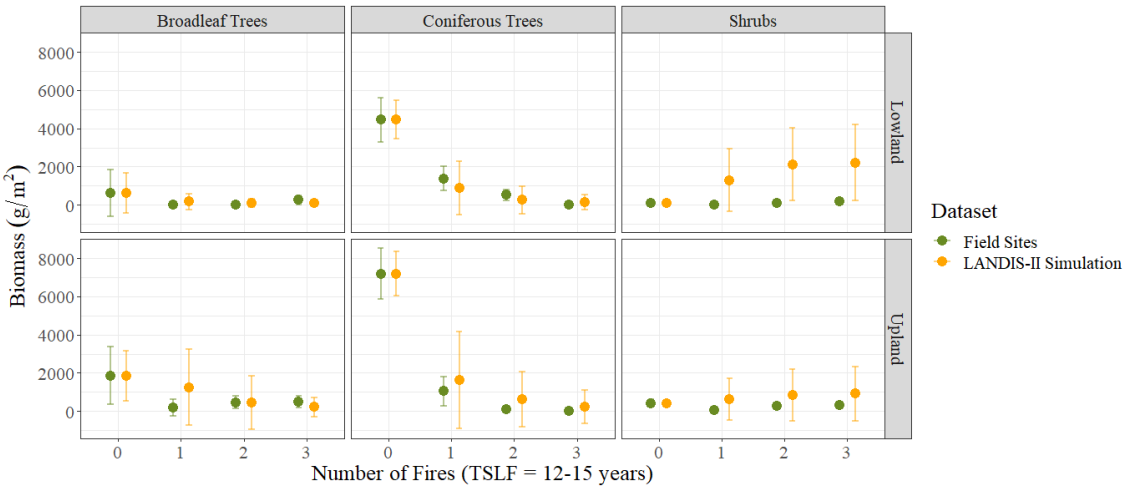

Figure 16. Comparisons of biomass of different functional groups in upland vs. lowland locations measured at field sites to test simulations. Test simulations were initiated with data from unburned reference plots (Number of Fires=0) and had a most recent fire 12-15 years ago for burned sites.

Landscape Trends

The greatest increases in landscape biomass occurred under climate change, and this was primarily driven by increases in willow and alder biomass, which increased more than 43-fold and 26-fold, respectively between the start and end of the simulation (Figure 17). However, tree biomass for all tree species except for tamarack experienced declines of 45% (black spruce) up to 69% (paper birch).

Changes in relative extent occurred most often in cells on the landscape which experienced wildfire; cells that did not experience any fire retained their relative proportions of vegetation types across the landscape, regardless of the climate scenario used (Figure 18a). Type changes overall were more common for those cells which experienced one or more wildfires during the simulation period across all scenario types, both historic and climate change. Rates of transition away from a conifer vegetation type increased in the latter half of the century under climate change (Figure 19). In cells that experienced fire(s), the largest declines in vegetation type occurred within the conifer under climate change and were most dramatic when more than one fire took place (Figure 18b-d). The largest increases in vegetation occurred for the broadleaf group, with the greatest increases taking place under the GFDL climate change scenario.

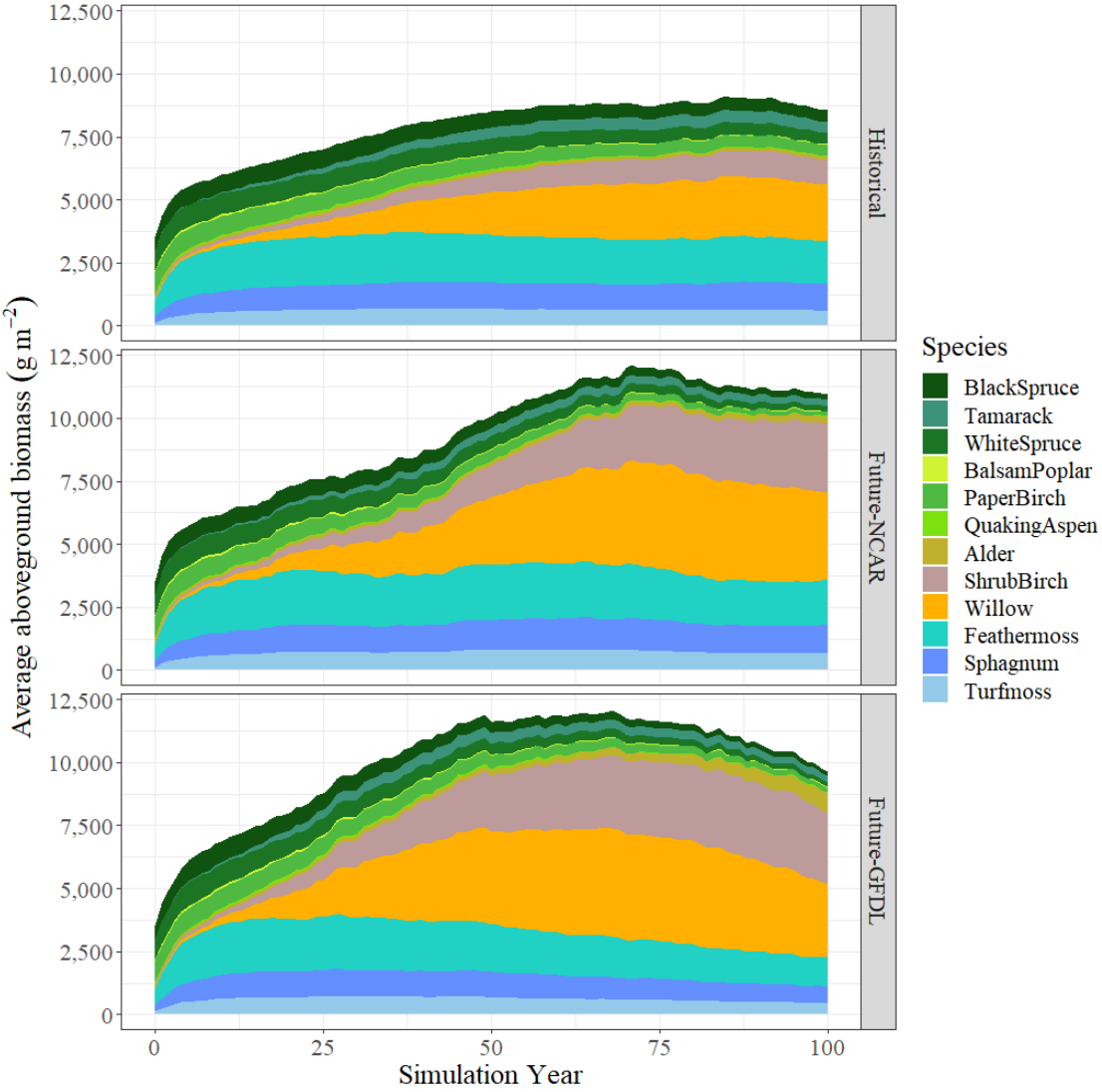

Figure 17. Trends in biomass (gm^{-2}) for each species averaged across replicates for each scenario over time.

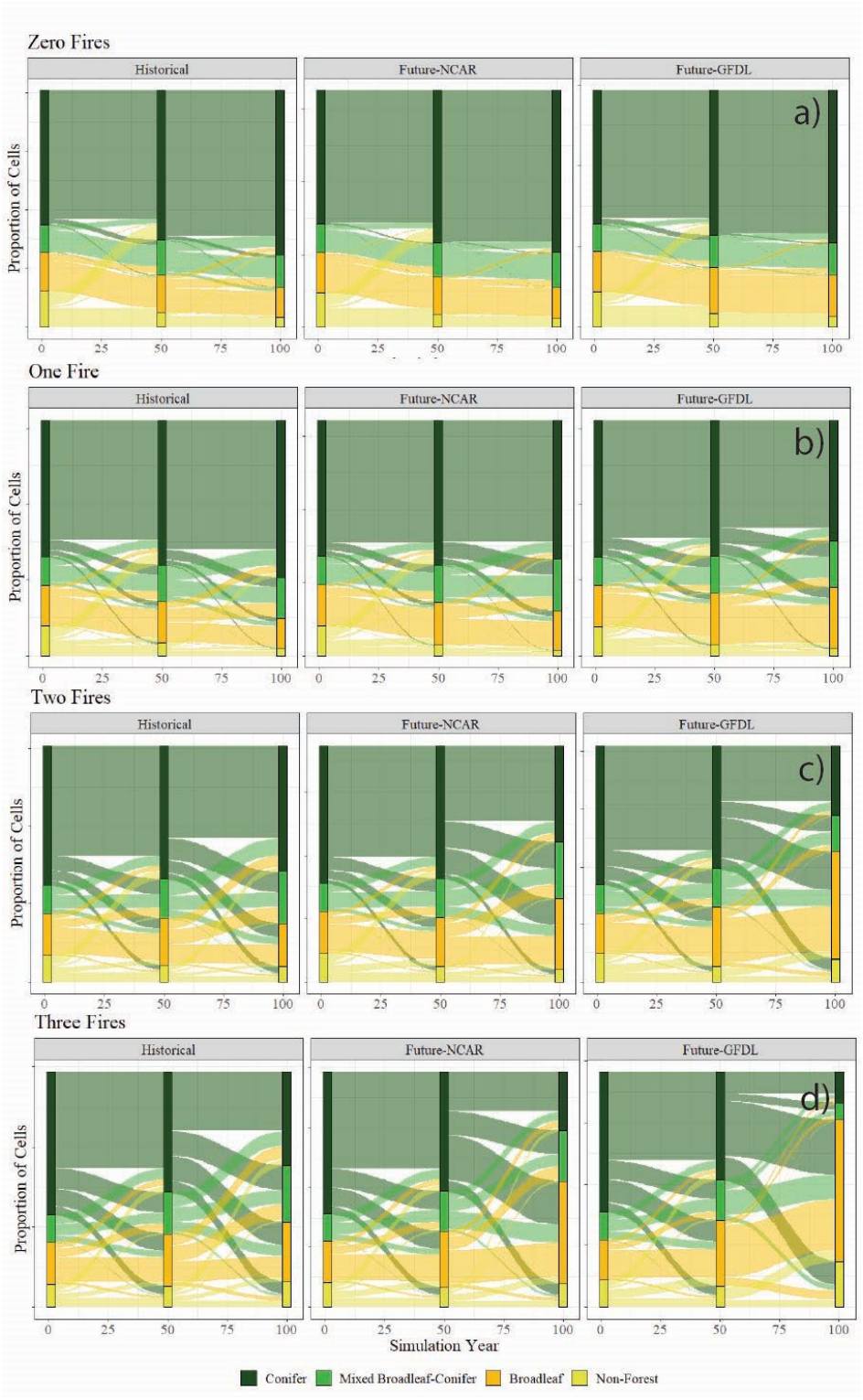

Figure 18a-d. Plots of proportions of cells within each vegetation type for each scenario at years 0, 50, and 100, with pathways taken to the next consecutive vegetation type noted for cells that experienced zero (a), one (b), two (c), and three (d) fires throughout the simulation period.

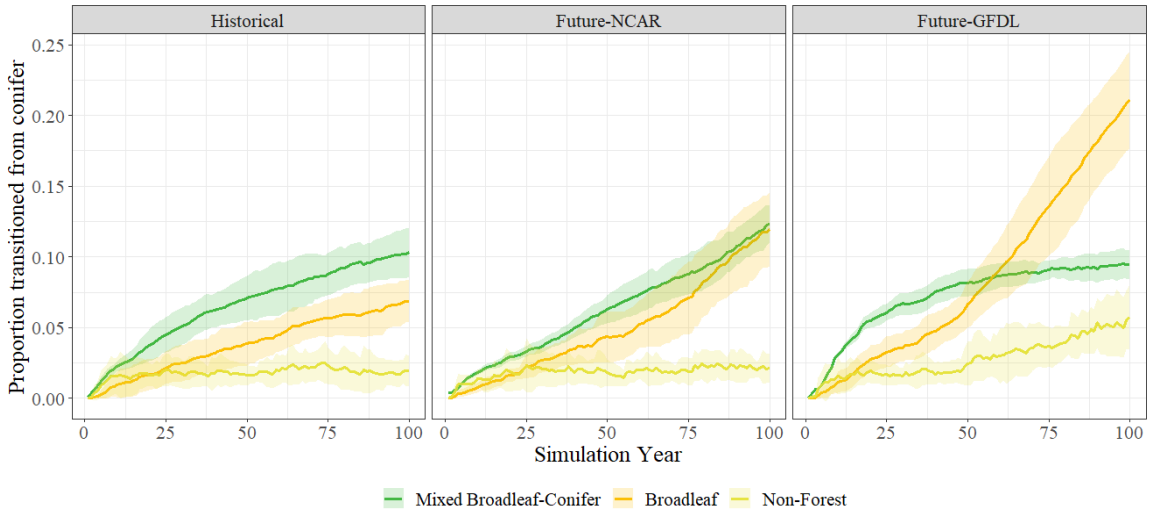

Figure 19. Proportions of cells that transitioned to a new vegetation state from conifer at each timestep for each scenario. Lines represent the averages across replicates and the band represents the stand deviation.

Burned Cell Trends

The random forests were able to classify conifer retention vs. transition with good accuracy on the independent test set and performed best on the one-time fires, and least well on the three-time fires (1x accuracy= 85.7% (+/- 1.6%), 2x accuracy= 77.0% (+/- 2.0%), 3x accuracy= 76% (+/- 2%)). Across all scenarios, rates of conifer retention declined with the number of fires experienced, while the number of cells which converted to an alternative vegetation type increased (Figure 20). Conversion rates to a mixed broadleaf deciduous-conifer vegetation type remained relatively constant between two and three fires after increasing between one and two fires (Figure 20). Climate change scenarios yielded more dramatic increases in cells which converted to broadleaf vegetation types, and when three fires were experienced under climate change, cells that had converted to a broadleaf vegetation type outpaced those where conifer dominance was maintained.

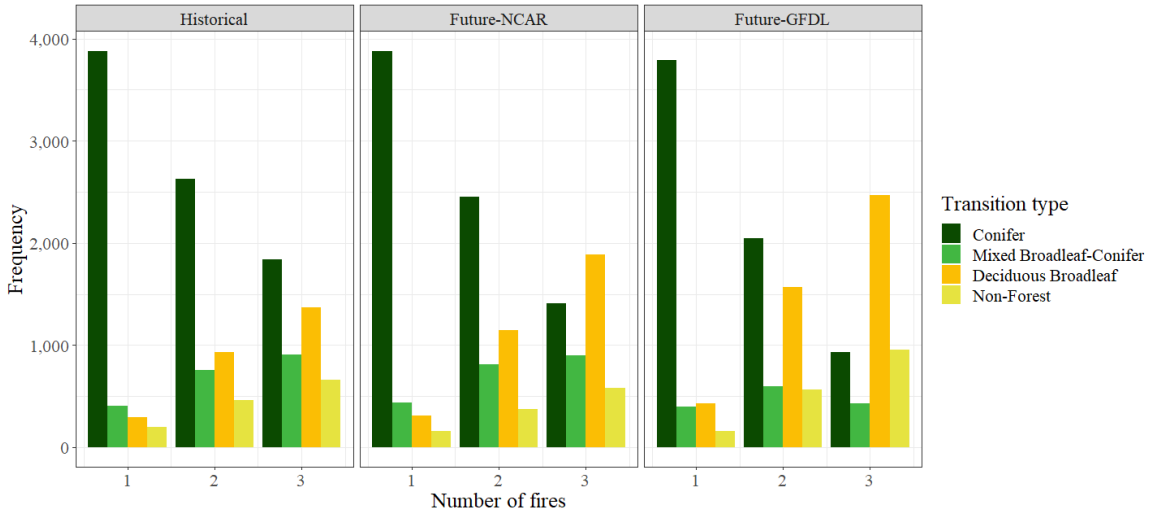

Figure 20. Frequency of cells that are classified under each vegetation type 10 years post-most-recent-fire by the number of fires ad scenario. All cells began the simulation as conifer vegetation type.

Using random forest classification models for each fire history type, similar variables played an important role in predicting conifer retention vs. transition for once burned, twice burned, and thrice burned. However, there were differences in the relative importance between them. Across all random forest analyses, the variable with the highest conditional importance for predicting the vegetation state of a cell 10 years post-fire was the percent biomass loss (i.e. vegetation mortality) during the fire (Figures 21a-c). This variable was most important by a large margin across all analyses; however, this margin was greatest for the single fire random forest classifier, and for two and three fire classifiers, the importance of additional variables became relatively closer in importance to the percent biomass lost. Additional variables that were important to the prediction of the post-fire vegetation state included starting deciduous fraction, percent of total carbon removed (post- - pre-fire carbon), and the number of adjacent cells containing mature

conifer biomass (Figures 21a-c). For a full list of variables and their conditional permutation importance values, see Appendix E.

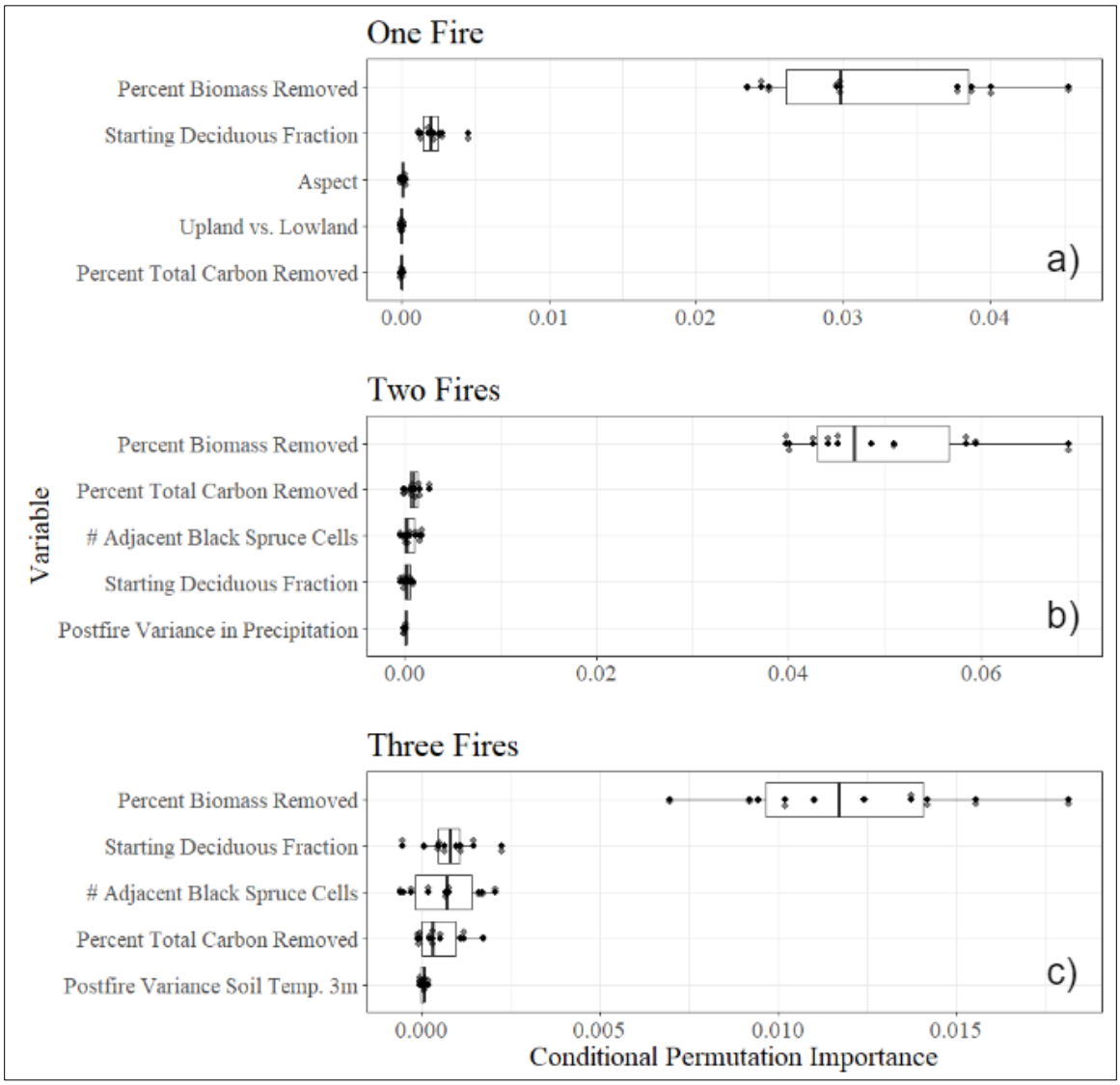

Figures 21a-c. Boxplots of the top five conditional permutation importance values for each variable from random forest classifiers of vegetation transition 10 years following one (a), two (b), and three (c) fires.

Cells that did not maintain conifer dominance postfire tended to experience higher percentages of aboveground biomass loss from fire than those where conifer was retained. However, this difference in biomass loss was most distinct for single fire cells

(Figure 22). The percent aboveground biomass removed also interacted with the number of surrounding cells with conifer biomass across the range of fires experienced. Two and three fire cells that retained conifer dominance tended to have greater numbers of surrounding mature conifer cells (i.e., potential seed sources) when they had lost more biomass (percent biomass removed; Figure 23). This trend was not found for single fire cells, however, which tended to have greater overall numbers of surrounding mature cells than those cells which experienced multiple fires (Figure 23).

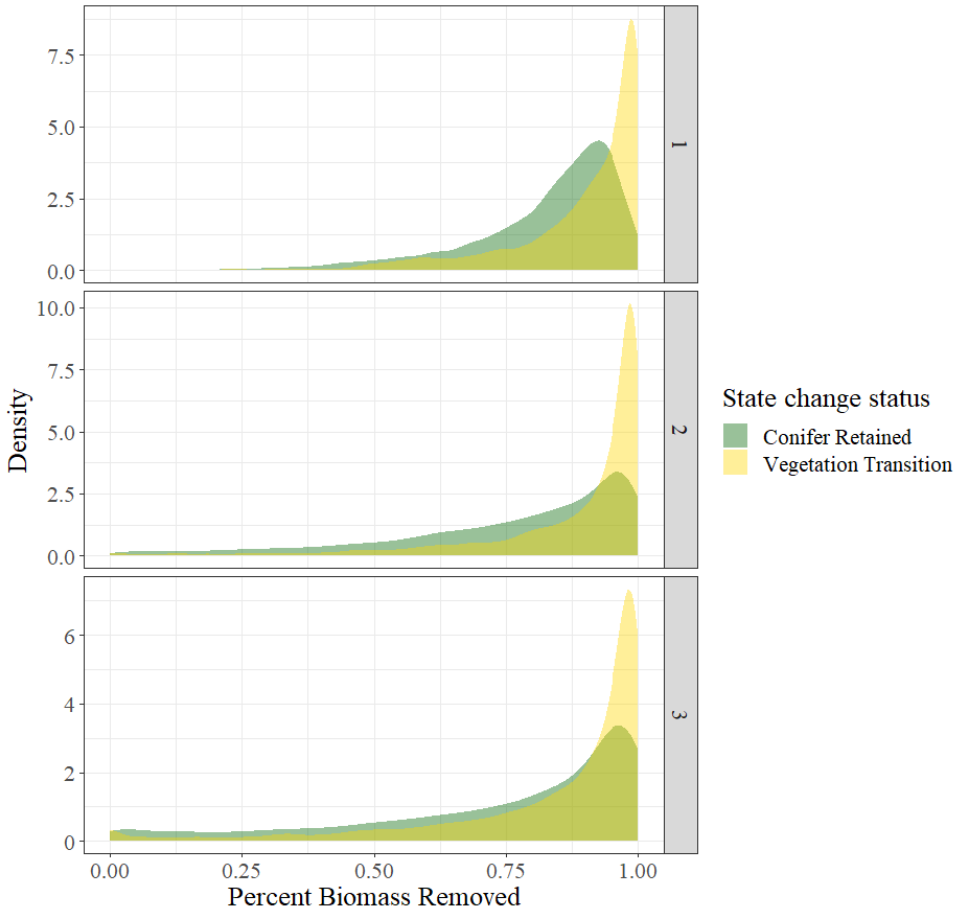

Figure 22. Density plot of percent biomass removed for cells that experienced one, two, and three fires and whether vegetation status changed 10 years post-fire.

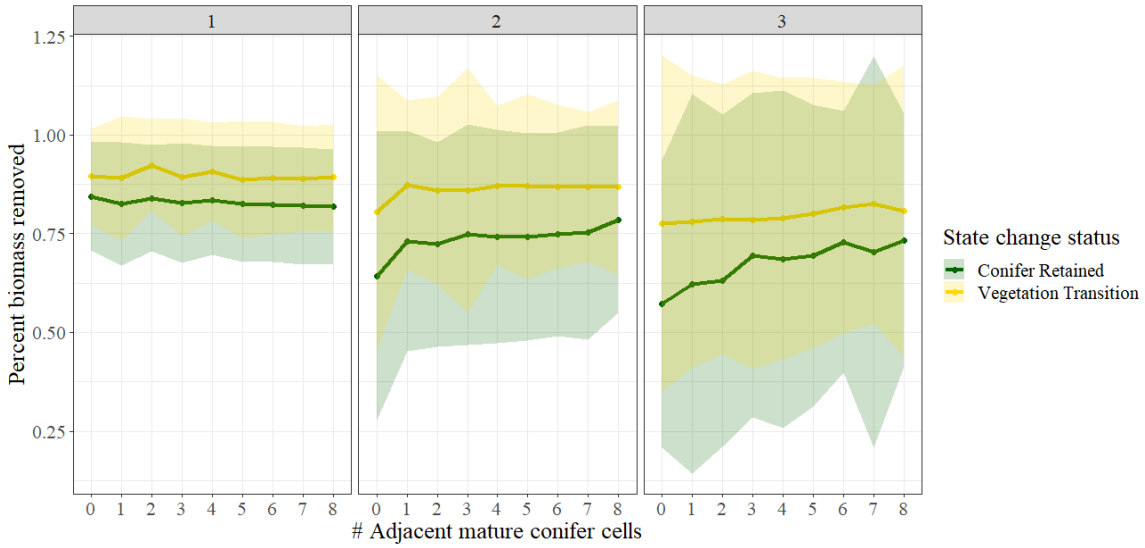

Figure 23. The average percentage of biomass removed of those cells that either retain conifer or transitioned, depending on the number of fires experienced and how many adjacent cells had mature black spruce. Bands represent standard deviation.

For single fires, having a lower starting deciduous fraction was more associated with conifer retention, however, this effect smoothed out with multiple fires (Figure 24). For reburns, state transitions happened more when starting deciduous fraction was lower, especially in thrice burned cells that transitioned to non-forest. The percentage of total carbon removed was also an important predictor across the number of fires experienced. For single fire cells, cells that transitioned to non-forest had higher levels of total carbon removal (Figure 25). Cells, where conifer was retained, exhibited a bimodal pattern regarding total carbon removed, peaking at around 20% and 40%. Cells that experienced multiple fires in general had lower percentages of carbon removed.

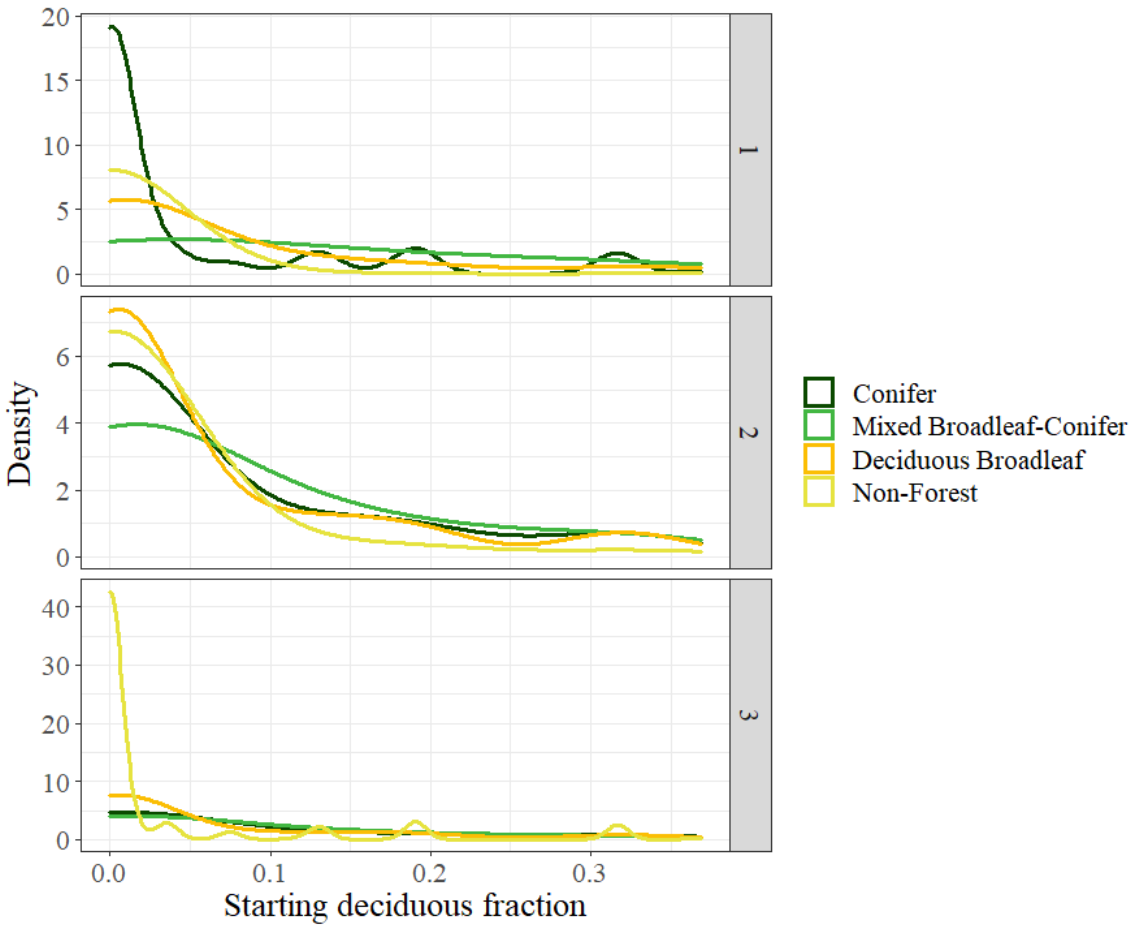

Figure 24. Density plots of cell values for starting deciduous fraction based on the number of fires experienced and the cell's associated vegetation type.

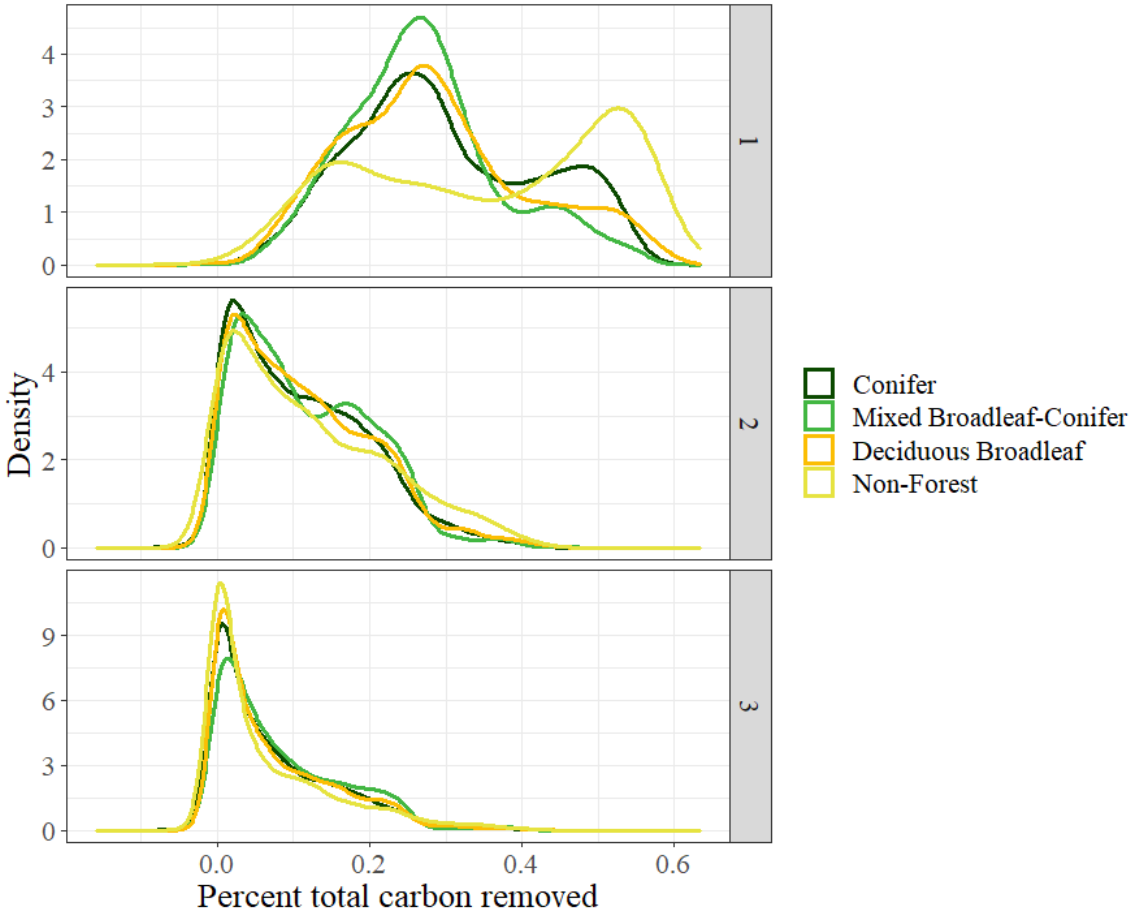

Figure 25. Density plots of cell values for the percentage of total carbon removed based on the number of fires experienced and the cell's associated vegetation type.

Discussion

The increase in biomass, largely driven by the increase in shrub biomass landscape-wide, observed here is consistent with studies documenting and projecting woody species expansion into tundra landscapes under climate change. Winter warming in the tundra has been linked to increases in shrub abundance and greening patterns in boreal North American and Russia (Bunn & Goetz, 2006; Forbes et al., 2010; Sturm et al., 2005; Tape et al., 2006). These patterns are attributed to feedbacks from shrubs being positively correlated with greater snow depths, and thus greater winter soil temperatures

and soil microbial activity, allowing for greater levels of plant-available nitrogen in the soil which then spurs shrub growth in the subsequent growing season (Myers-Smith et al., 2011; Sturm et al., 2005). While these studies have focused on these trends and relationships within the tundra, similar interactions may be taking place in Alaska's interior as well.

Important to note, is the increase in shrub biomass even under historic climate conditions. This could point to a potential process being absent from this modeling experiment that would otherwise limit the large accumulation of the willow and dwarf birch biomass in all three scenarios. Not represented in this study, is the process of herbivory by moose (*Alces alces*) and snowshoe hare (*Lepus americanus*), and which is known to influence boreal shrub communities (Bryant et al., 2014; Christie et al., 2015; Myers-Smith et al., 2011), though the relative strength of their influence how this may transpire under climate change warrants greater study (Christie et al., 2015). One study evaluated shrub radial growth in northern interior Alaska to examine the effect of browse pressure on climate-driven enhanced shrub growth and found that the positive warming effect on shrubs was in part, offset by browsing, though not entirely (Frank, 2020). Without the inclusion of this process within the modeling framework, it is difficult to conclude what the potential effect and interaction of this additional disturbance would be, or how the herbivores would be impacted by direct and indirect effects of climate, vegetation, and fire processes. However, it is possible that they would at least, partially moderate the strong growth response observed in this functional group.

Conifer forest type extent declined most when there were multiple fires and under climate change and most frequently transitioned to a broadleaf vegetation type by the end

of the simulated century. These findings are consistent with field studies that examined the effects of multiple and/or short-interval fires, which have consistently found that when fires have burned with greater frequency (Hayes & Buma, 2021), severity (Johnstone et al., 2020; Johnstone, et al., 2010), or with shorter than typical intervals (Brown & Johnstone, 2012; Johnstone & Chapin, 2006c; Whitman et al., 2019), transitions from a conifer dominant state occurred. These transitions have been tied to a decline in seed availability (Brown & Johnstone, 2012) and changes in the post-fire depth of the soil organic layer (Hayes & Buma, 2021; Johnstone et al., 2020; Johnstone et al., 2010), as well as interactions with climate (e.g., drought; Whitman et al., 2019).

Drivers of transition were similar regardless of the number of fires experienced during the simulation period, and most important was the percentage of aboveground biomass killed during the most recent fire, which can be thought of here as a dimension of fire severity in boreal forests. Fire severity in field studies is often defined using composite burn indices in remote sensing work or by measuring the consumption of the soil organic layer in field studies (Boby et al., 2010). Overall, studies have found that higher severity wildfire tends to promote the recruitment of broadleaf deciduous species postfire. These findings reflect the importance of residual aboveground biomass postfire in shaping relative dominance. Across simulations, the percent vegetation mortality from wildfire was high (mean= 80.3%, sd=27.3%), which is characteristic of wildfire in black spruce ecosystems (Boby et al., 2010; Hollingsworth et al., 2013). Variation in those levels of biomass loss, however, appears to have a strong predictive power of postfire composition. This is consistent with the findings of Hollingsworth et al. (2013)who found

that postfire community composition was primarily related to severity gradients, as measured via combustion of biomass and residual vegetation.

Beyond vegetation consumption, total carbon removed by wildfire, which is inclusive of the belowground carbon pool, was also found to be an important conditional predictor of postfire black spruce retention/transition in the twice burned and three times burned random forest models. While the DGS extension does not capture the effect of soil organic matter depth on seedling establishment (via exposed mineral soil), it does give greater access to soil moisture to species with adventitious roots (in this study only black spruce), and in this way gives those species a competitive advantage when growing on top of permafrost. The importance of total carbon loss could indicate other effects of belowground organic matter consumption, such as soil temperature and subsequent permafrost freeze/thaw dynamics, on top of aboveground reductions. Reduction in soil organic matter postfire has been found to contribute to permafrost degradation and increase soil microbial activity, releasing nutrients and moisture and providing an advantage to species with greater rooting depths and nutrient needs that would otherwise be restricted by permafrost and a shallow active layer (e.g., broadleaf deciduous species; Sturm et al., 2005). Within DGS, vegetation type, associated soil characteristics, and landscape position influence the belowground thermal dynamics. Rooting depths are specified for each species and a cohort's ability to access water and nutrients is limited to unfrozen soil layers, such that those species with deeper rooting depths would be advantaged by permafrost degradation on a site they occupy. It is possible that these dynamics represented in the model encouraged vegetation transitions when fire severity was high and would promote permafrost thaw.

Other important factors for predicting conifer retention or transition were cell adjacency of mature black spruce in the most recent fire year and starting proportion of broadleaf deciduous biomass. When additional fires were experienced (reburns), these additional factors beyond biomass removal alone became relatively more important in determining whether self-replacement of the conifer vegetation type. Black spruce does not have a great seeding distance (typically within 80 m; Tuskin and Laughlin 1991; Johnston, 1971) exceeded by the straight-line distance of the 4-ha cells (200-283 m) used in this study, and making it so that within the model, for seed dispersal to take place from a source outside of a given cell, it must come from an adjacent cell. This relatively short seeding distance makes the species vulnerable to seed source limitation and immaturity risk, should existing nearby seed sources become less available or are below the age of sexual maturity (Johnstone & Chapin, 2006b; Viglas et al., 2013). Results show that cells that have more potential seed sources as neighbors (adjacent mature conifer cells) are buffered against the effect of higher biomass loss events more than their counterparts with fewer adjacent seed sources. Additionally, when broadleaf deciduous species have less of a foothold (i.e., lower relative biomass) at the start of the simulation, this increases conifer retention postfire. This result is consistent with field studies, which have found that high densities of prefire black spruce are advantageous for postfire reestablishment (Johnstone, Chapin, et al., 2010; Johnstone & Chapin, 2006b).

Under climate change, transitions to a broadleaf deciduous forest type were observed at greater rates following wildfire than a mixed-deciduous forest type, which includes levels of conifer biomass and broadleaf biomass both within 33-66% of total tree biomass. This indicates that under combined pressures of multiple fires and/or climate

change, when conifer-dominated forest transitions to an alternate state, it does so by swiftly transitioning into a broadleaf-dominated forest, rather than gradually shifting species' relative dominance over time. This type of abrupt transition is characteristic of nonlinear behavior and a system approaching an ecological tipping point (Lenton, 2012; Scheffer & Carpenter, 2003). Tipping points imply that there are positive feedbacks internal to the system promoting self-amplification of a given state (Lenton, 2012). In interior Alaska, past work has supported the existence of these internal feedbacks promoting either conifer or broadleaf dominance as each given state creates and perpetuates specific soil temperature, nutrient, and microbial feedbacks (Chapin et al., 2004; J. F. Johnstone et al., 2016; Kurkowski et al., 2008). Under the singular pressures of greater numbers of fires (which necessitates a lower mean fire return interval in these 100-year simulations) under historic climate, transition rates to broadleaf forest type nearly doubled after two fires (increased by 84%) and increased an additional 24% after three fires. With climate change, those rates of transition to broadleaf increased even more aggressively and outpaces conifer retention rates after three fires in the Future-GFDL climate scenario. This combination of climate pressure and multiple fires could represent a threshold whereupon the broadleaf forest type transitions become equally or more likely.

Other process modeling work from interior Alaska boreal forests have projected state shifts from conifer to broadleaf deciduous dominance at large scales when simulating climate change and wildfire, finding that the interaction of these two pressures to be critical drivers of forest type change (Foster et al., 2019; Hansen et al., 2021; Mann et al., 2012; Mekonnen et al., 2019). Mekonnen et al. (2019) and Foster et al. (2019)

included below-ground dynamics in their simulations and found climate-induced changes on these processes were a key mechanism for reinforcing changes in vegetation composition. Similarly, in this study, climate change was an exacerbating factor in accelerating transitions to the alternate broadleaf forest state, likely due to increases in soil temperatures that both increase thaw depths (i.e., increasing the potential rooting zone) and accelerate nitrogen mineralization. Hansen et al. (2021) tested the stability of a newly transitioned deciduous state in their simulation study, and consistent with findings that the broadleaf deciduous forest state was highly resilient. This further supports the idea of there being a critical threshold between conifer and deciduous dominated states, with mixed-conifer forest types being a relatively less common transition, as was observed in this study.

As in Chapter 2, this study was limited by data available to use as model inputs for interior Alaska. One example of this is climate data. The daily temporal resolution required to run the SCRPPLE extension constrained options for downscaled GCM data sources, and available climate data were relatively coarse in spatial resolution (20 km). This may be one reason for the low importance of climate variables in the random forest classification; there may have been a mismatch between the scale at which climate influences operate on some postfire successional processes that were not able to be captured here.

Overall, I observed increases in landscape biomass over time, and especially large increases in willow and dwarf birch, pointing toward the potential for shrubs to play an increasing role in interior Alaska boreal forest communities under a warming climate, though the role that herbivory could play in moderating these potential increases remains

an unknown. I also observed vegetation transitions from a conifer-dominant state to deciduous dominance accelerate under climate change and with increasing pressure from wildfires, with factors related to fire severity and vegetation community context (e.g. starting relative dominance and seed source) being important to predicting these transitions. These findings have potential implications for identifying areas at particular risk for conifer dominance loss under climate change and illustrate the potential for continued large fire years and high severity fires to exert a strong influence on future forest composition in this region.

CHAPTER 4

FUTURE IMPACTS ON CARBON POOLS AND PRODUCTIVITY UNDER CLIMATE CHANGE AND INCREASING FIRE ACTIVITY IN INTERIOR ALASKA

Introduction

The boreal forest biome is a critically important global carbon (C) sink, storing an estimated one-third of the world's forest C (Pan et al., 2011). In these regions, most of the carbon is concentrated belowground in soils and peat, where decomposition proceeds slowly due to the cool annual temperatures, substrate quality, and often waterlogged soils, allowing organic material to accumulate over time (Bradshaw & Warkentin, 2015; Hobbie et al., 2000). Where permafrost is present, heterotrophic soil respiration is limited to the portion of soil near the surface, which thaws each growing season, only to refreeze again in winter. This portion of the soil is called the 'active layer' (Schuur et al., 2008). This results in boreal forests accumulating more carbon each year than they emit and holding vast quantities of carbon in its below ground pools, with only a small fraction of those pools available to be decomposed and released back into the atmosphere each year (Van Cleve et al. 1991, Schuur et al., 2008).

Carbon storage in boreal forests is sensitive to temperature, making it susceptible to change as global temperatures continue to increase into the 21st century; Van Cleve & Yarie 1986). High latitudes are experiencing warming at a faster rate than more temperate regions so arctic and boreal ecosystems are particularly vulnerable to the effects of climate change (McGuire et al. 2009). At locations where permafrost occurs, the depth of thaw is impacted by climate change and as thaw depths increase, this also increases the

amount of soil carbon that is available for decomposition and release into the atmosphere (Goulden et al., 1998; Schuur et al., 2008). Losses in soil carbon associated with higher soil temperatures in North American boreal forests have been documented across numerous field studies (Shabaga et al., 2022; Eliasson et al. 2005; Melillo et al. 2017) as well as simulated (Euskirchen et al., 2006; Genet et al., 2013; Koven et al., 2011).

Changes in fire frequency also threaten belowground processes that promote carbon storage. When adequate time is allowed between fires, fires will leave behind residual organic material (Harden et al., 2000; Melvin et al., 2015). These unburned stores of accumulated soil organic carbon within the residual soil organic layer have been termed 'legacy C' (Walker et al., 2019). These older carbon stores increase with stand age and are more common at mesic or wet sites, where incomplete combustion of the soil organic layer is more likely. Legacy C is vulnerable when multiple fires are experienced with inadequate time for the soil organic layer can rebuild or when burn depths are high (Walker et al., 2019). When legacy C combusts, this can tip the balance from a site being a net sink for carbon to a net source (Walker et al., 2019). Turetsky et al. (2011) analyzed black spruce and peatland sites in interior Alaska and found that carbon loss was twice as high for sites that burned in years with a greater annual area burned and/or in late-season fires due to increased burn depths that occur under these conditions (Turetsky et al., 2011). Increases in annual area burned, fire season length, and fire severity is expected under climate change in the circumboreal zone (Flannigan et al., 2009) increasing the probability of soil carbon loss from future fires. Fire regime changes are also likely to alter vegetation dynamics in boreal forests, and subsequent changes in aboveground composition impact belowground processes. Trends toward greater broadleaf deciduous

dominance across the North American boreal landscape driven by greater wildfire activity, have been observed and are predicted to continue under climate change (Beck et al., 2011; Mekonnen et al., 2019). Deciduous species are favored by shorter fire return intervals and greater consumption of the soil organic layer during fires (Hayes & Buma, 2021; Johnstone & Chapin, 2006).

These shifting vegetation trajectories post-fire impact soil temperature dynamics and decomposition rates. Conifer and broadleaf deciduous-dominated forests tend to have opposite patterns in soil temperature, carbon pools, and nutrient turnover. Black spruce-dominated stands are often associated with cooler soil temperatures, often growing atop permafrost soils, and have slower rates of decomposition and primary productivity (Nossov et al., 2013; Yoshikawa et al., 2003). Moss cover is particularly important to ground temperature dynamics because in winter months because higher moisture content causes moss to conduct heat, allowing it to escape the ground, while in summer when moss is dry, it insulates and prevents heat from moving into the soil (O'Donnell et al., 2009). These seasonal patterns keep soils cool and slow decomposition, leading to lower heterotrophic respiration rates and greater retention of permafrost and carbon stores belowground (Fisher et al., 2016). Broadleaf deciduous stands tend to have more rapid nutrient cycling, higher nutrient concentrations in foliage and litter, and higher rates of productivity (Johnstone, Chapin, et al., 2010; Melvin et al., 2015). Without the thick insulating layer of organic material, broadleaf deciduous soil temperatures tend to be warmer and have more rapid turnover of nutrients (Johnstone et al., 2010). At sites where transitions from a stand previously dominated by black spruce to one dominated by broadleaf deciduous species, there have been greater carbon losses from the soil

(Euskirchen et al., 2006; Melvin et al., 2015) and higher temperatures (Shabaga et al., 2022). Despite these differences, overall ecosystem stocks between these two forest types have been found to be similar (Melvin et al., 2015). There is uncertainty, however, around whether net ecosystem exchange would remain unchanged at larger scales should shifts in vegetation occur and persist. Mack et al. (2021) found that there was rapid accumulation of carbon via high rates of net primary productivity following high severity fire along a chronosequence in interior Alaska that overall counteracted soil carbon losses. However, fire history has also been found to impact this balance; one study found that when multiple fires occurred with short return intervals (< 50 years) separating them, biomass and primary productivity of understory plants were significantly reduced and ultimately made sites unable to offset the high rates of heterotrophic respiration driven by warmer postfire soils (Shabaga et al., 2022).

A variety of large-scale models have been used to project carbon dynamics under climate change in boreal regions including TEM, ecosys, and ALFRESCO (Euskirchen et al., 2006, 2009; Genet et al., 2013; Mekonnen et al., 2019; Rupp et al., 2007). These efforts have captured effects on soil temperature, active layer depth, and respiration as well as vegetation-driven changes in primary productivity. While many of these past studies have also included wildfire effects and associated feedbacks (Genet et al., 2013; Mekonnen et al., 2019; Rupp et al., 2007), these focused on broader regional patterns at coarse spatial scales (e.g., quarter or half a degree) and often without individual vegetation species being represented, instead using plant functional types). These studies have largely converged in their simulated outcomes for carbon in boreal forest ecosystems; agreeing that climate change can produce meaningful changes in net primary

productivity across plant functional types, with particularly high increases for broadleaf deciduous species, and increases in microbial decomposition associated with higher temperatures and permafrost degradation (Euskirchen et al., 2006; Mekonnen et al., 2019), both of which can be exacerbated by fire activity (Genet et al., 2013). Building on this work, this study also seeks to capture these processes and drivers within a spatially explicit modeling framework, but at a finer spatial scale, inclusive of individual plant species and their competitive interactions, and with analysis focused on how fire history can mediate outcomes for carbon stocks in interior Alaska boreal forests. In doing so I ask:

1. How do carbon pools change over time across a large landscape in interior Alaska under climate change and greater fire activity?; and
2. How does fire history (reburning) impact postfire vegetation productivity and carbon storage?

Materials and Methods

Modeling Domain and Simulations

As in prior chapters, I used the landscape simulation model, LANDIS-II. The same modeling domain and simulation experiments were used for this study as those used in chapters one and two, a total of 380,400 ha in interior Alaska, encompassing locations of reference plots from field studies of short interval fire effects on vegetation and soil dynamics (Hayes & Buma, 2021; Shabaga et al., 2022; Figure 2). The same simulation outputs as were used in chapters one and two were analyzed here as well. They represent three climate scenarios- one historical (using back casted NCAR-CCSM4 climate data

from 1970-2000) and two climate change scenarios representing the RCP 8.5 scenario (NCAR-CCSM4 and GFDL-CM3) for 2000-2100, with 10 replicates each for a total of 30 simulations.

Parameterization and Validation of Soil Temperature, Nutrient, and Moisture Dynamics

The DAMM-GIPL-SHAW Succession (DGS) extension of LANDIS-II is the module responsible for simulating carbon-nitrogen dynamics as well as soil moisture and temperature. The Damm-McNIP module is responsible for soil carbon and nitrogen cycling; it tracks multiple soil pools which are sensitive to soil moisture, soil temperature, oxygen concentrations, and substrate CN stoichiometry. The GIPL module is responsible for modeling ground temperature and active layer thickness within DGS and does so using a nonlinear heat equation with phase change, and phase changes are influenced by daily air temperatures and snow variables. The SHAW module simulates energy and water fluxes along a soil-vegetation-atmosphere continuum and the snow, surface vegetation, and litter that it simulates affect these dynamics. While each of these modules are separate models in themselves that are applied outside of the DGS model, within DGS, they are coupled to provide relevant information to one another. For example, SHAW provides the water and ice content values used by GIPL. Damm-McNIP and GIPL parameters were derived from a combination of field estimates and published literature values. SHAW module (hydrology) parameters were initiated using literature estimates and field data and then optimized from a GLUE analysis conducted by (Marshall et al., 2021).

The performance of DGS was calibrated and tested using field data specific to three sites representing different vegetation and successional states (a burned site, a black spruce-dominated site, and a deciduous site) and running single cell simulations as representations of each site. The performance of DGS was tested against a similar LANDIS-II extension, NECN, which lacks the complexity in its representation of soil pools and fluxes, and dynamics with soil moisture and ground temperature. DGS has been shown to outperform NECN at sites in interior Alaska in representing seasonal trends in soil moisture and temperature (Lucash et al. *in prep*).

Vegetation growth is also simulated within the DGS extension. Details on the parameterization and validation of the vegetation growth parameters within the DGS extension can be found in Chapter 2.

Analysis

Analysis was aimed at examining differences in carbon pools between scenarios and how different levels of fire activity impact these patterns. At the landscape level, patterns in average annual net primary productivity, net ecosystem exchange, and heterotrophic respiration were aggregated across replicates and compared between climate scenarios. The DGS extension tracks individual carbon pools at the landscape level, including which components of the soil are frozen and thus unavailable for decomposition and heterotrophic respiration. The difference between total soil carbon and unfrozen soil carbon was taken at each time step and plotted over simulation time to examine changes in unfrozen soil carbon across scenarios. Soil pools representing

average live and dead woody material, and total soil organic matter were aggregated across replicates, and trends over simulated time were summarized.

In addition to examining overall changes in carbon pools and fluxes across the entire simulated landscape, specific variables are tracked at the cell level within DGS, including total carbon, annual net primary productivity, and net ecosystem exchange. Within DGS, Net ecosystem exchange represents the difference between heterotrophic respiration and net primary productivity within each cell. These cell-level data were matched to their respective vegetation type and fire histories (the cumulative number of fires) for each time step within every replicate. To better understand how fire impacted changes in carbon storage and postfire productivity across the simulated landscapes, cells that had burned between one and three times before year 75 in the simulation were isolated, and their values for total carbon, net ecosystem exchange, and annual net primary productivity were compared at 25 years postfire across scenarios and fire histories up to three fires. The statistical significance of pairwise comparisons was tested using Wilcoxon rank sum test statistics, evaluated at a 0.05 threshold for significance.

Results

Landscape Trends

Rates of net primary productivity, heterotrophic respiration, and net ecosystem exchange all show seasonal variation, peaking during the growing season across all three scenarios (Figure 26). Monthly values across these fluxes were also higher during the last 25 years of the simulations, including the winter months. This was also true for the

simulations run with historical climate, indicating that these changes in flux may be responding both to the effect of cumulative fires over time as well as climate.

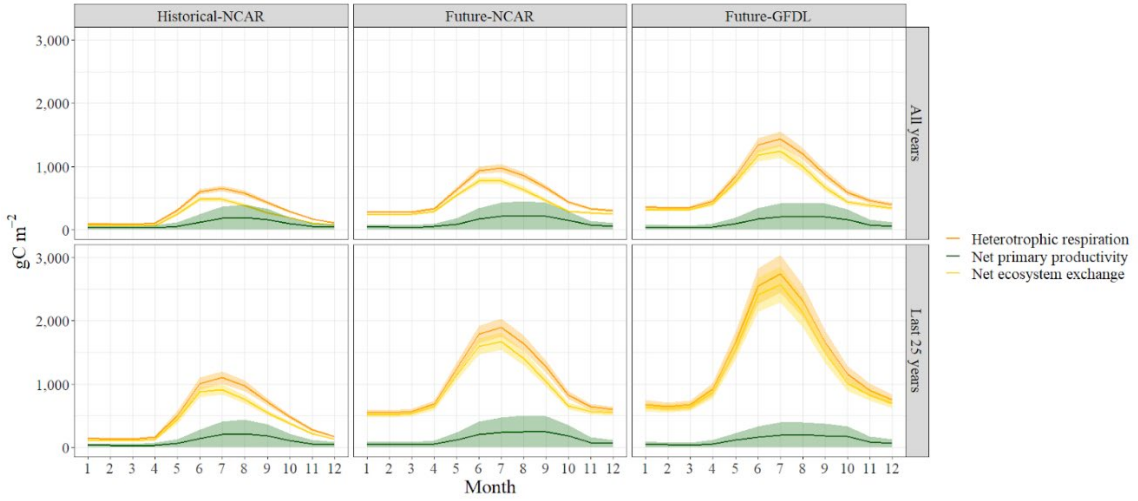

Figure 26. Average monthly net primary productivity (gC $m^{-2}mo^{-1}$), heterotrophic respiration (gC $m^{-2}mo^{-1}$), and net ecosystem exchange (gC $m^{-2}mo^{-1}$) across all years (top) and the average for just the last 25 years of simulations (bottom) by scenario.

Under climate change, the average available soil carbon, or the amount of total unfrozen soil carbon that is available for respiration, across the landscape increases and eventually converges with total soil carbon, indicating great amounts of permafrost thaw under climate change (Figure 27). This happens most rapidly under the GFDL scenario, which had the strongest warming and largest increase in precipitation (Chapter 2, Figure 2). Unfrozen soil carbon converges with total carbon by year 25 across replicates, while under the NCAR scenario, this convergence occurs after 60 years. Under historical climate, soil carbon difference remains constant, though it is more variable than in climate change scenarios. It is important to note that these values represent landscape averages, so while they indicate that there is rapid permafrost degradation, they do not necessarily imply a total loss of permafrost in the climate change scenarios.

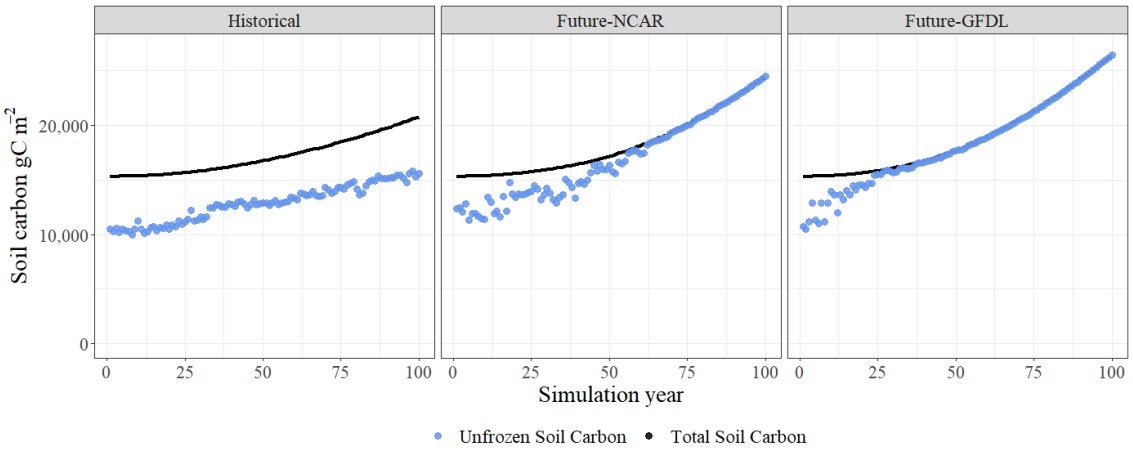

Figure 27. Total landscape soil carbon (gC m^{-2}, black) and unfrozen soil carbon (gC m^{-2}, blue) over time.

Dead and alive aboveground wood carbon pools increase over time at the landscape level across all simulations, as does soil organic matter (Figure 28). The Future GFDL climate scenario yields the largest increases across all groups, followed by Future NCAR. Carbon from live woody material plateaus after mid-century across scenarios and does so earliest in the Future GFDL scenario before beginning to decline by the end of the century. Dead woody material, however, continues to increase for the duration of the simulation, though at a slower rate by the end of the century. Increases in soil organic carbon are continuous throughout the simulation.

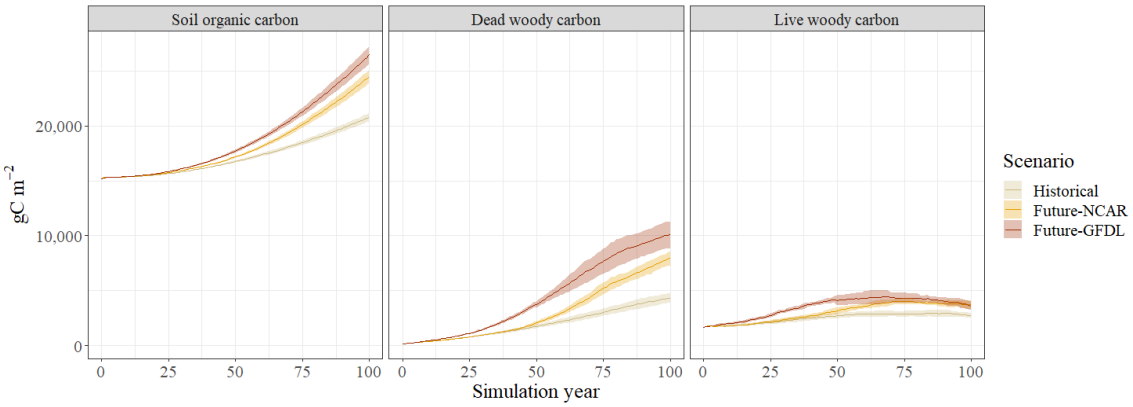

Figure 28. Average carbon across the landscape in soil carbon, dead woody carbon, and live woody carbon pools (gC m^{-2}) over time and compared across scenarios.

Burned Cell Trends

Twenty-five years postfire, within cells that burned one to three times, average annual aboveground net primary productivity was lower than net primary productivity for the overall landscape for each scenario ($p < 0.001$; Figure 29). When comparing trends between cells that had experienced differing amounts of fire (controlling for time since fire) during the simulation, there were significant differences in overall aboveground net primary productivity between cells that burned once and those that burned twice, across all climate change groups (all p-values < 0.001), with the single burn having the highest net primary productivity among numbers of fires. However, there were no significant differences between the two-burned and three-burned ($p_{hist}=0.56$, $p_{ncar}=0.83$, $p_{gfdl}=0.12$; Figure 29). Future scenarios had higher rates of net primary productivity relative to the historic scenario, regardless of the number of fires experienced (all p values < 0.01), and there were no significant differences between the two future climate groups for any number of fires ($p_{1fire}=0.19$, $p_{2fires}=0.72$, $p_{3fires}=0.07$).

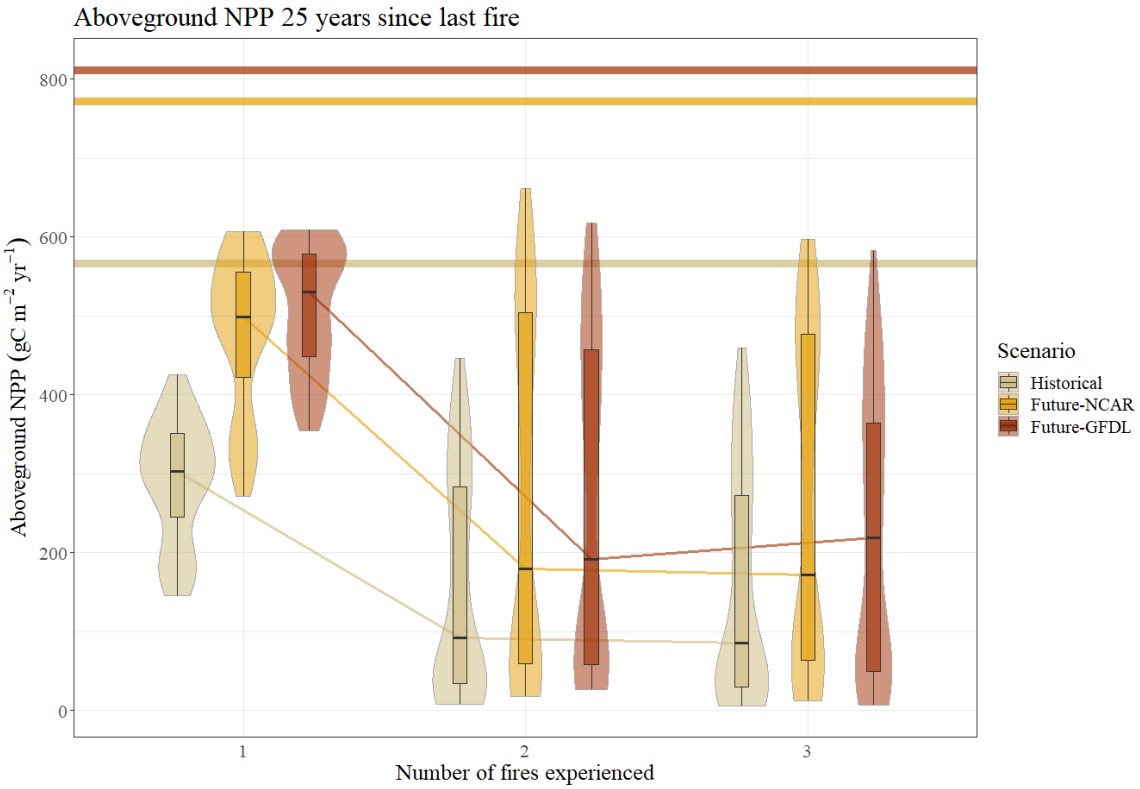

Figure 29. Aboveground net primary productivity for cells experiencing different numbers of fires across scenarios. Thin lines between boxplots connect median values between climate scenarios, and thick horizontal lines are equal to the overall landscape average aboveground net primary productivity for each scenario ($gCm^{-2}yr^{-1}$).

On average, the overall landscape had greater amounts of carbon than burned cells 25 years postfire within each scenario (all p-values < 0.001; Figure 30). Within burned cells, total carbon was greater under climate change regardless of the cumulative number of fires (all p-values < 0.001) and was greatest under the most extreme climate change scenario (GFDL; all p-values < 0.05). The reburned areas had the greatest variability in total carbon observed across all simulations, pointing toward varied trajectories in carbon storage within reburns. Overall, however, total carbon across reburns was mostly similar between numbers of fires, though there were significant differences between the one and three fire cells for the historic and Future-GFDL

scenarios (p=0.01 and p=0.03, respectively); increasing under historical climate and decreasing under Future-GFDL.

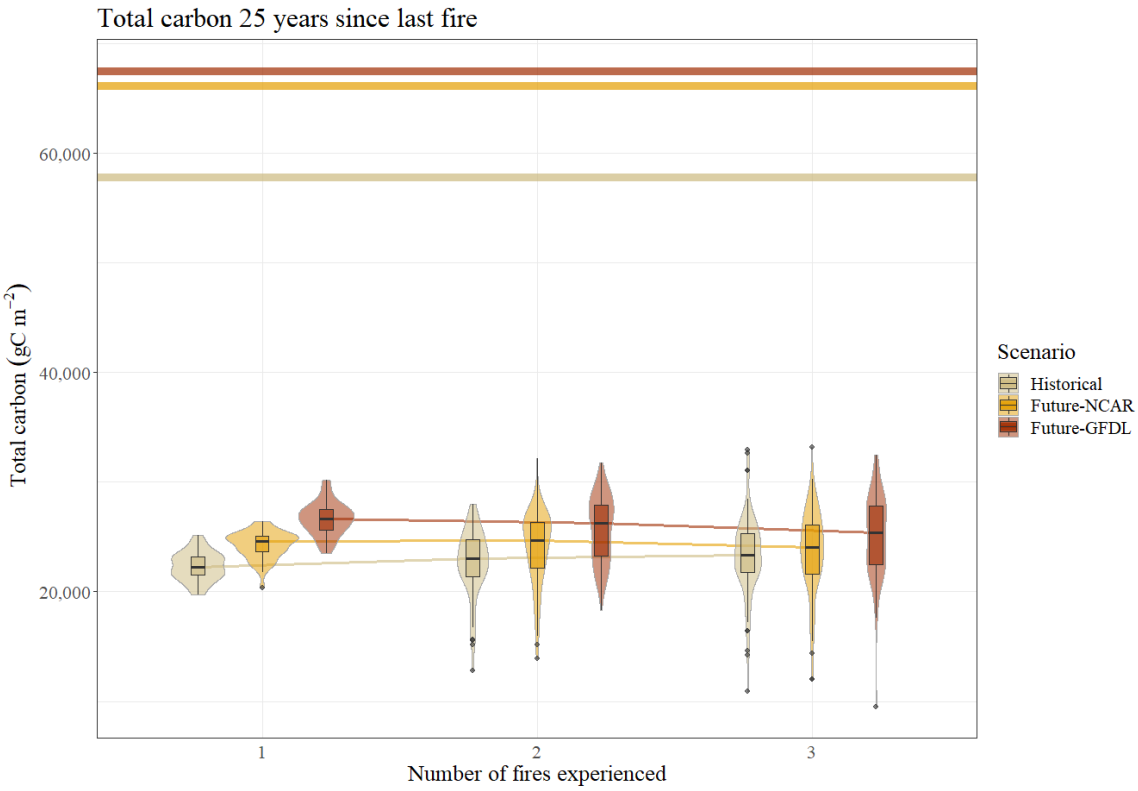

Figure 30. Boxplots of total carbon density for cells experiencing different numbers of fires across scenarios. Thin lines between boxplots connect median values between climate scenarios, and thick horizontal lines are equal to the overall landscape average total carbon for each scenario (gCm^{-2}).

Average annual rates of net ecosystem exchange within burned cells 25 postfire were in some cases similar to average landscape net ecosystem exchange within each scenario (Figure 31); rates were similar between the landscape average and a single fire under historical climate (p=0.74), and under both climate change scenarios, landscape averages were similar to all three burn frequencies (all p values > 0.1). Annual average rates of net ecosystem exchange increased with between one and two fires for all

scenarios (all p-values < 0.01) and one and three fires for all scenarios (all p-values < 0.05) but were similar between two and three fires for all scenarios (all p values > 0.1). Where significant differences did occur, there were increases in net ecosystem exchange between historical and climate change scenarios. Within each burn group, rates of net ecosystem exchange were significantly different between each pair of scenarios and increased from historical to future NCAR, and from future NCAR to future GFDL scenarios (all p-values < 0.001). Variability in the net ecosystem exchange also increased with the number of fires, especially for future scenarios.

Figure 31. Boxplots of net ecosystem exchange for cells experiencing different numbers of fires across scenarios. Thin lines between boxplots connect median values between climate scenarios, and thick horizontal lines are equal to the overall landscape average net ecosystem exchange for each scenario ($gCm^{-2}yr^{-1}$). Note that values are plotted on a log scale. This was done due to a large number of outliers which made comparison difficult to observe.

Discussion

Interior Alaska's boreal forest is temperature-limited in terms of productivity, with low temperatures that restrict biological activity and nutrient availability (Van Cleve & Yarie 1986). This study showed increases in net primary productivity under climate change scenarios, consistent with results from other modeling studies from northern temperate and boreal ecosystems (Duveneck & Thompson, 2017; Euskirchen et al., 2006; Peng & Apps, 1999; Reyer et al., 2014). Net primary productivity in boreal forests is influenced by multiple complex and interacting factors including climate change. Growing season length is one such factor, and past work found that under climate change, an increase in growing season length led to overall increases in annual primary productivity (Duveneck & Thompson, 2017; Euskirchen et al., 2006). There was not an increase in the growing season observed in this study, although growth rates in April were higher under climate change (Figure 25). In field experiments (Binkley et al., 1994; Hobbie et al., 2000) and modeling studies (Mekonnen et al., 2019; Peng & Apps, 1999), enhanced nitrogen mineralization from warming has also been linked to increased growth rates. This may have played a role here as warming increased thaw depths in permafrost-affected areas, freeing up stocks of soil organic material for mineralization. Stand age dynamics also play a role in the productivity of forest ecosystems. While very young stands tend to have relatively lower rates of productivity, net primary productivity tends to peak as they reach maturity (Goulden et al., 2011) and so the distribution of disturbances, temporally and spatially, can alter forest stand age composition at a landscape-scale, affecting overall net primary productivity.

Some past modeling work has incorporated positive effects of CO_2 fertilization into their modeling frameworks (Duveneck & Thompson, 2017; Euskirchen et al., 2006; Peng & Apps, 1999), which is not included in this study. Increasing concentrations of CO_2 are associated with increased growth rates and greater water use efficiency in plants until the point that the optimum growth temperature is surpassed (Eamus, 1991); however, enhanced growth can also reduce nutrient availability, slowing gains (Elmore et al., 2016). Peng & Apps, 1999 found that including CO_2 fertilization effects increased NPP by 35% for simulated forests in central Canada. However, there are still uncertainties as to whether and the extent to which elevated CO_2 levels will increase carbon sequestration in high latitude ecosystems, and where this is more likely to occur (Peñuelas et al., 2011). If NPP does increase significantly in response to increased CO_2 concentrations, this study could be underestimating carbon sequestration which would further counterbalance potential future soil carbon losses due to changes in the regional temperature regime and associated permafrost thaw.

Despite increasing fire activity across the landscape and increasing rates of soil respiration, live and dead woody carbon as well as total soil organic carbon increased over the simulation period and increase the most under climate change. This corresponds with elevated rates in primary productivity that were also observed under climate change, accelerating the accumulation of live carbon, which then contributes to the dead woody carbon pool once live vegetation dies, and eventually the soil organic carbon pool as that material beaks down. These carbon sources accumulated over the simulation period. This is in part, likely due to forest age also increasing over the simulation period, where on average stand age landscape-wide increases from less than 50 years at the start of the

simulation to between 73 and 82 years by the end of the century, depending on the scenario (Chapter 2, Figure 9, left panel). This is consistent with patterns of carbon accumulation in boreal landscapes, where older stands tend to hold more carbon (Alexander & Mack, 2016) and cool annual temperatures tend to allow material to accumulate more rapidly than it breaks down (Bradshaw & Warkentin, 2015; Hobbie et al., 2000), a pattern that was sustained in the simulations, even under climate change scenarios. Dead woody material comprised about 35% of aboveground carbon under historical climate, 40% under Future-NCAR, and 48% under Future-GFDL climate, ranging from approximately four to 10 kgm^{-2}, depending on the scenario (Figure 27). These values are consistent with field data from Manitoba, Canada, which found that dead woody material makes significant contributions to carbon storage, and they modeled that 10-60% of the deep carbon pool at upland sites, which contained an estimated 7-10 kgm^{-2}, was derived from dead woody biomass, although these levels of contribution are moderated by fire frequency, net primary productivity, and decay rates (Manies et al., 2005). Studies within the last decade have observed comparable amounts of carbon storage between different forest types in interior Alaska along chronosequences, with the rapid growth of broadleaf deciduous species compensating for belowground soil carbon losses over time (Alexander & Mack, 2016; Mack et al., 2021). Simulations in this study projected an increase in broadleaf deciduous dominance by the end of the century under climate change, a decline in non-forest vegetation type, and noted large increases in shrub and moss biomasses, all of which together could be driving increases in aboveground live carbon pools. Mosses and shrubs are two vegetation groups that are frequently neglected

from analyses of stocks in field modeling work in this region, though these findings lend support that they will potentially account for a substantial portion of total future carbon.

Despite overall increases in net primary productivity and corresponding increases in carbon stocks at the landscape scale, high rates of heterotrophic respiration counteracted this, ultimately resulting in a positive net ecosystem exchange across all scenarios. High rates of respiration were not only higher in the growing season but also persisted into the winter months in the climate change scenarios, reflecting higher winter temperatures under climate change. Early winter soil respiration has been quantified on the North Slope of Alaska as an increasing source of carbon emissions (Commane et al., 2017). Winter soil respiration across both the tundra and boreal Alaska was recently quantified in a separate study as accounting for 15% of regional soil respiration (Watts et al., 2021). Simulations indicate that these trends are likely to continue, making winter soil respiration an increasing source of CO_2 that should be accounted for in Earth System Models (Commane et al., 2017).

Also likely contributing to these increases in heterotrophic respiration were large increases in the amount of available soil organic carbon, which by the end of the century, converged with total soil carbon landscape-wide under climate change. This trend indicates large-scale permafrost thaw and a deepening of the active layer, freeing up a large and previously unavailable source of organic material. As deeper soil layers become unfrozen, this becomes an additional source of carbon that is susceptible to accelerated decomposition rates with increasing soil temperature (Davidson & Janssens, 2006; Fang & Moncrieff, 2001; Lloyd J., Taylor, 1994). These newly available deep soil carbon pools are particularly vulnerable to loss under climate change. Across a reburn gradient in

interior Alaska, Shabaga et al. (2022) noted that multiple fires resulted in increased soil temperature and soil respiration within these reburned sites. They found that reburn sites were more sensitive to temperature relative to mature sites, indicating that multiple fires accelerate the availability of deeper, more sensitive, soil pools to decomposition. Simulations from this study showed rates of net ecosystem increase with the number of fires and under climate change, indicating that respiration rates in this study are consistent with the accelerated rates of carbon loss within reburns observed in the field. Large-scale losses of permafrost and increasing active layer depth under climate change have been projected elsewhere at high latitudes using other models (Lawrence et al., 2008; McGuire et al., 2018) and a recent field study quantified the effect of including permafrost subsidence in estimates of thaw depths finding that accounting for subsidence increased estimated thawed carbon by between 37 and 113 percent (Rodenhizer et al., 2020). This lends further support to the concern that rapid degradation of permafrost will be a potentially large source of carbon emissions in the future.

Surprisingly, carbon stocks did not as a rule decline with a greater number of fires in these simulations; they become more variable and in under historic conditions were slightly elevated after the third fire when compared to one fire. One contributing factor to this was the higher rates of net primary productivity observed under climate change and given the large increases in shrub and moss biomasses also observed in the climate change simulation (Chapter 3, Figure 16), the levels of net primary productivity across the landscape include not only tree species, but also the understory. This trend toward increased shrub productivity under climate change is also reflected in field studies of shrub expansion on the North Slope of Alaska (Bunn & Goetz, 2006; Forbes et al., 2010;

Sturm et al., 2005; Tape et al., 2006). The understory may be driving a substantial proportion of the increases in net primary productivity following multiple fires within the boreal forest under a changing climate as well. These understory components in the boreal forest are increasingly proving to play important roles in overall carbon cycling and in areas that are experiencing a shifting disturbance regime. Shabaga et al. (2022) noted that understory plants were responsible for a large proportion of ecosystem productivity in recently burned and reburned sites, in part driven by greater light availability for understory plants postfire. They found that understory productivity was highest following one fire, even compared to a mature site. However, following the first fire event, subsequent fires yielded lower levels of productivity. Aboveground net primary productivity for burned cells in this study was found to be lower in reburned cells as well, although lacked the magnitude of the initial bump in productivity postfire that Shabaga et al. (2022) quantified, although it should be noted that their study accounted only for understory and ground vegetation productivity and respiration. These findings overall underscore the importance of assessing species and community dynamics and accounting for the effects of a broad range of vegetation types present when modeling the effects of climate change and fire on carbon balance.

Lastly, it is important to note that overall rates of soil respiration and net ecosystem exchange were exceptionally high across simulation scenarios, with respiration rates exceeding those of field studies from the region. For example, a recent study that used random forest modeling to impute soil respiration levels based on eddy covariance tower data found maximum levels of soil respiration around 400 $gCm^{-2}yr^{-1}$ for the 2016-2017 year (Watts et al., 2021), while within historical climate scenarios,

estimates of respiration averaged close to 500 gCm-2 month^{-1} in June and July, alone. Such high simulated rates of respiration prompt concerns over whether model calibration of this process has yielded results that sufficiently capture this process. Soil respiration was calibrated at the single-cell scale, which is a commonly accepted practice, and calibration results aligned well with flux measurements from field data (Lucash et al. *in prep*), however, issues of scaling up processes can present challenges to modelers, especially when complex parameter sets interact in a non-linear manner to drive processes (Gustafson, 2013; Urban, 2005). Therefore, it is recommended that respiration results presented here be interpreted with caution and the parameter set used in this study should be investigated further to better understand and report on the sensitivities of these model parameters.

This study had several limitations that should be considered along with the results. The interpretation of these simulation results is constrained by the assumptions inherent in the LANDIS-II modeling framework and DGS model extension. For example, DGS does not capture the effect of CO_2 fertilization on primary productivity, so estimates of net primary productivity exclude that potential influence. Additionally, DGS model outputs at the cell level do not separate carbon pools into above and belowground C stocks, so the cell-level analysis here is confined to examining differences between total carbon between different fire histories, making it difficult to determine how each pool at each site has responded to wildfire activity within these simulations and further understand what is driving the landscape level increases in carbon. For this reason, additional site-specific analysis should be undertaken upon the further development of

the DGS extension to verify and better understand the patterns in soil carbon from this experiment.

CHAPTER 5

CONCLUSIONS

These studies used the SCRPPLE and DGS model extensions to LANDIS-II to simulate above and belowground forest landscape processes that are currently underway within interior Alaska boreal forests: wildfire, vegetation succession, permafrost dynamics, and carbon dynamics. DGS captures these processes in a spatially explicit and interactive manner that is necessary for better understanding the relative importance of these processes and how they may respond to the pressures of climate change and increasing wildfire frequency.

Simulations of wildfire agree with other studies predicting increasing wildfire activity in western North America (Flannigan et al. 2005, Foster et al. 2022) as well as other large-scale modeling studies; that climate change promotes greater fire activity in this region. This study further builds on this understanding by examining the potential for continued fire activity in areas that have already burned within the last century. While pointed toward a negative vegetation feedback to fire based on stand age, more extreme climate change scenarios were more likely to burn within relatively younger stands that under less extreme climate scenarios and overall reburn rates increased under climate change.

This study also sought to model future successional trajectories in areas experiencing greater fire activity using random forest classification to predict shifts away from the dominant forest type at the start of the simulation, black spruce, following different numbers of fires. The percentage of biomass removed in the most recent fire

emerged as an important predictor variable of forest transition, and high levels of starting conifer biomass, as well as seed sources from surrounding cells, were important in moderating the impact of increasing fire activity. These simulations also showed large increases in willow and dwarf birch biomass across the landscape, indicating that interspecific dynamics with shrubs may play an increasingly important role in these ecosystems in the future. While shrub expansion under climate change has been noted in the tundra, it has been less explored in the boreal forest zone of interior Alaska, but future work could focus on better understanding the role of shrubs in a landscape undergoing change driven by an interacting combination of climatic factors and wildfire.

Simulations predicted increases in net primary productivity that are in part promoted by a large-scale shift to an alternative forest type (see Chapter 3). However, this was coupled with large increases in heterotrophic respiration, promoted by the thawing of permafrost and accelerated decomposition of deep, previously unavailable soil layers, which ultimately led to a positive net ecosystem exchange. Fire activity further exacerbated this effect and lowered net primary productivity after single fires and reburns even after more than two decades post-fire. Soil microbial feedbacks are an important process to include in earth system models, however, their representation is often relatively simplistic (e.g., confined to broad soil carbon pools representing 'passive', 'slow', and 'active' components with decomposition represented as a first-order decay function; Luo et al., 2016; Peng & Apps, 1999). The DGS model is the first to simulate temperature and soil moisture at user-defined depths down to 75 meters, and integrate those measurements with vegetation, fire, and soil with measurable C and N pools (including microbial pools). This is an important step in modeling this region and making

valuable predictions of future interactions and impacts of climate change. Future work refining the calibration of these processes will be useful to confirm the findings of this study and further explore underlying drivers of future trends.

APPENDIX A: SPECIES SIMULATED

Scientific Names	**Common Names**
Picea mariana	Black spruce
Picea glauca	White spruce
Betula neoalaskana	Alaska paper birch, resin birch
Populus tremuloides	Quaking aspen
Populus balsamifera	Balsam poplar
Larix laricina	Tamarack
Salix spp.	Willow
Alnus spp.	Alder
Betula nana	Dwarf birch
Sphagnum spp.	Sphagnum peatmoss
Feathermoss functional group includes: *Hylocomium* spp., *Pleurozium* spp., *Thuidium* spp., *Kindbergia* spp., *Brachythecium* spp.	Feathermoss
Turfmoss functional group. Includes: *Bryum* spp., *Mnium* spp., *Polytrichum* spp.	Turfmoss

Appendix Table 1. Species simulated in this study.

APPENDIX B: SCRPPLE PARAMETERIZATION GRAPHS

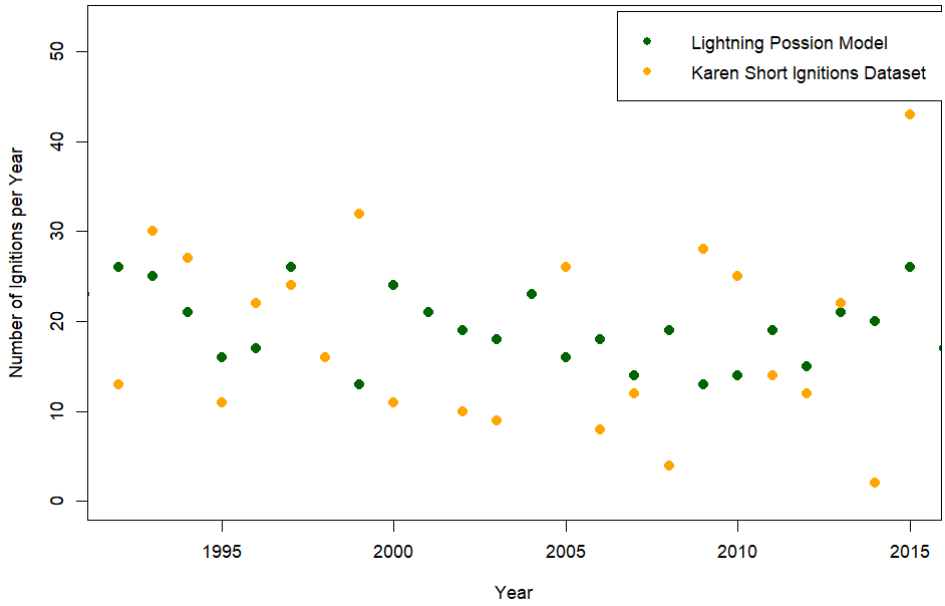

Appendix Figure 1. Comparison between reference lighting ignitions data (Short, 2021) and the number of ignitions modeled using a Poisson model relating fire weather index to the probability of ignition.

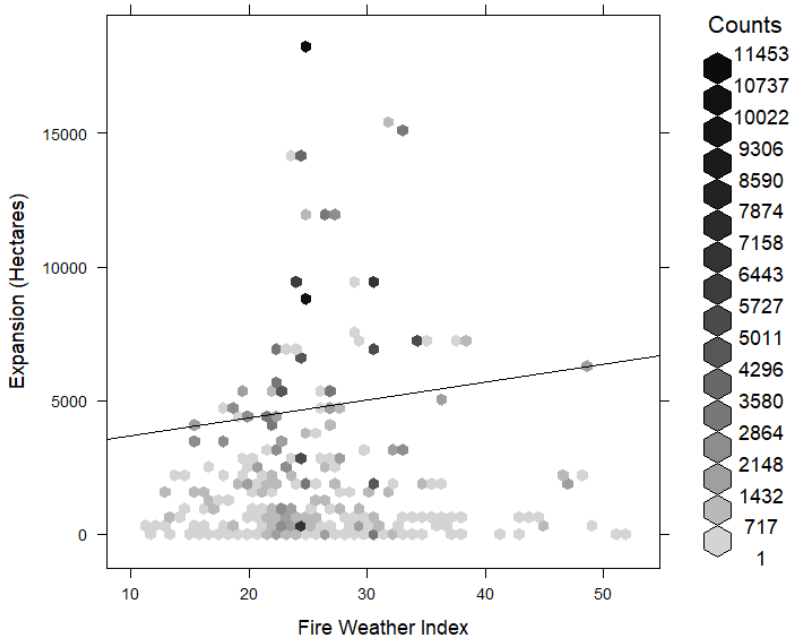

Appendix Figure 2. Modeled expansion (area of fire increase) response relative to the fire weather index for estimating SCRPPLE spread parameters. Expansion data was sourced from the GeoMac daily fire perimeters database (GeoMAC, 2019, 2020).

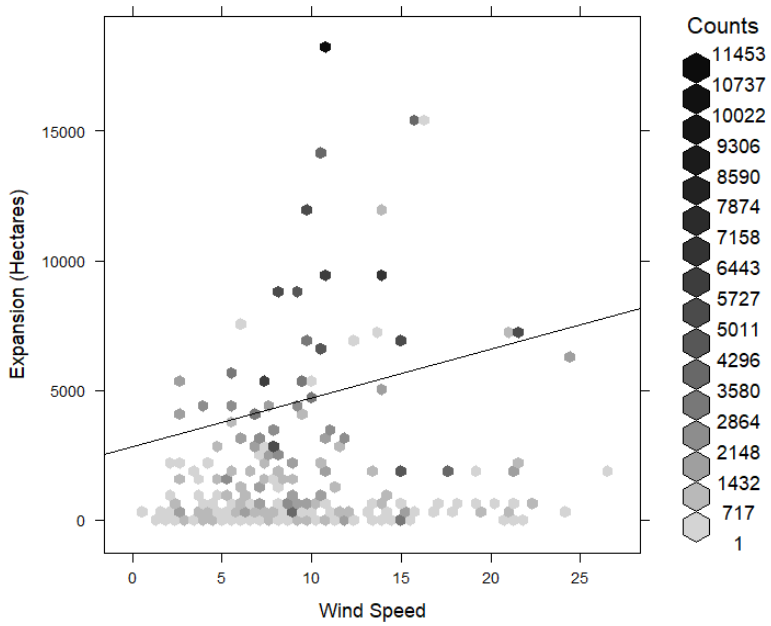

Appendix Figure 3. Modeled expansion (area of fire increase) response relative to wind speed for estimating SCRPPLE spread parameters. Expansion data was sourced from the GeoMac daily fire perimeters database (GeoMAC, 2019, 2020).

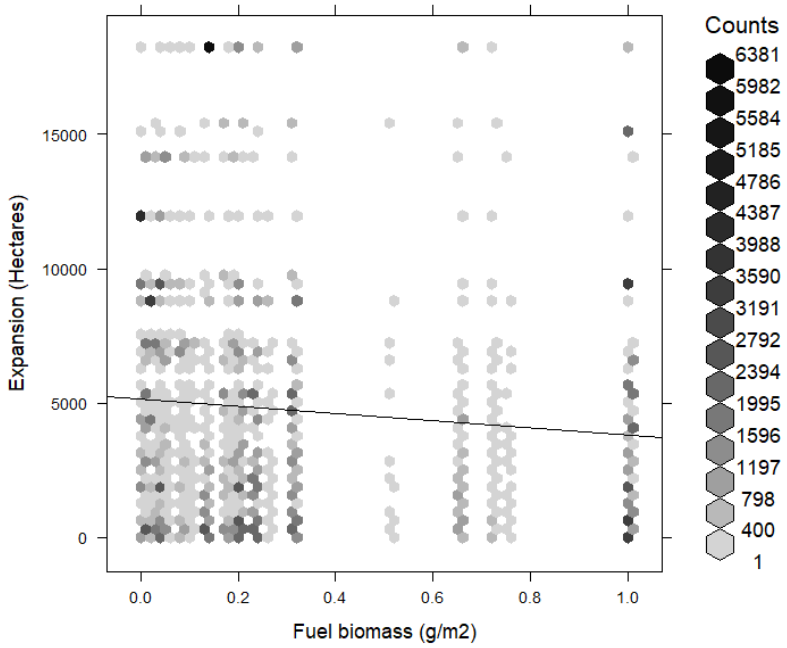

Appendix Figure 4. Modeled expansion (area of fire increase) response relative fuel biomass for estimating SCRPPLE spread parameters. Expansion data was sourced from a daily fire perimeters database (GeoMAC, 2019, 2020).

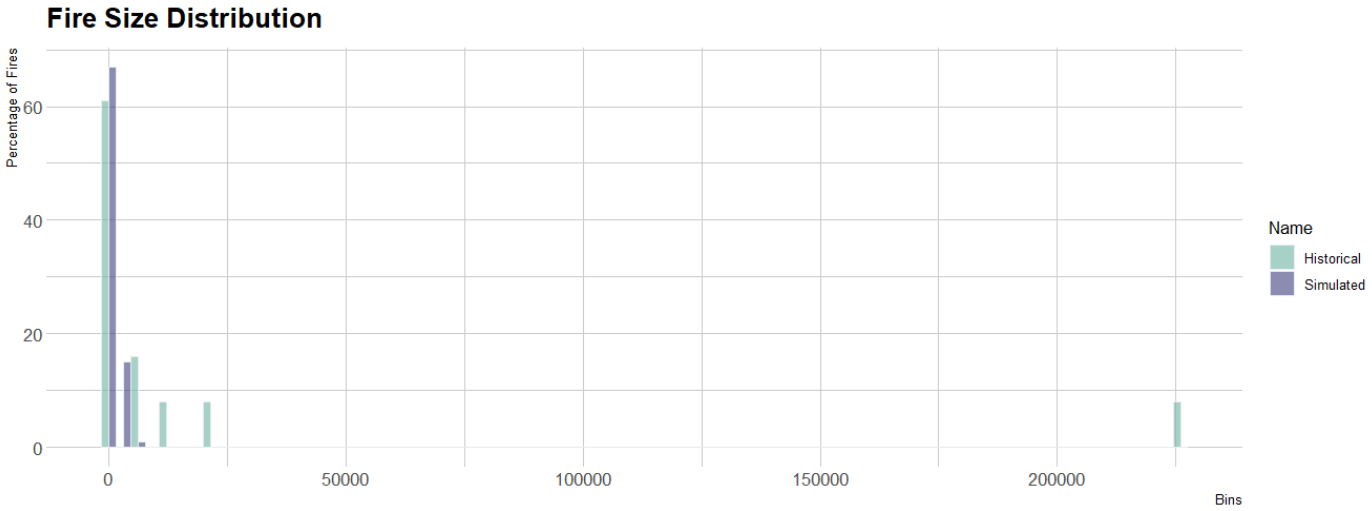

Appendix Figure 5. Resulting fire size distribution from all ten simulated historical replicates ("Simulated") compared with reference data from the Alaska Large Fires Database for the years 1970-2000 ("Historical", FRAMES, 2016).

APPENDIX C: SOIL TEMPERATURE AND SOIL MOISTURE RESPONSE CURVES FOR SPECIES FUNCTIONAL GROUPS

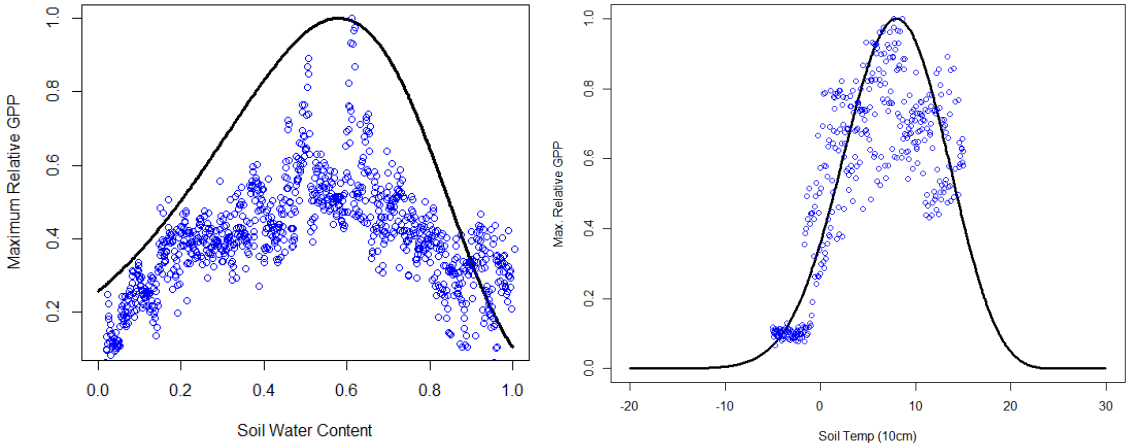

Appendix Figure 6. Conifer species functional type soil moisture (left; %) and soil temperature (right; Celsius) response curves (black), fit to Ameriflux data (blue) sampled at 10 cm from sites dominated by black spruce (US-Prr and US-Uaf; Kobayashi et al., 2019; Ueyama et al., 2018b).

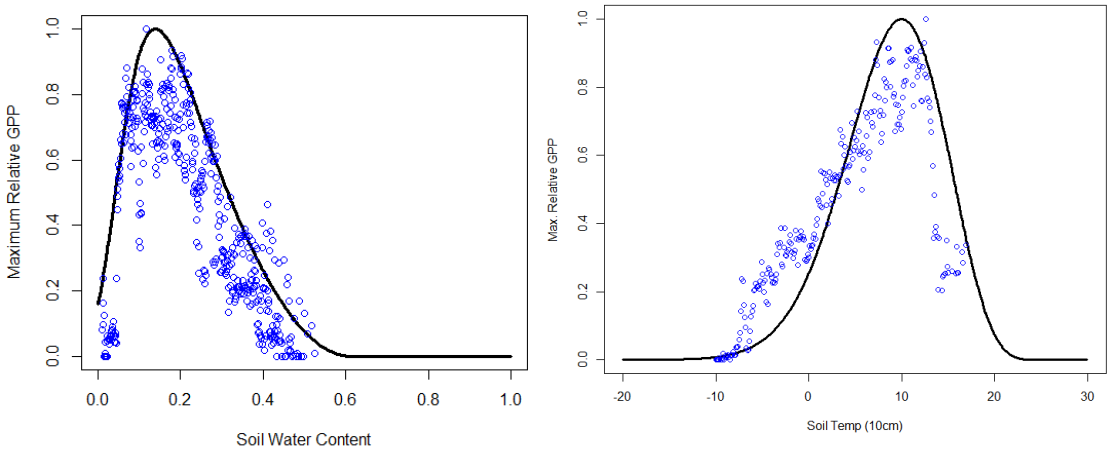

Appendix Figure 7. Broadleaf deciduous species functional type soil moisture (left; %) and soil temperature (right; Celsius) response curves (black), fit to Ameriflux data (blue) sampled at 10 cm from a site dominated by deciduous trees and shrubs (US-Rpf ; (Ueyama et al., 2019a).

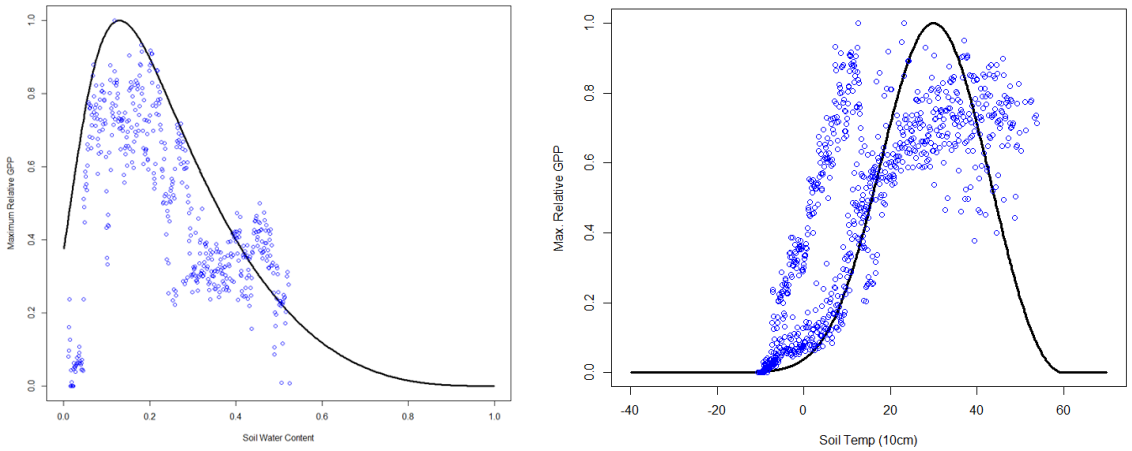

Appendix Figure 8. Shrub species functional type soil moisture (left; %) and soil temperature (right, Celsius) response curves (black), fit to Ameriflux data (blue) sampled at 10 cm from a site dominated by deciduous trees and shrubs, and open shrubland (US-Rpf and US-Fcr; Ueyama et al., 2019a, 2019b).

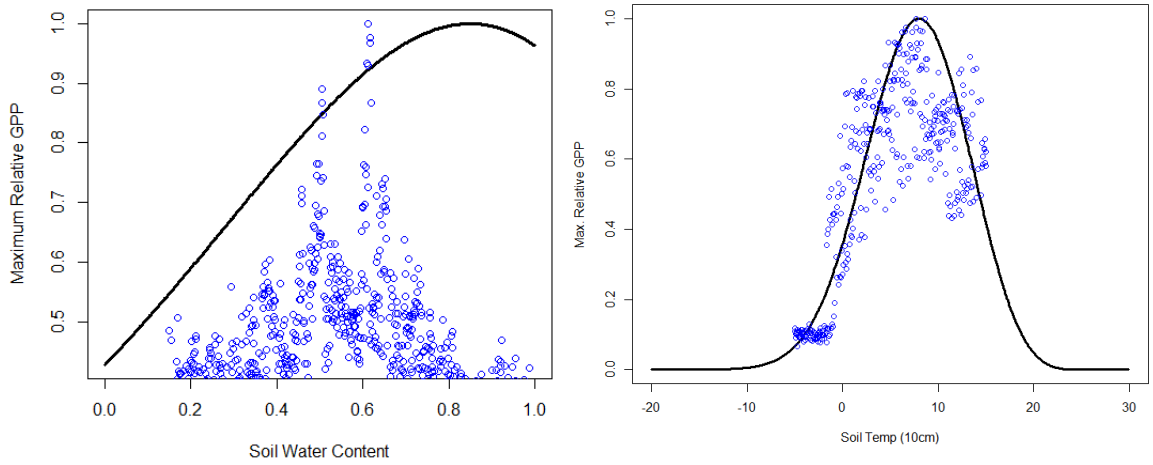

Appendix Figure 9. Moss species functional type soil moisture (left, %) and soil temperature (right, Celsius) response curves (black), fit to Ameriflux data (blue) sampled at 10 cm from a site dominated by mature black spruce, with the assumption that mosses would be associated with this forest type (US-Prr and US-Uaf; Kobayashi et al., 2019; Ueyama et al., 2018b). Soil water content curve was adjusted such that productivity does not substantially decline with greater soil moisture, with the understanding that mosses are often found in sites of very high moisture (e.g., bogs).

APPENDIX D: CALIBRATION OF SPECIES' GROWTH

To calibrate species growth trajectories, I ran a series of single-cell simulations populated with just a single, one year old cohort of the species of interest. The species of interest included one species from each modeled functional group (conifer, broadleaf deciduous, shrubs, mosses). The resulting biomass trends for each species were plotted and evaluated iteratively while adjusting variables with a range of uncertainty around them due to lack of data or literature values (KLAI, MaxANPP, FCFRAC, MAXLAI, and a competition index (K)) using an automated particle swarm optimization algorithm to choose the values on each run using the hydroPSO package in R (Zambrano-Bigiarini & Rojas, n.d.). Biomass trends were compared to the maximum relative biomasses of the species of interest plotted by stand age from FIA plot data, with the aim of the modeled trajectory matching the top edge of the FIA data. This method best captures the maximum growth potential, which will then be subject to internal factors (e.g., competition, moisture stress) during full-scale model runs.

Appendix Figure 10. Biomass growth trajectory (green) for black spruce compared to relative maximum biomasses of black spruce within FIA plots plotted by stand age.

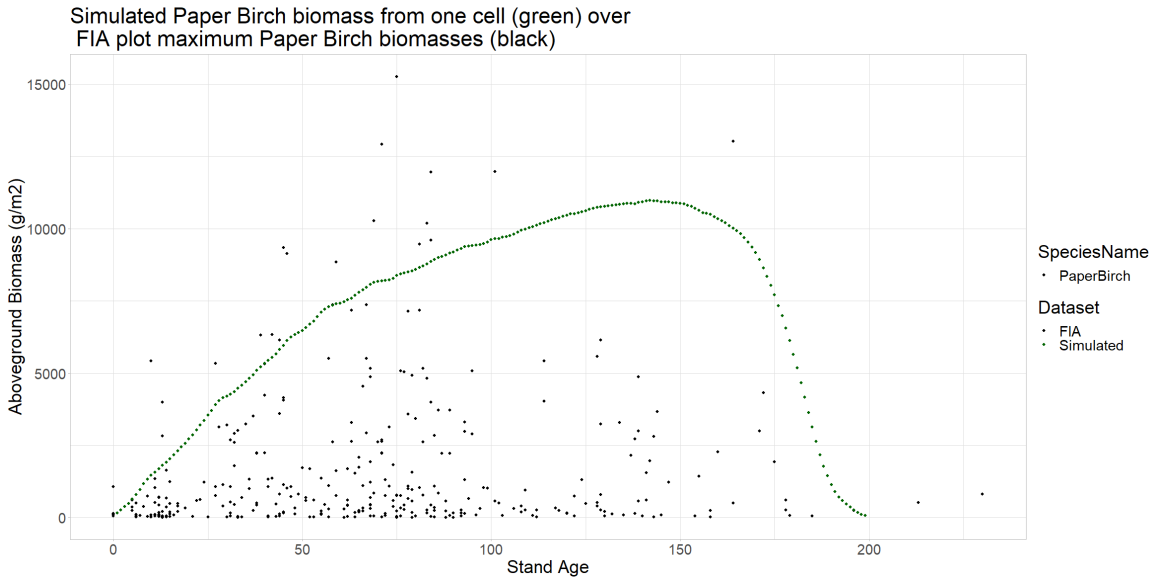

Appendix Figure 11. Biomass growth trajectory (green) for paper birch compared to relative maximum biomasses of paper within FIA plots plotted by stand age.

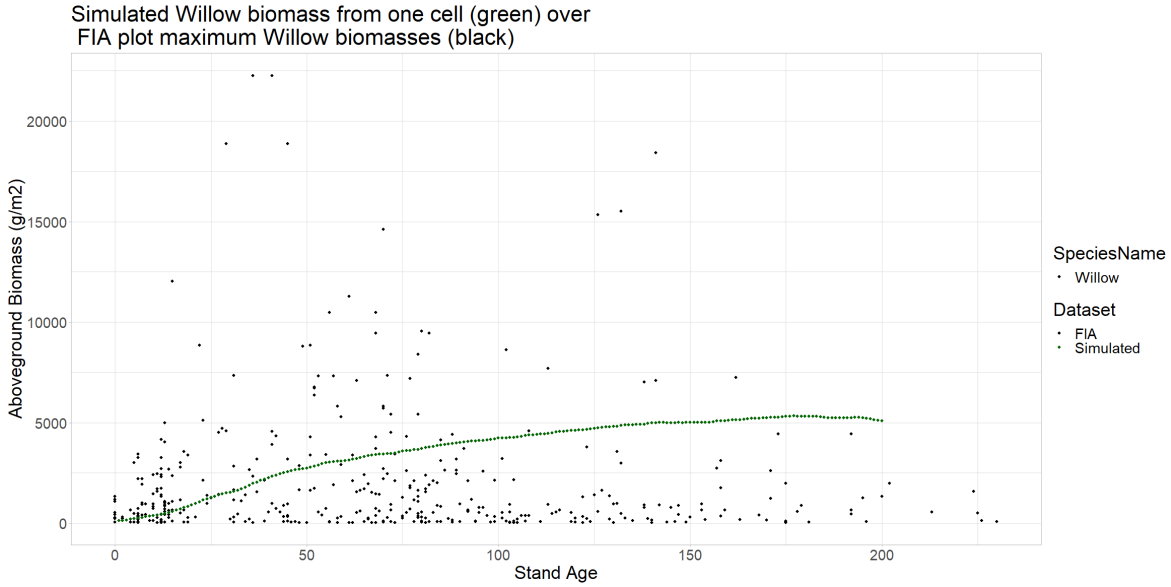

Appendix Figure 12. Biomass growth trajectory (green) for willow compared to relative maximum biomasses of willow within FIA plots plotted by stand age.

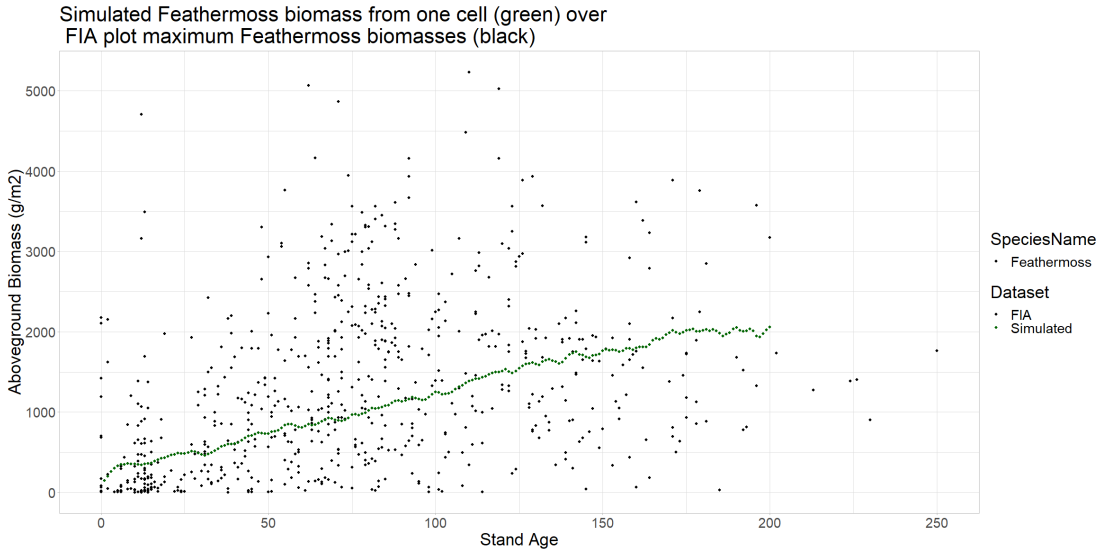

Appendix Figure 13. Biomass growth trajectory (green) for feathermoss compared to relative maximum biomasses of feathermoss within FIA plots plotted by stand age.

APPENDIX E: RANDOM FOREST CONDITIONAL PERMUTATION IMPORTANCE VALUES

	Conditional Permutation Importance		
Variable	**One Fire**	**Two Fires**	**Three Fires**
Percent biomass removed	0.032402135	0.049814947	0.012085409
Starting deciduous fraction	0.002179715	0.000272598	0.000782918
Aspect	9.36E-05	-2.21E-05	3.91E-06
Lowland vs Upland	1.78E-05	3.31E-05	-2.03E-05
Percent total carbon removed	1.71E-05	0.000982562	5.00E-04
Variance in total annual precipitation postfire	1.46E-05	4.38E-05	2.88E-05
Variance in mean annual temperature postfire	1.28E-05	1.67E-05	1.87E-19
Time 1 soil temperature at 3 m	1.25E-05	2.35E-05	3.56E-06
Variance in soil temperature 3m postfire	9.25E-06	-1.32E-05	3.06E-05
Soil temperature 3m postfire	3.91E-06	-2.31E-05	-3.56E-07
Mean annual temperature change	3.91E-06	-7.12E-07	-1.42E-06
GCM	2.85E-06	-3.56E-07	-1.78E-06
Mean annual temperature all years	2.49E-06	6.41E-06	4.27E-06
Total annual precipitation variance	7.12E-07	7.47E-06	5.69E-06
Scenario	7.12E-07	3.56E-07	0
Total annual precipitation postfire	7.12E-07	7.12E-06	7.47E-06
# Adjacent mature black spruce cells	3.56E-07	3.56E-07	1.60E-05
Scenario	3.56E-07	-7.12E-07	3.56E-07
Average total annual precipitation all years	-7.12E-07	-2.14E-06	-2.85E-06
Mean annual temperature postfire	-1.78E-06	-8.54E-06	-2.85E-06
Change in total annual precipitation	-2.14E-06	3.56E-07	-7.83E-06
Mean annual temperature variance all years	-2.85E-06	1.10E-05	-2.49E-06
Time 1 soil moisture at 0.55m	-2.85E-06	1.64E-05	-1.10E-05
Soil moisture at 0.55m	-9.61E-06	-3.91E-06	2.24E-05
Number of adjacent mature black spruce cells	-1.57E-05	0.000542705	0.000618861
Soil moisture variance at 0.55m postfire	-2.14E-05	-2.85E-06	-6.05E-05
Fire year	-3.63E-05	-2.31E-05	-2.49E-06

Appendix Table 2. Table of input variables for random forest models and corresponding conditional permutation importance values.

REFERENCES CITED

Abramoff, R. Z., Davidson, E. A., & Finzi, A. C. (2017). A parsimonious modular approach to building a mechanistic belowground carbon and nitrogen model. *Journal of Geophysical Research: Biogeosciences*, *122*(9), 2418–2434. https://doi.org/10.1002/2017JG003796/FORMAT/PDF

AKCCS. (2019). *Alaska Vegetation and Wetland Composite Map*. https://accscatalog.uaa.alaska.edu/dataset/alaska-vegetation-and-wetland-composite

Alexander, H. D., & Mack, M. C. (2016). A canopy shift in interior Alaskan boreal forests: consequences for above- and belowground carbon and nitrogen pools during post-fire succession. *Ecosystems*, *19*(1), 98–114. https://doi.org/10.1007/s10021-015-9920-7

Bachelet, D., Lenihan, J., Neilson, R., Drapek, R., & Kittel, T. (2005). Simulating the response of natural ecosystems and their fire regimes to climatic variability in Alaska. *Canadian Journal of Forest Research*, *35*(9), 2244–2257. https://doi.org/10.1139/x05-086

Balshi, M. S., McGuire, A. D., Duffy, P., Flannigan, M., Walsh, J., & Melillo, J. (2009). Assessing the response of area burned to changing climate in western boreal North America using a Multivariate Adaptive Regression Splines (MARS) approach. *Global Change Biology*, *15*(3), 578–600. https://doi.org/10.1111/j.1365-2486.2008.01679.x

Beck, P. S. A., Goetz, S. J., Mack, M. C., Alexander, H. D., Jin, Y., Randerson, J. T., & Loranty, M. M. (2011). The impacts and implications of an intensifying fire regime on Alaskan boreal forest composition and albedo. *Global Change Biology*, *17*, 2853–2866. https://doi.org/10.1111/j.1365-2486.2011.02412.x

Begét, J. E., Stone, D., & Verbyla, D. L. (2006). Regional overview of interior Alaska. In *Alaska's Changing Boreal Forest* (pp. 12–20).

Berner, L. T., Alexander, H. D., Loranty, M. M., Ganzlin, P., Mack, M. C., Davydov, S. P., & Goetz, S. J. (2015). Biomass allometry for alder, dwarf birch, and willow in boreal forest and tundra ecosystems of far northeastern Siberia and north-central Alaska. *Forest Ecology and Management*, *337*, 110–118. https://doi.org/10.1016/j.foreco.2014.10.027

Berner, L. T., Beck, P. S. A., Bunn, A. G., Lloyd, A. H., & Goetz, S. J. (2011). High-latitude tree growth and satellite vegetation indices: Correlations and trends in Russia and Canada (1982-2008). *Journal of Geophysical Research: Biogeosciences*, *116*(1), 1–13. https://doi.org/10.1029/2010JG001475

Bieniek, P. A., Bhatt, U. S., Walsh, J. E., Rupp, T. S., Zhang, J., Krieger, J. R., & Lader, R. (2016). Dynamical Downscaling of ERA-Interim Temperature and Precipitation for Alaska. *Journal of Applied Meteorology and Climatology*, *55*(3), 635–654. https://doi.org/10.1175/JAMC-D-15-0153.1

Binkley, D., Stottlemyer, R., Suarez, F., Cortina, J., & Taylor, P. (1994). Soil nitrogen availability in some arctic ecosystems in northwest Alaska: Responses to temperature and moisture. *Ecoscience*, *1*(1), 64–70.

Boby, L. A., Schuur, E. A. G., Mack, M. C., Verbyla, D., & Johnstone, J. F. (2010). Quantifying fire severity, carbon, and nitrogen emissions in Alaska' s boreal forest. *Ecological Applications*, *20*(6), 1633–1647.

Boyd, M. A., Berner, L. T., Doak, P., Goetz, S. J., Rogers, B. M., Wagner, D., Walker, X. J., & Mack, M. C. (2019). Impacts of climate and insect herbivory on productivity and physiology of trembling aspen (Populus tremuloides) in Alaskan boreal forests. *Environmental Research Letters*, *14*(8). https://doi.org/10.1088/1748-9326/ab215f

Bradshaw, C. J. A., & Warkentin, I. G. (2015). Global estimates of boreal forest carbon stocks and flux. *Global and Planetary Change*, *128*, 24–30. https://doi.org/10.1016/j.gloplacha.2015.02.004

Bret-Harte, M. S., Shaver, G. R., & Chapin, F. S. (2002). Primary and secondary stem growth in arctic shrubs: Implications for community response to environmental change. *Journal of Ecology*, *90*(2), 251–267. https://doi.org/10.1046/j.1365-2745.2001.00657.x

Brown, C. D., & Johnstone, J. F. (2012). Once burned, twice shy: Repeat fires reduce seed availability and alter substrate constraints on Picea mariana regeneration. *Forest Ecology and Management*, *266*, 34–41. https://doi.org/10.1016/j.foreco.2011.11.006

Bryant, J. P., Joly, K., Chapin, F. S., DeAngelis, D. L., & Kielland, K. (2014). Can antibrowsing defense regulate the spread of woody vegetation in arctic tundra? *Ecography*, *37*(3), 204–211. https://doi.org/10.1111/j.1600-0587.2013.00436.x

Buma, B., Hayes, K., Weiss, S., & Lucash, & M. (2022). Short-interval fires increasing in the Alaskan boreal forest as fire self-regulation decays across forest types. *Scientific Reports* |, *12*, 4901. https://doi.org/10.1038/s41598-022-08912-8

Bunn, A. G., & Goetz, S. J. (2006). Trends in satellite-observed circumpolar photosynthetic activity from 1982 to 2003: The influence of seasonality, cover type, and vegetation density. *Earth Interactions*, *10*(12), 1–19. https://doi.org/10.1175/EI190.1

Calef, M. P., Varvak, A., McGuire, A. D., Chapin, F. S., & Reinhold, K. B. (2015). Recent changes in annual area burned in interior Alaska: The impact of fire management. *Earth Interactions*, *19*(5), 1–17. https://doi.org/10.1175/EI-D-14-0025.1

Carmean, W. H., Hahn, J. T., & Jacobs, R. D. (1989). Site index curves for forest tree species in the eastern United States. *General Technical Report NC-128. St. Paul, MN: US Dept. of Agriculture, Forest Service, North Central Forest Experiment Station*, *128*.

Chapin, F. S., Callaghan, T. v., Bergeron, Y., Fukuda, M., Johnstone, J. F., Juday, G., & Zimov, S. A. (2004). Global change and the boreal forest: Thresholds, shifting states or gradual change? *Ambio*, *33*(6), 361–365. https://doi.org/10.1579/0044-7447-33.6.361

Chapin, F. S., Shaver, G. R., Giblin, A. E., Nadelhoffer, K. J., & Laundre, J. A. (1995). Responses of Arctic Tundra to Experimental and Observed Changes in Climate Published by : Wiley on behalf of the Ecological Society of America Stable URL : https://www.jstor.org/stable/1939337 REFERENCES Linked references are available on JSTOR for this a. *Ecology*, *76*(3), 694–711.

Christie, K. S., Bryant, J. P., Gough, L., Ravolainen, V. T., Ruess, R. W., & Tape, K. D. (2015). The Role of Vertebrate Herbivores in Regulating Shrub Expansion in the Arctic: A Synthesis. *BioScience*, *65*(12), 1123–1133. https://doi.org/10.1093/biosci/biv137

Commane, R., Lindaas, J., Benmergui, J., Luus, K. A., Chang, R. Y. W., Daube, B. C., Euskirchen, E. S., Henderson, J. M., Karion, A., Miller, J. B., Miller, S. M., Parazoo, N. C., Randerson, J. T., Sweeney, C., Tans, P., Thoning, K., Veraverbeke, S., Miller, C. E., & Wofsy, S. C. (2017). Carbon dioxide sources from Alaska driven by increasing early winter respiration from Arctic tundra. *Proceedings of the National Academy of Sciences of the United States of America*, *114*(21), 5361–5366. https://doi.org/10.1073/pnas.1618567114

Davidson, E. A., & Janssens, I. A. (2006). Temperature sensitivity of soil carbon decomposition and feedbacks to climate change. *Nature*, *440*(7081), 165–173. https://doi.org/10.1038/nature04514

Duveneck, M. J., & Thompson, J. R. (2017). Climate change imposes phenological trade-offs on forest net primary productivity. *Journal of Geophysical Research: Biogeosciences*, *122*(9), 2298–2313. https://doi.org/10.1002/2017JG004025

Eamus, D. (1991). The interaction of rising CO2 and temperatures with water use efficiency. *Plant, Cell, and the Environment*, *14*, 843–852.

Eliasson, P. E., McMurtrie, R. E., Pepper, D. A., Strömgren, M., Linder, S., & Ågren, G. I. (2005). The response of heterotrophic CO2 flux to soil warming. *Global Change Biology*, *11*(1), 167–181. https://doi.org/10.1111/j.1365-2486.2004.00878.x

Elmore, A. J., Nelson, D. M., & Craine, J. M. (2016). Earlier springs are causing reduced nitrogen availability in North American eastern deciduous forests. *Nature Plants*, *2*(10), 1–5. https://doi.org/10.1038/nplants.2016.133

Euskirchen, E. S., Mcguire, A. D., Chapin, F. S., Yi, S., & Thompson, C. C. (2009). Changes in vegetation in northern Alaska under scenarios of climate change, 2003-2100: implications for climate feedbacks. In *Ecological Applications* (Vol. 19, Issue 4).

Euskirchen, E. S., McGuire, A. D., Kicklighter, D. W., Zhuang, Q., Clein, J. S., Dargaville, R. J., Dye, D. G., Kimball, J. S., McDonald, K. C., Melillo, J. M., Romanovsky, V. E., & Smith, N. v. (2006). Importance of recent shifts in soil thermal dynamics on growing season length, productivity, and carbon sequestration in terrestrial high-latitude ecosystems. *Global Change Biology*, *12*(4), 731–750. https://doi.org/10.1111/j.1365-2486.2006.01113.x

Fang, C., & Moncrieff, J. B. (2001). The dependence of soil CO2 efflux on temperature. *Soil Biology and Biochemistry*, *33*(2), 155–165. https://doi.org/10.1016/S0038-0717(00)00125-5

Fastie, C. L., & Ott, R. A. (2006). Successional Processes in the Alaskan Boreal Forest. In *Alaska's Changing Boreal Forest* (Issue May). https://doi.org/10.1093/oso/9780195154313.003.0012

Fisher, J. P., Estop-Aragonés, C., Thierry, A., Charman, D. J., Wolfe, S. A., Hartley, I. P., Murton, J. B., Williams, M., & Phoenix, G. K. (2016). The influence of vegetation and soil characteristics on active-layer thickness of permafrost soils in boreal forest. *Global Change Biology*, *22*(9), 3127–3140. https://doi.org/10.1111/gcb.13248

Flannigan, M. D., Krawchuk, M. A., de Groot, W. J., Wotton, B. M., & Gowman, L. M. (2009). Implications of changing climate for global wildland fire. *International Journal of Wildland Fire*, *18*(5), 483–507. https://doi.org/10.1071/WF08187

Flannigan, M., Stocks, B., Turetsky, M., & Wotton, M. (2009). Impacts of climate change on fire activity and fire management in the circumboreal forest. *Global Change Biology*, *15*(3), 549–560. https://doi.org/10.1111/j.1365-2486.2008.01660.x

Flerchinger, G. N. (2000). *The Simultaneous Heat and Water (SHAW) Model: Technical Documentation*.

Forbes, B. C., Fauria, M. M., & Zetterberg, P. (2010). Russian Arctic warming and "greening" are closely tracked by tundra shrub willows. *Global Change Biology*, *16*(5), 1542–1554. https://doi.org/10.1111/j.1365-2486.2009.02047.x

Foster, A. C., Armstrong, A. H., Shuman, J. K., Shugart, H. H., Rogers, B. M., Mack, M. C., Goetz, S. J., & Ranson, K. J. (2019). Importance of tree- and species-level interactions with wildfire, climate, and soils in interior Alaska: Implications for forest change under a warming climate. *Ecological Modelling*, *409*(August), 108765. https://doi.org/10.1016/j.ecolmodel.2019.108765

Foster, A. C., Shuman, J. K., Rogers, B. M., Walker, X. J., Mack, M. C., Bourgeau-Chavez, L. L., Veraverbeke, S., & Goetz, S. J. (2022). Bottom-up drivers of future fire regimes in western boreal North America. *Environmental Research Letters*, *17*(2). https://doi.org/10.1088/1748-9326/ac4c1e

FRAMES. (2016). *The Alaska Large Fire Database*.

Frank, P. (2020). *Herbivory Moderates the Positive Effect of Climate Warming on Shrub Growth in Northern Interior Alaska* (Issue May).

Genet, H., McGuire, A. D., Barrett, K., Breen, A., Euskirchen, E. S., Johnstone, J. F., Kasischke, E. S., Melvin, A. M., Bennett, A., Mack, M. C., Rupp, T. S., Schuur, A. E. G., Turetsky, M. R., & Yuan, F. (2013). Modeling the effects of fire severity and climate warming on active layer thickness and soil carbon storage of black spruce forests across the landscape in interior Alaska. *Environmental Research Letters*, *8*(4). https://doi.org/10.1088/1748-9326/8/4/045016

GeoMAC. (2019). *Historic Perimeters Combined 2000-2018. U.S. Geological Survey*. . https://data-nifc.opendata.arcgis.com/datasets/nifc::historic-perimeters-combined-2000-2018/about

GeoMAC. (2020). *Historic Perimeters 2019, U.S. Geological Survey*. https://data-nifc.opendata.arcgis.com/datasets/nifc::historic-perimeters-2019/about

Goulden, M. L., Mcmillan, A. M. S., Winston, G. C., Rocha, A. v., Manies, K. L., Harden, J. W., & Bond-Lamberty, B. P. (2011). Patterns of NPP, GPP, respiration, and NEP during boreal forest succession. *Global Change Biology*, *17*(2), 855–871. https://doi.org/10.1111/j.1365-2486.2010.02274.x

Goulden, M. L., Wofsy, S. C., Harden, J. W., Trumbore, S. E., Crill, P. M., Gower, S. T., Fries, T., Daube, B. C., Fan, S. M., Sutton, D. J., Bazzaz, A., & Munger, J. W. (1998). Sensitivity of boreal forest carbon balance to soil thaw. *Science*, *279*(5348), 214–217. https://doi.org/10.1126/science.279.5348.214

Greene, D. F., Macdonald, S. E., Haeussler, S., Domenicano, S., Noël, J., Jayen, K., Charron, I., Gauthier, S., Hunt, S., Gielau, E. T., Bergeron, Y., & Swift, L. (2007). The reduction of organic-layer depth by wildfire in the North American boreal forest and its effect on tree recruitment by seed. *Canadian Journal of Forest Research*, *37*(6), 1012–1023. https://doi.org/10.1139/X06-245

Gudmundsson, L., & Gudmundsson, M. L. (2012). Package 'qmap.' *Methods*, *2012*(16), 3383–3390.

Gustafson, E. J. (2013). When relationships estimated in the past cannot be used to predict the future: using mechanistic models to predict landscape ecological dynamics in a changing world. *Landscape Ecology*, *28*, 1429–1437. https://doi.org/10.1007/s10980-013-9927-4

Hansen, W. D., Fitzsimmons, R., Olnes, J., & Williams, A. P. (2021). An alternate vegetation type proves resilient and persists for decades following forest conversion in the North American boreal biome. *Journal of Ecology*, *109*(1), 85–98. https://doi.org/10.1111/1365-2745.13446

Harden, J. W., Trumbore, S. E., Stocks, B. J., Hirsch, A., Gower, S. T., O'Neill, K. P., & Kasischke, E. S. (2000). The role of fire in the boreal carbon budget. *Global Change Biology*, *6*(SUPPLEMENT 1), 174–184. https://doi.org/10.1046/j.1365-2486.2000.06019.x

Hart, S. J., Henkelman, J., McLoughlin, P. D., Nielsen, S. E., Truchon-Savard, A., & Johnstone, J. F. (2019). Examining forest resilience to changing fire frequency in a fire-prone region of boreal forest. *Global Change Biology*, *25*(3), 869–884. https://doi.org/10.1111/gcb.14550

Hayes, K., & Buma, B. (2021). Effects of short-interval disturbances continue to accumulate, overwhelming variability in local resilience. *Ecosphere*, *12*(3). https://doi.org/10.1002/ecs2.3379

Héon, J., Arseneault, D., & Parisien, M. A. (2014). Resistance of the boreal forest to high burn rates. *Proceedings of the National Academy of Sciences of the United States of America*, *111*(38), 13888–13893. https://doi.org/10.1073/pnas.1409316111

Hessilt, T. D., Abatzoglou, J. T., Chen, Y., Randerson, J. T., Scholten, R. C., van der Werf, G., & Veraverbeke, S. (2022). Future increases in lightning ignition efficiency and wildfire occurrence expected from drier fuels in boreal forest ecosystems of western North America. *Environmental Research Letters*, *17*(5). https://doi.org/10.1088/1748-9326/ac6311

Higuera, P. E., Brubaker, L. B., Anderson, P. M., Hu, F. S., & Brown, T. A. (2009). Vegetation mediated the impacts of postglacial climate change on fire regimes in the south-central Brooks Range, Alaska. *Ecological Monographs*, *79*(2), 201–219. https://doi.org/10.1890/07-2019.1

Hinzman, L. D., Viereck, L. A., Adams, P. C., Romanovsky, V. E., & Yoshikawa, K. (2006). Climate and permafrost dynamics of the Alaskan boreal forest. In F. S. Chapin, M. W. Oswood, K. van Cleve, L. A. Viereck, & D. L. Verbyla (Eds.), *Alaska's Changing Boreal Forest* (pp. 39–61). Oxford University Press.

Hobbie, S. E., Schimel, J. P., Trumbore, S. E., & Randerson, J. R. (2000). Controls over carbon storage and turnover in high-latitude soils. *Global Change Biology*, *6*(S1), 196–210. https://doi.org/10.1046/j.1365-2486.2000.06021.x

Hoecker, T. J., & Turner, M. G. (2022). A short-interval reburn catalyzes departures from historical structure and composition in a mesic mixed-conifer forest. *Forest Ecology and Management*, *504*. https://doi.org/10.1016/j.foreco.2021.119814

Hollingsworth, T. N., Johnstone, J. F., Bernhardt, E. L., & Chapin, F. S. (2013). Fire Severity Filters Regeneration Traits to Shape Community Assembly in Alaska's Boreal Forest. *PLoS ONE*, *8*(2). https://doi.org/10.1371/journal.pone.0056033

Hoy, E. E., Turetsky, M. R., & Kasischke, E. S. (2016). More frequent burning increases vulnerability of Alaskan boreal black spruce forests. *Environmental Research Letters*, *11*(9). https://doi.org/10.1088/1748-9326/11/9/095001

Hu, F. S., Brubaker, L. B., Gavin, D. G., Higuera, P. E., Lynch, J. A., Rupp, T. S., & Tinner, W. (2006). How climate and vegetation influence the fire regime of the Alaskan boreal biome: The Holocene perspective. *Mitigation and Adaptation Strategies for Global Change*, *11*(4), 829–846. https://doi.org/10.1007/s11027-005-9015-4

Johnston, W. F. (1971). *Management guide for the Black Spruce type in the Lake States. Research Paper NC-64*. *NC-64*, 12.

Johnstone, J., Boby, L., Tissier, E., Mack, M., Verbyla, D., & Walker, X. (2009). Postfire seed rain of black spruce, a semiserotinous conifer, in forests of interior Alaska. *Canadian Journal of Forest Research*, *39*(8), 1575–1588. https://doi.org/10.1139/X09-068

Johnstone, J. F., Allen, C. D., Franklin, J. F., Frelich, L. E., Harvey, B. J., Higuera, P. E., Mack, M. C., Meentemeyer, R. K., Metz, M. R., Perry, G. L. W., Schoennagel, T., & Turner, M. G. (2016). Changing disturbance regimes, ecological memory, and forest resilience. *Frontiers in Ecology and the Environment*, *14*(7), 369–378. https://doi.org/10.1002/fee.1311

Johnstone, J. F., Celis, G., Chapin, F. S., Hollingsworth, T. N., Jean, M., & Mack, M. C. (2020). Factors shaping alternate successional trajectories in burned black spruce forests of Alaska. *Ecosphere*, *11*(5). https://doi.org/10.1002/ecs2.3129

Johnstone, J. F., & Chapin, F. S. (2006a). Effects of soil burn severity on post-fire tree recruitment in boreal forest. *Ecosystems*, *9*(1), 14–31. https://doi.org/10.1007/s10021-004-0042-x

Johnstone, J. F., & Chapin, F. S. (2006b). Fire interval effects on successional trajectory in boreal forests of northwest Canada. *Ecosystems*, *9*(2), 268–277. https://doi.org/10.1007/s10021-005-0061-2

Johnstone, J. F., Chapin, F. S., Hollingsworth, T. N., Mack, M. C., Romanovsky, V., & Turetsky, M. (2010). Fire, climate change, and forest resilience in interior Alaska. *Canadian Journal of Forest Research*, *40*, 1302–1312. https://doi.org/10.1139/X10-061

Johnstone, J. F., Hollingsworth, T. N., Chapin, F. S., & Mack, M. C. (2010). Changes in fire regime break the legacy lock on successional trajectories in Alaskan boreal forest. *Global Change Biology*, *16*, 1281–1295. https://doi.org/10.1111/j.1365-2486.2009.02051.x

Jorgenson, M. T., Romanovsky, V., Harden, J., Shur, Y., Donnell, J. O., Schuur, E. A. G., & Kanevskiy, M. (2010). Resilience and vulnerability of permafrost to climate change. *Canadian Journal of Forest Research*, *40*, 1219–1236.

Kasischke, E. S., Verbyla, D. L., Rupp, T. S., Mcguire, A. D., Murphy, K. A., Jandt, R., Barnes, J. L., Hoy, E. E., Duffy, P. A., Calef, M., & Turetsky, M. R. (2010). Alaska's changing fire regime - implications for the vulnerability of its boreal forests. *Canadian Journal of Forest Research*, *40*, 1313–1324.

Kelly, R., Chipman, M. L., Higuera, P. E., Stefanova, I., Brubaker, L. B., & Hu, F. S. (2013). Recent burning of boreal forests exceeds fire regime limits of the past 10,000 years. *Proceedings of the National Academy of Sciences of the United States of America*, *110*(32), 13055–13060. https://doi.org/10.1073/pnas.1305069110

Kobayashi, H., Ikawa, H., & Suzuki, R. (2019). *AmeriFlux BASE US-Prr Poker Flat Research Range Black Spruce Forest (Dataset)*. https://doi.org/https://doi.org/10.17190/AMF/1246153

Koven, C. D., Ringeval, B., Friedlingstein, P., Ciais, P., Cadule, P., Khvorostyanov, D., Krinner, G., & Tarnocai, C. (2011). Permafrost carbon-climate feedbacks accelerate global warming. *Proceedings of the National Academy of Sciences of the United States of America*, *108*(36), 14769–14774. https://doi.org/10.1073/pnas.1103910108

Kurkowski, T. A., Mann, D. H., Rupp, T. S., & Verbyla, D. L. (2008). Relative importance of different secondary successional pathways in an Alaskan boreal forest. *Canadian Journal of Forest Research*, *38*(7), 1911–1923. https://doi.org/10.1139/X08-039

Kurz, W. A., Stinson, G., & Rampley, G. (2008). Could increased boreal forest ecosystem productivity offset carbon losses from increased disturbances? *Philosophical Transactions of the Royal Society B: Biological Sciences*, *363*(1501), 2261–2269. https://doi.org/10.1098/rstb.2007.2198

Lader, R., Walsh, J. E., Bhatt, U. S., & Bieniek, P. A. (2017). Projections of Twenty-First-Century Climate Extremes for Alaska via Dynamical Downscaling and Quantile Mapping. *Journal of Applied Meteorology and Climatology*, *56*(9), 2393–2409. https://doi.org/10.1175/JAMC-D-16-0415.1

Lawrence, D. M., Slater, A. G., Romanovsky, V. E., & Nicolsky, D. J. (2008). Sensitivity of a model projection of near-surface permafrost degradation to soil column depth and representation of soil organic matter. *Journal of Geophysical Research: Earth Surface*, *113*(2), 1–14. https://doi.org/10.1029/2007JF000883

Lenton, T. M. (2012). Arctic climate tipping points. *Ambio*, *41*(1), 10–22. https://doi.org/10.1007/s13280-011-0221-x

Lloyd J., Taylor, J. A. (1994). On the Temperature Dependence of Soil Respiration Author (s): J . Lloyd and J . A . Taylor Published by : British Ecological Society Stable URL : http://www.jstor.org/stable/2389824 REFERENCES Linked references are available on JSTOR for this article : *Functional Ecology*, *8*(3), 315–323.

Lucash, M. S., Ruckert, K. L., Nicholas, R. E., Scheller, R. M., & Smithwick, E. A. H. (2019). Complex interactions among successional trajectories and climate govern spatial resilience after severe windstorms in central Wisconsin, USA. *Landscape Ecology*, *34*(12), 2897–2915. https://doi.org/10.1007/s10980-019-00929-1

Lucash, M. S., Scheller, R. M., J. Gustafson, E., & R. Sturtevant, B. (2017). Spatial resilience of forested landscapes under climate change and management. *Landscape Ecology*, *32*(5), 953–969. https://doi.org/10.1007/s10980-017-0501-3

Luo, Y., Ahlström, A., Allison, S. D., Batjes, N. H., Brovkin, V., Carvalhais, N., Chappell, A., Ciais, P., Davidson, E. A., Finzi, A., Georgiou, K., Guenet, B., Hararuk, O., Harden, J. W., He, Y., Hopkins, F., Jiang, L., Koven, C., Jackson, R. B., … Zhou, T. (2016). Toward more realistic projections of soil carbon dynamics by Earth system models. *Global Biogeochemical Cycles*, 40–56. https://doi.org/10.1002/2015GB005239.Received

Lynch, J. A., Clark, J. S., Bigelow, N. H., Edwards, M. E., & Finney, B. P. (2002). Geographic and temporal variations in fire history in boreal ecosystems of Alaska. *Journal of Geophysical Research*, *107*, 8152. https://doi.org/10.1029/2001jd000332

Mack, M. C., Treseder, K. K., Manies, K. L., Harden, J. W., Schuur, E. A. G., Vogel, J. G., Randerson, J. T., & Iii, F. S. C. (2008). Recovery of Aboveground Plant Biomass and Productivity After Fire in Mesic and Dry Black Spruce Forests of Interior Alaska. *Ecosystems*, *11*, 209–225. https://doi.org/10.1007/s10021-007-9117-9

Mack, M. C., Walker, X. J., Johnstone, J. F., Alexander, H. D., Melvin, A. M., Jean, M., & Miller, S. N. (2021). Carbon loss from boreal forest wildfires offset by increased dominance of deciduous trees. *Science*, *372*, 280–283. http://science.sciencemag.org/

Maechler, M., Rousseeuw, P., Struyf, A., Hubuert, M., & Hornik, K. (2021). *cluster: Cluster Analysis Basics and Extensions. R package version 2.1.2.*

Manies, K. L., Harden, J. W., Bond-Lamberty, B. P., & O'Neill, K. P. (2005). Woody debris along an upland chronosequence in boreal Manitoba and its impact on long-term carbon storage. *Canadian Journal of Forest Research*, *35*(2), 472–482. https://doi.org/10.1139/x04-179

Mann, D., Rupp, T., Olson, M., & Duffy, P. (2012). Is Alaska's boreal forest now crossing a major ecological threshold? *Arctic, Antarctic, and Alpine Research*, *44*(3), 319–331. https://doi.org/10.1657/1938-4246-44.3.319

Marchenko, S., Romanovsky, V., & Tipenko, G. (2008). Numerical modeling of spatial permafrost dynamics in Alaska. *Proceedings of the Ninth International Conference on Permafrost*, *29*, 1125–1130.

Marshall, A. M., Link, T. E., Flerchinger, G. N., & Lucash, M. S. (2021). Importance of parameter and climate data uncertainty for future changes in boreal hydrology. *Water Resources Research*, *57*(8), 1–20. https://doi.org/10.1029/2021WR029911

McGuire, A. D., Lawrence, D. M., Koven, C., Clein, J. S., Burke, E., Chen, G., Jafarov, E., MacDougall, A. H., Marchenko, S., Nicolsky, D., Peng, S., Rinke, A., Ciais, P., Gouttevin, I., Hayes, D. J., Ji, D., Krinner, G., Moore, J. C., Romanovsky, V., … Zhuang, Q. (2018). Dependence of the evolution of carbon dynamics in the northern permafrost region on the trajectory of climate change. *Proceedings of the National Academy of Sciences of the United States of America*, *115*(15), 3882–3887. https://doi.org/10.1073/pnas.1719903115

Mekonnen, Z. A., Riley, W. J., Randerson, J. T., Grant, R. F., & Rogers, B. M. (2019). Expansion of high-latitude deciduous forests driven by interactions between climate warming and fire. *Nature Plants*, *5*(9), 952–958. https://doi.org/10.1038/s41477-019-0495-8

Melillo, J. M., Frey, S. D., DeAngelis, K. M., Werner, W. J., Bernard, M. J., Bowles, F. P., Pold, G., Knorr, M. A., & Grandy, A. S. (2017). Long-term pattern and magnitude of soil carbon feedback to the climate system in a warming world. *Science*, *358*(6359), 101–105. https://doi.org/10.1126/science.aan2874

Melvin, A. M., Mack, M. C., Johnstone, J. F., David McGuire, A., Genet, H., & Schuur, E. A. G. (2015). Differences in ecosystem carbon distribution and nutrient cycling linked to forest tree species composition in a mid-successional boreal forest. *Ecosystems*, *18*(8), 1472–1488. https://doi.org/10.1007/s10021-015-9912-7

Menne, M. J., Durre, I., Vose, R. S., Gleason, B. E., & Houston, T. G. (2012). An Overview of the global historical climatology network-daily database. *Journal of Atmospheric and Oceanic Technology*, *29*(7), 897–910. https://doi.org/10.1175/JTECH-D-11-00103.1

Myers-Smith, I. H., Forbes, B. C., Wilmking, M., Hallinger, M., Lantz, T., Blok, D., Tape, K. D., MacIas-Fauria, M., Sass-Klaassen, U., Lévesque, E., Boudreau, S., Ropars, P., Hermanutz, L., Trant, A., Collier, L. S., Weijers, S., Rozema, J., Rayback, S. A., Schmidt, N. M., … Hik, D. S. (2011). Shrub expansion in tundra ecosystems: Dynamics, impacts and research priorities. *Environmental Research Letters*, *6*(4). https://doi.org/10.1088/1748-9326/6/4/045509

Nicolsky, D. J., Romanovsky, V. E., Panda, S. K., Marchenko, S. S., & Muskett, R. R. (2017). Applicability of the ecosystem type approach to model permafrost dynamics across the Alaska North Slope. *Journal of Geophysical Research: Earth Surface*, *122*(1), 50–75. https://doi.org/10.1002/2016JF003852

Nossov, D. R., Torre Jorgenson, M., Kielland, K., & Kanevskiy, M. Z. (2013). Edaphic and microclimatic controls over permafrost response to fire in interior Alaska. *Environmental Research Letters*, *8*(3). https://doi.org/10.1088/1748-9326/8/3/035013

O'Donnell, J. A., Romanovsky, V. E., Harden, J. W., & David McGuire, A. (2009). The effect of moisture content on the thermal conductivity of moss and organic soil horizons from black spruce ecosystems in interior Alaska. *Soil Science*, *174*(12), 646–651. www.lter.uaf.edu

Pan, Y., Birdsey, R. A., Fang, J., Houghton, R., Kauppi, P. E., Kurz, W. A., Phillips, O. L., Shvidenko, A., Lewis, S. L., Canadell, J. G., Ciais, P., Jackson, R. B., Pacala, S. W., McGuire, A. D., Piao, S., Rautiainen, A., Sitch, S., & Hayes, D. (2011). A large and persistent carbon sink in the world's forests. *Science*, *333*(August), 988–993.

Peng, C., & Apps, M. J. (1999). Modelling the response of net primary productivity (NPP) of boreal forest ecosystems to changes in climate and fire disturbance regimes. *Ecological Modelling*, *122*(3), 175–193. https://doi.org/10.1016/S0304-3800(99)00137-4

Peñuelas, J., Canadell, J. G., & Ogaya, R. (2011). Increased water-use efficiency during the 20th century did not translate into enhanced tree growth. *Global Ecology and Biogeography*, *20*(4), 597–608. https://doi.org/10.1111/j.1466-8238.2010.00608.x

PRISM Climate Group: Oregon State University. (2021). Recent 30 year normals (1981-2021). In *Oregon State University*. https://prism.oregonstate.edu/recent/.

Reyer, C., Lasch-Born, P., Suckow, F., Gutsch, M., Murawski, A., & Pilz, T. (2014). Projections of regional changes in forest net primary productivity for different tree species in Europe driven by climate change and carbon dioxide. *Annals of Forest Science*, *71*(2), 211–225. https://doi.org/10.1007/s13595-013-0306-8

Rodenhizer, H., Ledman, J., Mauritz, M., Natali, S. M., Pegoraro, E., Plaza, C., Romano, E., Schädel, C., Taylor, M., & Schuur, E. (2020). Carbon Thaw Rate Doubles When Accounting for Subsidence in a Permafrost Warming Experiment. *Journal of Geophysical Research: Biogeosciences*, *125*(6), 1–16. https://doi.org/10.1029/2019JG005528

Rupp, T. S., Chen, X., Olson, M., & McGuire, A. D. (2007). Sensitivity of simulated boreal fire dynamics to uncertainties in climate drivers. *Earth Interactions*, *11*(3), 1–21.

Scheffer, M., & Carpenter, S. R. (2003). Catastrophic regime shifts in ecosystems: Linking theory to observation. *Trends in Ecology and Evolution*, *18*(12), 648–656. https://doi.org/10.1016/j.tree.2003.09.002

Scheller, R., Kretchun, A., Hawbaker, T. J., & Henne, P. D. (2019). A landscape model of variable social-ecological fire regimes. *Ecological Modelling*, *401*, 85–93. https://doi.org/10.1016/J.ECOLMODEL.2019.03.022

Scheller, R. M., Domingo, J. B., Sturtevant, B. R., Williams, J. S., Rudy, A., Gustafson, E. J., Mladenoff, D. J., & Service, U. F. (2007). Design, development, and application of LANDIS-II, a spatial landscape simulation model with flexible temporal and spatial resolution. *Ecological Modelling*, *201*, 409–419. https://doi.org/10.1016/j.ecolmodel.2006.10.009

Scheller, R. M., & Mladenoff, D. J. (2004). A forest growth and biomass module for a landscape simulation model, LANDIS: design, validation, and application. *Ecological Modelling*, *180*, 211–229. https://doi.org/10.1016/j.ecolmodel.2004.01.022

Schuur, E. A. G., Bockheim, J., Canadell, J. G., Euskirchen, E., Field, C. B., Goryachkin, S. v., Hagemann, S., Kuhry, P., Lafleur, P. M., Lee, H., Mazhitova, G., Nelson, F. E., Rinke, A., Romanovsky, V. E., Shiklomanov, N., Tarnocai, C., Venevsky, S., Vogel, J. G., & Zimov, S. A. (2008). Vulnerability of permafrost carbon to climate change: Implications for the global carbon cycle. *BioScience*, *58*(8), 701–714. https://doi.org/10.1641/B580807

Shabaga, J. A., Bracho, R., Klockow, P. A., Lucash, M. S., & Vogel, J. G. (2022). Shortened Fire Intervals Stimulate Carbon Losses from Heterotrophic Respiration and Reduce Understorey Plant Productivity in Boreal Forests. *Ecosystems*. https://doi.org/10.1007/s10021-022-00761-w

Shenoy, A., Johnstone, J. F., Kasischke, E. S., & Kielland, K. (2011). Persistent effects of fire severity on early successional forests in interior Alaska. *Forest Ecology and Management*, *261*(3), 381–390. https://doi.org/10.1016/j.foreco.2010.10.021

Short, K. C. (2021). *Spatial wildfire occurrence data for the United States, 1992-2018 [FPA_FOD_20210617]* (5th ed.).

Stralberg, D., Arseneault, D., Baltzer, J. L., Barber, Q. E., Bayne, E. M., Boulanger, Y., Brown, C. D., Cooke, H. A., Devito, K., Edwards, J., Estevo, C. A., Flynn, N., Frelich, L. E., Hogg, E. H., Johnston, M., Logan, T., Matsuoka, S. M., Moore, P., Morelli, T. L., … Whitman, E. (2020). Climate-change refugia in boreal North America: what, where, and for how long? *Frontiers in Ecology and the Environment*, *18*(5), 261–270. https://doi.org/10.1002/fee.2188

Strobl, C., Boulesteix, A. L., Kneib, T., Augustin, T., & Zeileis, A. (2008). Conditional variable importance for random forests. *BMC Bioinformatics*, *9*, 1–11. https://doi.org/10.1186/1471-2105-9-307

Sturm, M., Schimel, J., Michaelson, G., Welker, J. M., Oberbauer, S. F., Liston, G. E., Fahnestock, J., & Romanovsky, V. E. (2005). Winter biological processes could help convert arctic tundra to shrubland. *BioScience*, *55*(1), 17–26. https://doi.org/10.1641/0006-3568(2005)055[0017:WBPCHC]2.0.CO;2

Tape, K., Sturm, M., & Racine, C. (2006). The evidence for shrub expansion in Northern Alaska and the Pan-Arctic. *Global Change Biology*, *12*(4), 686–702. https://doi.org/10.1111/j.1365-2486.2006.01128.x

Turetsky, M. R., Kane, E. S., Harden, J. W., Ottmar, R. D., Manies, K. L., Hoy, E., & Kasischke, E. S. (2011). Recent acceleration of biomass burning and carbon losses in Alaskan forests and peatlands. *Nature Geoscience*, *4*(January). https://doi.org/10.1038/NGEO1027

Ueyama, M., Iwata, H., & Harazono, Y. (2018a). *AmeriFlux BASE US-Rpf Poker Flat Research Range: Succession from fire scar to deciduous forest, Ver. 6-5, AmeriFlux AMP, (Dataset).* . https://doi.org/https://doi.org/10.17190/AMF/1579540

Ueyama, M., Iwata, H., & Harazono, Y. (2018b). *AmeriFlux BASE US-Uaf University of Alaska, Fairbanks, Ver. 9-5, AmeriFlux AMP, (Dataset).* https://doi.org/https://doi.org/10.17190/AMF/1480322

Ueyama, M., Iwata, H., & Harazono, Y. (2019a). *AmeriFlux AmeriFlux US-Rpf Poker Flat Research Range: Succession from fire scar to deciduous forest (Dataset)*. https://doi.org/https://doi.org/10.17190/AMF/1579540

Ueyama, M., Iwata, H., & Harazono, Y. (2019b). *AmeriFlux BASE US-Fcr Cascaden Ridge Fire Scar (Dataset)*. https://doi.org/https://doi.org/10.17190/AMF/1562388

Urban, D. L. (2005). Modeling Ecological Processes Across Scales. *Ecology*, *86*(8), 242–242. https://doi.org/10.1111/j.1525-139X.1993.tb00152.x

USDA-Forest Service. (2018). *PNW-FIA Interior Alaska Database*. https://www.fs.usda.gov/pnw/tools/pnw-fia-interior-alaska-database

USGS. (2020a). *Alaska 2 Arc-second Digital Elevation Models (DEMs)*. https://data.usgs.gov/datacatalog/data/USGS:4bd95204-7a29-4bd4-acce-00551ecaf47a

USGS. (2020b). *LANDFIRE 2020 Fuel Characteristic Classification System (FCCS) AK 2022 Capable Fuels*. https://landfire.gov/metadata/lf2020/AK/LA22_FCCS_220.html

van Cleve, K., & Dyrness, C. T. (1983). Introduction and overview of a multidisciplinary research project: the structure and function of a black spruce (Picea mariana) forest in relation to other fire-affected taiga ecosystems. *Canadian Journal of Forest Research*, *13*, 695–702.

van Cleve, K., Dyrness, C. T., Viereck, L. A., Fox, J., Chapin, F. S., & Oechel, W. (1983). Taiga in Ecosystems Interior Alaska. *BioScience*, *33*(1), 39–44.

van Cleve, K., Oliver, L., Schlentner, R., Viereck, L. A., & Dyrness, C. T. (1983). Productivity and nutrient cycling in taiga forest ecosystems. *Canadian Journal of Forest Research*, *13*, 747–766.

Viereck, L. A. (1983). The Effects of Fire in Black Spruce Ecoystems of Alaska and Northern Canada. In R. W. Wein & D. A. MacLean (Eds.), *The Role of Fire in Northern Circumpolar Ecosystems* (pp. 201–220). John Wiley & Sons Ltd.

Viereck, L. A., Dyrness, C. T., van Cleve, K., & Foote, M. J. (1983). Vegetation, soils, and forest productivity in selected forest types in interior Alaska. *Canadian Journal of Forest Research*, *13*, 703–720.

Viereck, L., van Cleve, K., Chapin, F. S., Hollingsworth, T., & Ruess, R. (2010). *Vegetation Plots of the Bonanza Creek LTER Control Plots: Species Percent Cover (1975 - 2009): Vol. BNZ:174* (Issue http://www.lter.uaf.edu/data/data-detail/id/174). Bonanza Creek LTER - University of Alaska Fairbanks.

Viereck, L., van Cleve, K., Chapin, F. S., Ruess, R., & Hollingsworth, T. N. (2005). *Vegetation Plots of the Bonanza Creek LTER Control Plots: Species Count (1975 - 2004): Vol. BNZ:175* (Issue http://www.lter.uaf.edu/data/data-detail/id/175). Bonanza Creek LTER - University of Alaska Fairbanks. .

Viglas, J. N., Brown, C. D., & Johnstone, J. F. (2013). Age and size effects on seed productivity of northern black spruce. *Canadian Journal of Forest Research*, *43*(6), 534–543. https://doi.org/10.1139/cjfr-2013-0022

Walker, X. J., Baltzer, J. L., Cumming, S. G., Day, N. J., Ebert, C., Goetz, S., Johnstone, J. F., Potter, S., Rogers, B. M., Schuur, E. A. G., Turetsky, M. R., & Mack, M. C. (2019). Increasing wildfires threaten historic carbon sink of boreal forest soils. *Nature*, *572*, 520–525. https://doi.org/10.1038/s41586-019-1474-y

Wang, J. A., Sulla-Menashe, D., Woodcock, C. E., Sonnentag, O., Keeling, R. F., & Friedl, M. A. (2020). Extensive land cover change across Arctic–Boreal Northwestern North America from disturbance and climate forcing. *Global Change Biology*, *26*(2), 807–822. https://doi.org/10.1111/gcb.14804

Watts, J. D., Natali, S. M., Minions, C., Risk, D., Arndt, K., Zona, D., Euskirchen, E. S., Rocha, A. v., Sonnentag, O., Helbig, M., Kalhori, A., Oechel, W., Ikawa, H., Ueyama, M., Suzuki, R., Kobayashi, H., Celis, G., Schuur, E. A. G., Humphreys, E., … Edgar, C. (2021). Soil respiration strongly offsets carbon uptake in Alaska and Northwest Canada. *Environmental Research Letters*, *16*(8). https://doi.org/10.1088/1748-9326/ac1222

Whitman, E., Parisien, M. A., Thompson, D. K., & Flannigan, M. D. (2019). Short-interval wildfire and drought overwhelm boreal forest resilience. *Scientific Reports*, *9*(1), 1–12. https://doi.org/10.1038/s41598-019-55036-7

Whitman, E., Parks, S., Holsinger, L., & Parisien, M.-A. (2022). Climate-induced fire regime amplification in Alberta, Canada. *Environmental Research Letters*. https://doi.org/10.1088/1748-9326/ac60d6

Williams, A. P., Xu, C., & McDowell, N. G. (2011). Who is the new sheriff in town regulating boreal forest growth? *Environmental Research Letters*, *6*(4), 041004. https://doi.org/10.1088/1748-9326/6/4/041004

Yang, J., Cooper, D. J., Li, Z., Song, W., Zhang, Y., Zhao, B., Han, S., & Wang, X. (2020). Differences in tree and shrub growth responses to climate change in a boreal forest in China. *Dendrochronologia*, *63*(February), 125744. https://doi.org/10.1016/j.dendro.2020.125744

Yoshikawa, K., Bolton, W. R., Romanovsky, V. E., Fukuda, M., & Hinzman, L. D. (2003). Impacts of wildfire on the permafrost in the boreal forests of interior Alaska. *Journal of Geophysical Research: Atmospheres*, *108*(1). https://doi.org/10.1029/2001jd000438

Zambrano-Bigiarini, M., & Rojas, R. (n.d.). *hydroPSO: Particle Swarm Optimisation, with Focus on Environmental Models. R package version 0.5-1.* https://doi.org/DOI:10.5281/zenodo.1287350

Zasada, J. C., Sharik, T. L., & Nygren, M. (1992). The reproductive process in boreal forest trees. In *A Systems Analysis of the Global Boreal Forest* (pp. 85–125). https://doi.org/10.1017/cbo9780511565489.004

Zuur, A. F., Ieno, E. N., Walker, N. J., Saveliev, A. A., & Smith, G. M. (2009). *Zero-truncated and zero-inflated models for count data* (pp. 261–293). https://doi.org/10.1007/978-0-387-87458-6_11